AD-A033 969 GENERAL DYNAMICS SAN DIEGO CALIF CONVAIR AEROSPACE DIV F/G 1/3
CONTROL POWER CRITERIA FOR STATICALLY UNSTABLE AIRCRAFT.(U)
NOV 76 N00019-75-C-0355
UNCLASSIFIED CASD-NSC-76-003 NL

END

DATE FILMED 2-77

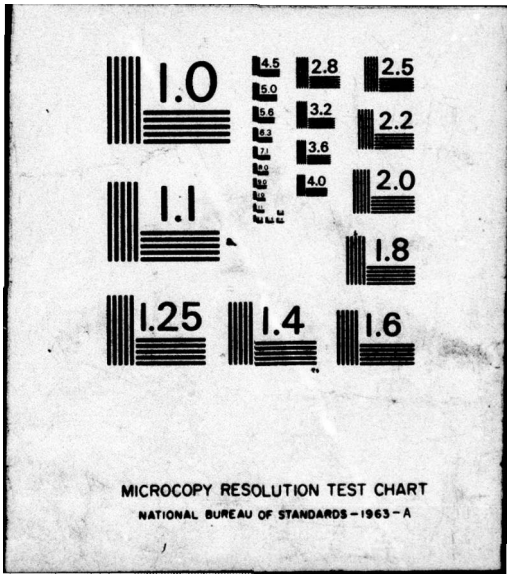
1.0
1.1
1.25
1.4
1.6
1.8
2.0
2.2
2.5
2.8
3.2
3.6
4.0
4.5
5.0
5.6
6.3
7.1
8.0
MICROCOPY RESOLUTION TEST CHART
NATIONAL BUREAU OF STANDARDS-1963-A

(14) REPORT CASD-NSC-76-003

(6) CONTROL POWER CRITERIA FOR STATICALLY UNSTABLE AIRCRAFT.

(9) FINAL REPORT.

(11) November 1976 (12) 70p.

United States Navy
Naval Air Systems Command
Plans and Programs Division
Washington D.C.

(15) Prepared Under
Contract N00019-75-C-0355

Prepared by
GENERAL DYNAMICS CONVAIR DIVISION
San Diego, California

406 258
6pgs

A

TABLE OF CONTENTS

BEST AVAILABLE COPY

LIST OF FIGURES

PAGE BLANK-NOT FILMED

LIST OF FIGURES, Contd

LIST OF FIGURES, Contd

LIST OF FIGURES, Contd

LIST OF TABLES

SUMMARY

e sensitivity of control power requirements during gust response to variations in
craft parameters and input disturbance levels has been investigated in an attempt to
vide data useful in establishing design criteria and margins of safety needed in the
sign of aerodynamically unstable aircraft. Both canard configured and a conven-
nal tail configured aircraft were used in this study. For both configurations the
tical flight conditions were during the low-speed power approach. The critical
st frequency in terms of critical power requirement for a (1-cos) type gust was
proximately twice the closed loop natural frequency of the aircraft.

tic margin was found to be the primary quantity influencing the control power
quirements. The sensitivity of required control power to variation in other aircraft
rameters is predictable by the manner in which these parametric variations alter
e static margin. The high angle of attack characteristics also had a significant
fect on the control power requirements -- indicating the need for a complete and
curate data base in this region. The gust upset boundaries dropped off sharply
en the discrete gust was applied at a significant angle from the vertical.

e control power requirements were found to be relatively insensitive to variations
the discrete gust mode shape in the absence of control surface rate saturation.
wever, the increases in required control power due to increased gust magnitude
re also relatively small when the surfaces were not rate saturated. When rate

SECTION 1

INTRODUCTION

Many studies in recent years have established the importance of the control configured vehicle (CCV) concept in improving the performance of fighter aircraft. In particular, it has been established that the use of relaxed static stability (RSS) results in significant decrease in trim drag (especially at the higher load factors), and a substantial increase in specific excess power. RSS implies a reduced (and even negative) static margin, which is a direct consequence of an aft shift in center of gravity (cg) or a forward shift in center of pressure. For an unaugmented aircraft, the reduction in static margin required to produce measurable performance benefits, generally results in unacceptable handling qualities. Consequently, the criteria for the most aft cg point acceptable must be predicated on the capabilities of an active feedback flight control system. In addition to ensuring stability/response characteristics at least as good as those for a statically stable conventional design, the flight control system must have the necessary control authority (control surface deflection and rate capability) to provide the pitching moment necessary to cope with "worst case" combinations of maneuver and gust.

In a conventional, statically stable fighter aircraft, such criteria as:

a. Trim $C_{L_{max}}$ at V_s,

b. Balance,

c. Nose gear unstick, and

d. Short period frequency requirements

generally predominate over the gust upset criterion; this may not be true for an RSS aircraft. Consequently, the consideration of the pitch control power to accommodate gust upset is now essential in the design of an RSS aircraft.

The primary aim of this study was to determine the sensitivity of control power requirements to variations in aircraft parameters and input disturbance levels for statically unstable fighter aircraft. Sensitivity studies of this type are the first step in arriving at design criteria for control power for unstable aircraft. An attempt is made at providing data useful in arriving at rational design criteria and margins of safety needed for control power in aerodynamically unstable aircraft.

1.1 BASELINE CONFIGURATIONS

Over the past several years, several aerospace companies have been working on canard configured and conventional configured advanced fighter aircraft that use the reduced static stability concept to obtain improved maneuvering performance. This study analyzes the sensitivity of control power requirements to parameter variations for both types of configurations.

1.1.1 CANARD CONFIGURATION. The canard configuration, Figure 1-1, has a low aspect ratio, highly swept, aerodynamically thin delta wing. A controllable canard was added to the basic configuration to enhance the aerodynamic characteristics of the wing. The canard contributes to positive lift during maneuvers, cruise, landing and takeoff. It has been positioned to generate favorable aerodynamic interference effects and to shift the aircraft aerodynamic center of lift forward, to reduce the longitudinal static stability margin. The canard incorporates a geared trailing-edge flap that operates in combination with the wing and elevons (deflected as flaps) to produce a high-lift system for low-speed flight. Coordination of canard and elevons for pitch control and trim is mechanized by a fly-by-wire flight control system to produce good lift-to-drag relationship for cruise, maneuvers, and landing/takeoff.

The aerodynamic data used in this study is based on wind tunnel test results. Figures 1-2 through 1-7 show the low-speed longitudinal characteristics up to 40 degrees angle of attack and a wide range of canard and elevon deflections. Since the canard flap is a direct function of canard deflection, only specific canard flap deflections are shown. The study used aerodynamic data over the complete speed range: low-speed, transonic, and supersonic. However, the majority of the work centered around the low-speed, high angle of attack region. Therefore, only this data is present. The pitching moment is referenced to 16.4% $\bar{c}$ and the range of cg studied were from 4% $\bar{c}$ to 32% $\bar{c}$.

Lift and pitching moment characteristics for the canard configuration at extreme angle of attack were obtained from wind tunnel tests. These tests provided data to angles of attack near 70 degrees. The canard configuration was designed to provide a nose-down pitching moment throughout the angle of attack range, with the aircraft balanced at the aft cg. Typical wind tunnel data is presented in Figure 1-8. The control deflections for this test are those that produce maximum nose-down pitching moments: +25 degrees elevon, -40 degrees canard, and -30 degrees canard flap. The data illustrated by Figure 1-8, along with data at other control deflections, was used in this study.

1.1.2 CONVENTIONAL CONFIGURATION. The conventional configuration, shown in Figure 1-9, has a relatively low thickness and aspect ratio wing with a relatively high leading-edge sweep. The wing is blended into the fuselage. A conventional all-moving horizontal tail provides pitch and roll control. Location of the wing on the fuselage is such that the concept of relaxed static stability can be applied for improvements in maneuver and trim drag.

	Unit	Actual	Exposed
Wing			
• Area	sq. ft.	415.92	270.05
• Aspect ratio		1.874	1.76
• Taper ratio		0.1297	0.16
• Span	ft.	27.85	21.81
• Sweep (LE)	deg.	60.0	60.0
• Dihedral	deg.	–	–
• Incidence	deg.	2.0	2.0
• Airfoil section	NACA 0004-65 Mod. with 20% span L.E. camber (Convair case XXIX)		
• Twist	deg.	0	0
• Elevon area/side	sq. ft.	27.17	27.17
Canard (all moveable)			
• Area	sq. ft.	80.00	80.00
• Aspect ratio		2.459	2.459
• Taper ratio		0.145	0.145
• Span (per side)	ft.	7.015	7.015
• Sweep (LE)	deg.	55	55
• Dihedral	deg.	–	–
• Airfoil section	NACA 0004-65 MOD with 20% span LE camber (Convair case XXIX)		
• Canard flap Area/side	sq. ft.	9.17	9.17
Vertical Tail			
• Area	sq. ft.	58.98	58.98
• Aspect ratio		1.867	1.867
• Taper ratio		0.2097	0.2097
• Span	ft.	7.93	7.93
• Sweep (LE)	deg.	55	55
• Airfoil sections		NACA 0004-65 Mod.	
• Rudder area	sq. ft.	16.81	16.81

	Unit	Actual	
Speed Brake (Tailcone Petal Type)			
• Area stowed	sq. ft.	25.7	
• Projected	sq. ft.	25.2	
Control Surface Travel			
• Elevon	deg.	±25	
• Canard	deg.	TE 30 up to 20 down	
• Canard flap	deg.	TE 20 up to 30 down	
• Rudder	deg.	±25	
• Speed brake	deg.	60	
Landing Gear			
• Main gear			
Tire size		30 x 8.8-15 22 PR	
Stroke	in.	22	
Static rolling radius	in.	12.9	
• Nose gear			
Tire size		22 x 6.75-10 18 PR	
Stroke	in.	19.5	
Static rolling radius	in.	10.52	
		Baseline	*Improved*
Propulsion		JTF22A-26A*	JTF22A-26C
• Thrust (SLS) rated	lb.	26,945	29,359
• Engine comp. face dia.	in.	37.9	37.9
• Engine length	in.	206.4	200.4
• Inlet capture area	sq. in.	1008	1008
Fuel Capacity			
• Internal capacity	lb.	9,495	9,433

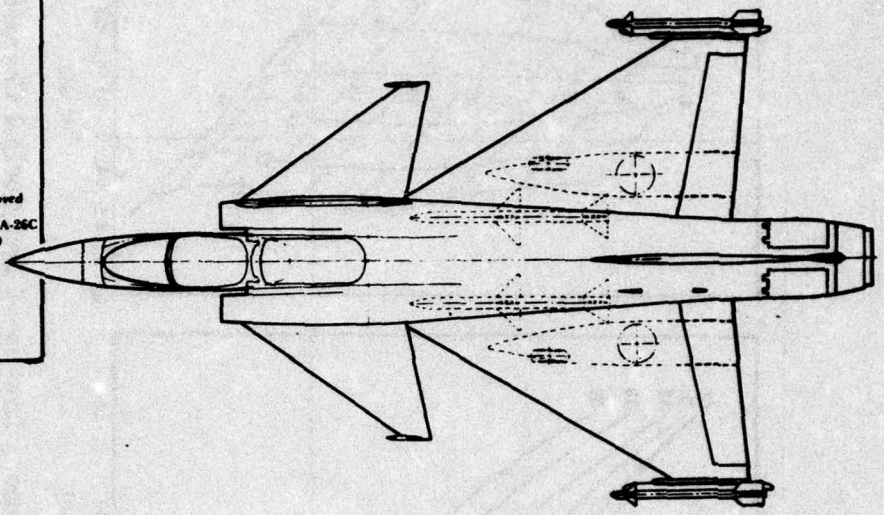

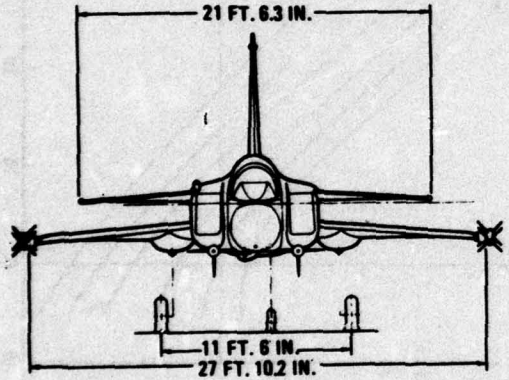

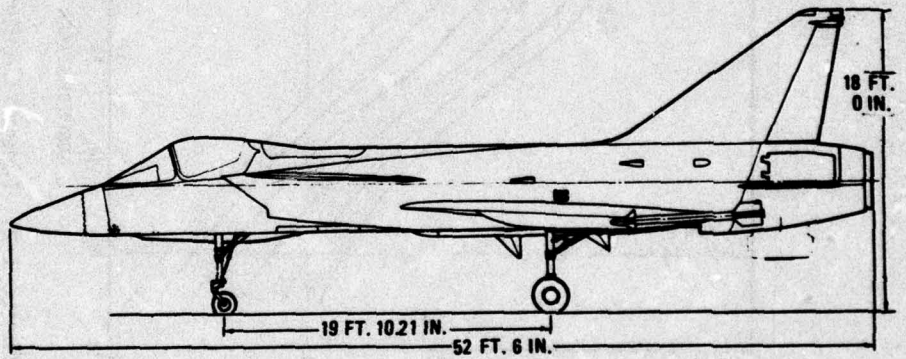

Figure 1-1. Study Canard Configuration

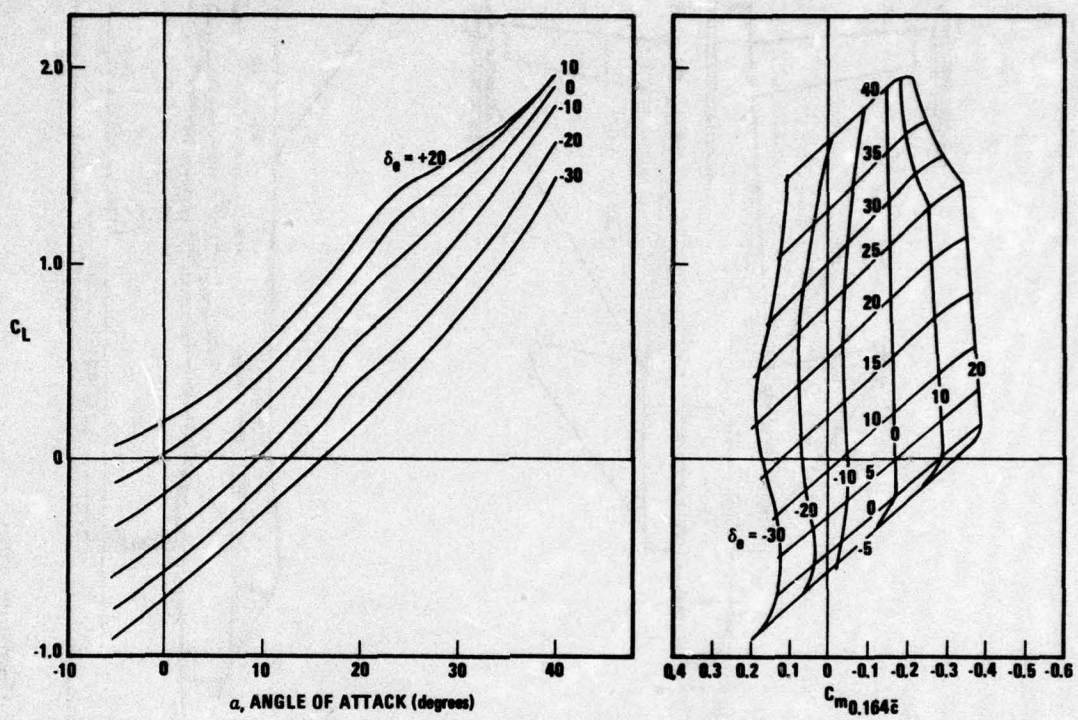

Figure 1-2. Canard Configuration, Low-Speed Longitudinal Characteristics, δ_c = -35, δ_f = -25 Degrees

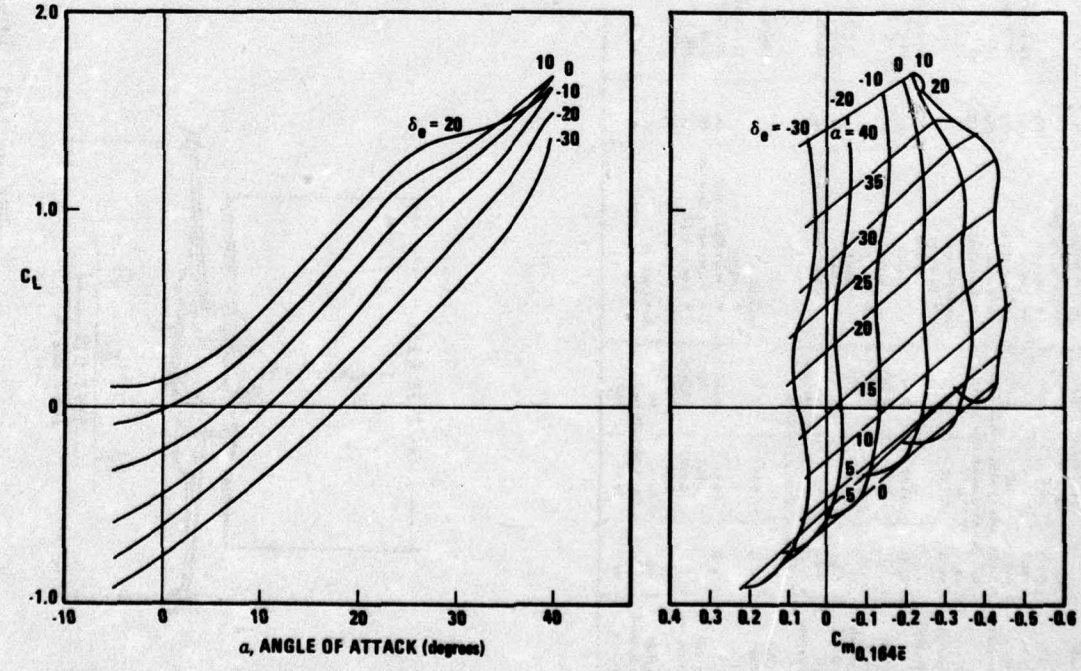

Figure 1-3. Canard Configuration, Low-Speed Longitudinal Characteristics, δ_c = -25, δ_f = -15 Degrees

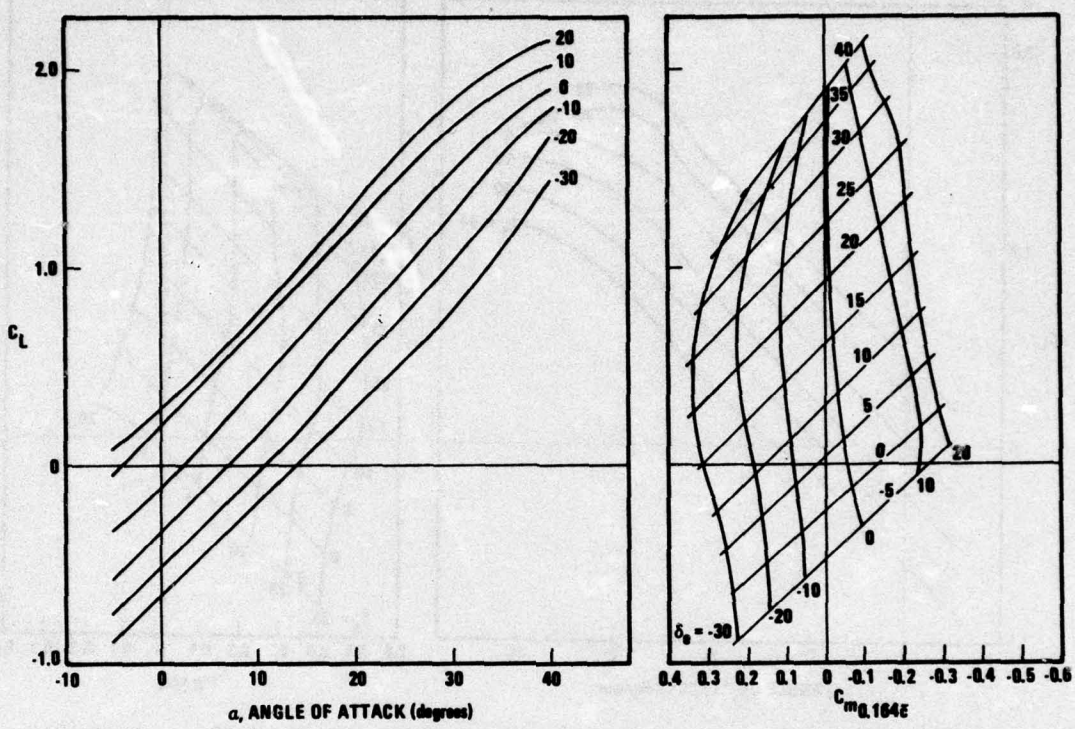

Figure 1-4. Canard Configuration, Low-Speed Longitudinal Characteristics, $\delta_c = -10$, $\delta_f = -0$ Degrees

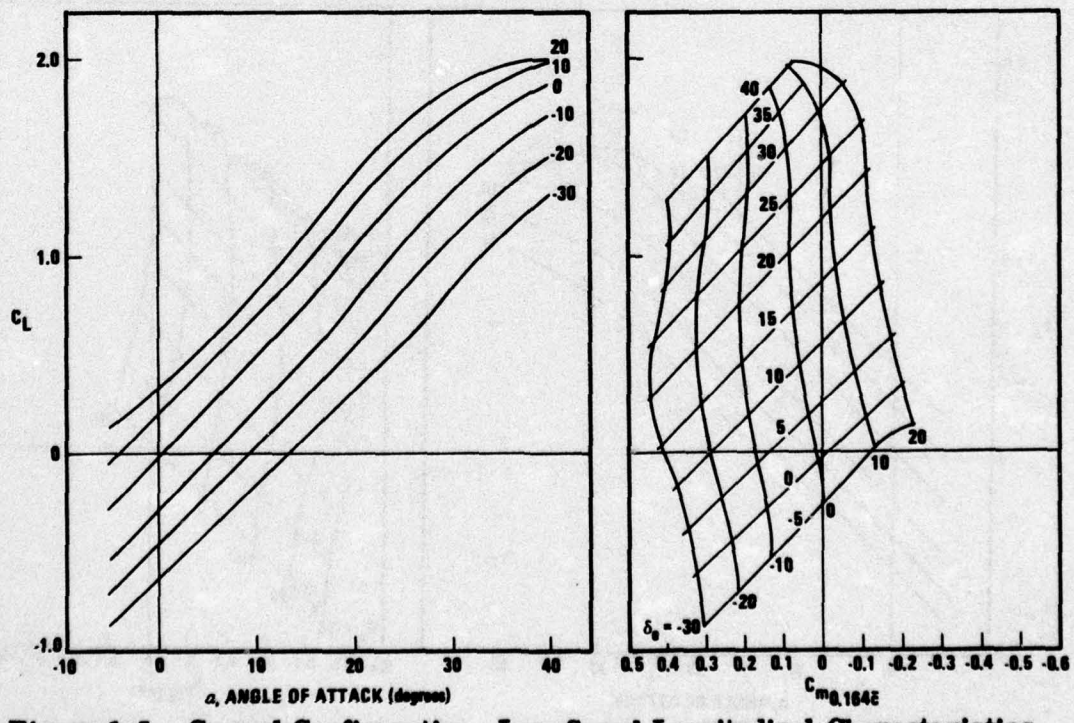

Figure 1-5. Canard Configuration, Low-Speed Longitudinal Characteristics, $\delta_c = 0$, $\delta_f = 10$ Degrees

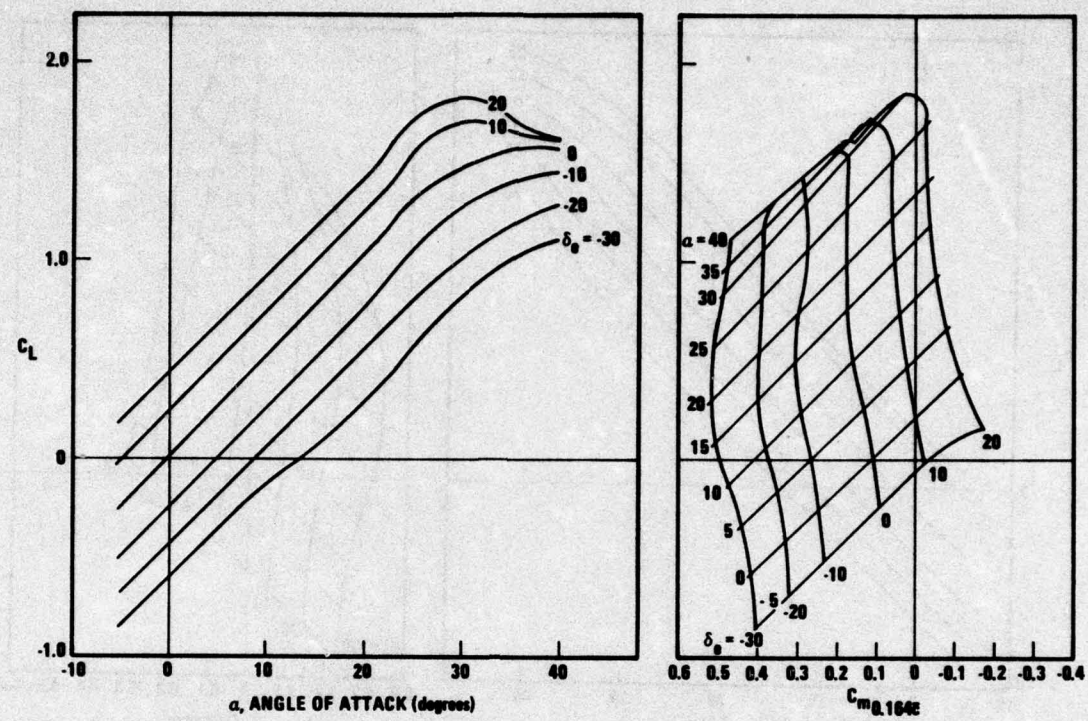

Figure 1-6. Canard Configuration, Low-Speed Longitudinal Characteristics, $\delta_c = 10$, $\delta_f = 20$ Degrees

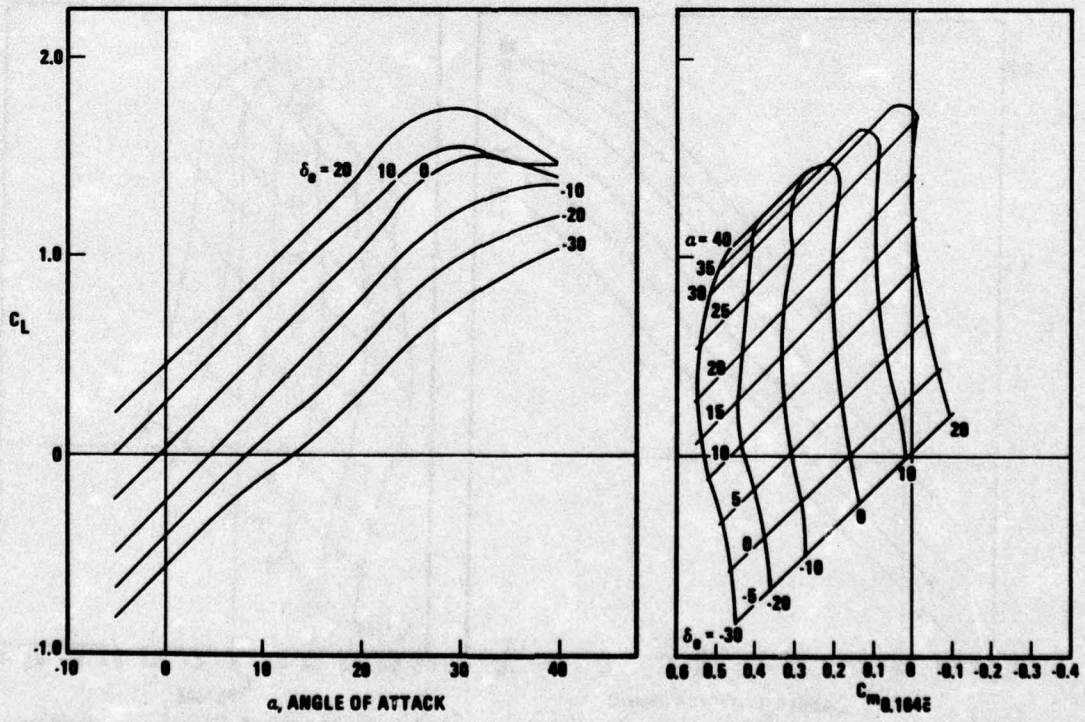

Figure 1-7. Canard Configuration, Low-Speed Longitudinal Characteristics, $\delta_c = 15$, $\delta_f = 25$ Degrees

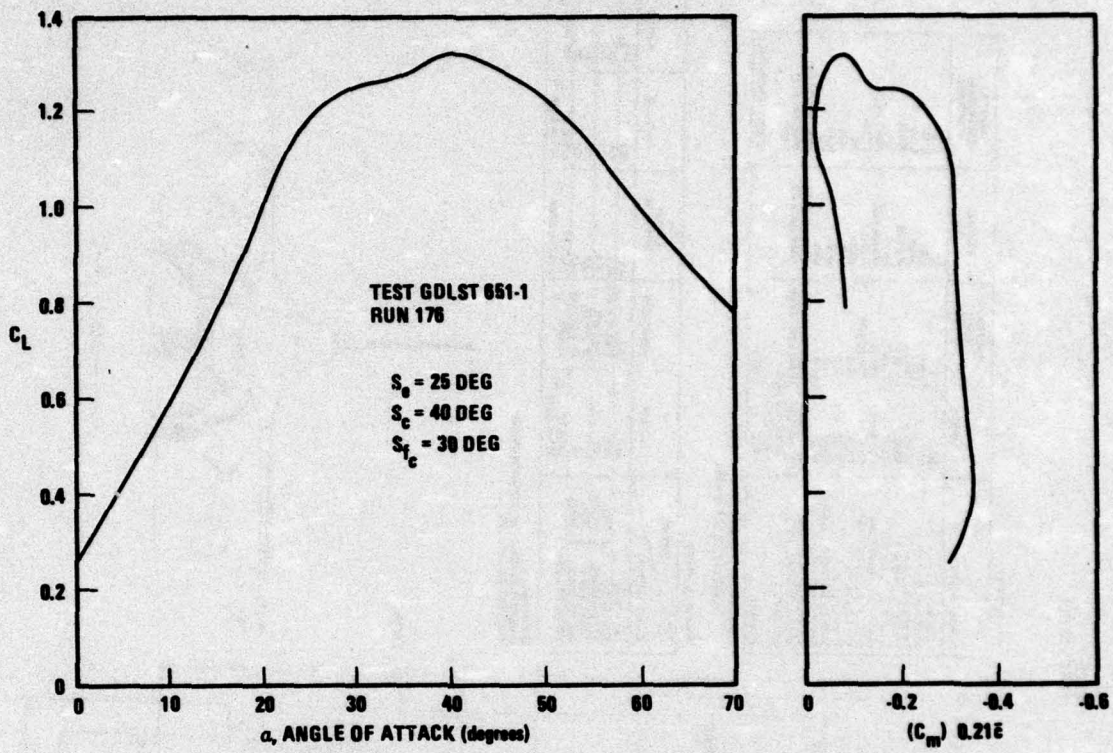

Figure 1-8. Canard Configuration, High Angle of Attack, Low Speed

The aerodynamic data used in this study is based upon wind tunnel data. Figure 1-10 is the low-speed longitudinal characteristics as a function of angle of attack and horizontal tail deflection (δ_e). This data is for angles up to 40 degrees. The pitching moment is referenced to 35% $\bar{c}$ and the range of cg studied was from 39% $\bar{c}$ to 55% $\bar{c}$.

Actual wind tunnel test data was available up to 26 degrees. It was necessary to extrapolate the wing-body lift and pitching moments, down-wash, and tail lift. The resulting data used in the conventional configuration aerodynamic data is shown in Figure 1-11. The extrapolations are based upon detailed configuration component wind tunnel tests conducted on similar configurations. The conventional configuration of this study was designed to have nose-down pitch moments at high angles of attack.

1.2 CONTROL SYSTEM

The control systems for both study configurations are fly-by-wire (FBW) in three axes. FBW allows the concept of relaxed static stability and provides the aircraft stability artifically and tailored flying qualities. This study did not concern itself with the degree of control system redundancy nor the evaluation of handling qualities. The control systems had, in previous analysis and design studies, been optimized for handling qualities.

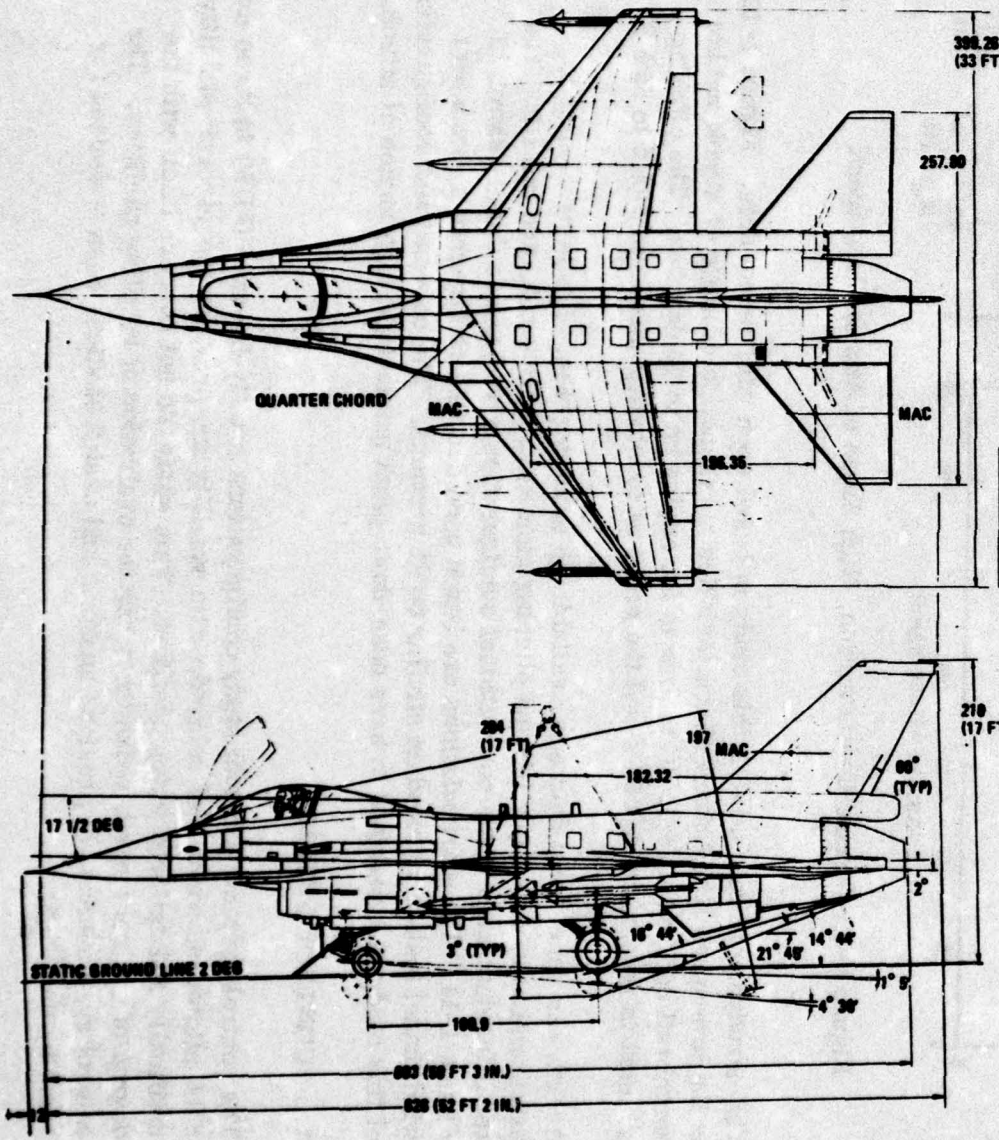

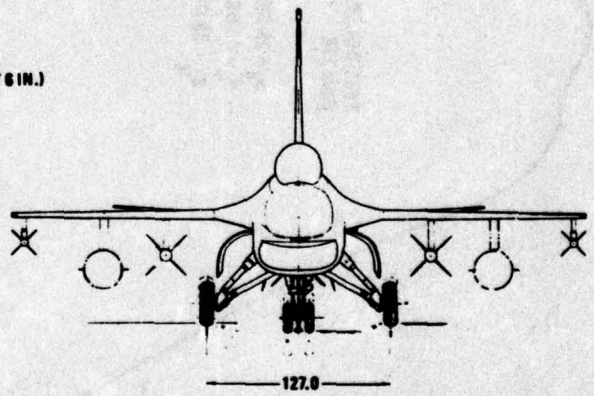

BASIC SURFACES

CHARACTERISTIC \ SURFACE	WING	HORIZONTAL TAIL (EXPOSED)	VERTICAL TAIL	VENTRAL (THEORETICAL PLANFORM)
AREA, SQ FT	300	75	70	15.28
ASPECT RATIO	3.0	2.000	1.304	0.3339
TAPER RATIO	0.2275	0.30	0.4370	0.7169
LEADING EDGE SWEEP	40 DEG	40 DEG	47.5 DEG	45 DEG
SPAN, IN.	300.30	162.00	114.21	15.0
ROOT CHORD LE LOCATION (FUSELAGE COORDINATES)	X231.98, Y0.0, Z180	X486.25 Y45.162, Z180	X446.36, Y0.0, Z121.75	X488.0, Y18.5 Z72.16
ROOT CHORD	216.94	88.10	122.01	630
TIP CHORD	48.33 (TRUE)	20.76	68.71	48.35
MEAN AERODYNAMIC CHORD, IN.	169.66	70.71	92.77	66.35
MAC SPANWISE LOCATION, IN.	70.69	34.32	49.65	6.69
AIRFOIL SECTION AT ROOT	NACA64A004	0.06t/c BICONVEX	0.060t/c BICONVEX	0.60t/c HEXSIDE
AIRFOIL SECTION AT TIP	NACA64A004	0.038t/c BICONVEX	0.03t/c BICONVEX	CONSTANT 0.60t
INCIDENCE	0 DEG AT Y81.80 -3 DEG AT TIP	(1)	-	0 DEG
DIHEDRAL	0 DEG	5 DEG	-	15 DEG FROM VERTICAL

(1) HORIZONTAL TAIL MAXIMUM DEFLECTION
25 DEG TE UP, 25 DEG TE DOWN

CONTROL SURFACES

CHARACTERISTIC \ SURFACE		LE FLAP	LE KRUEGER	LE FLAP EXTENSION	FLAPERON	RUDDER
AREA, SQ FT		45.7	24.5	8.4	33.0	14.0
SPAN, % OF BASIC SURFACE	INBD	28.4	28.4	22.8	22.8	62.0
	OUTBD	100	84.8	28.4	77.0	62.0
CHORD, % OF BASIC SURFACE	INBD	15	20	15.0	15.0	30
	OUTBD	30	20	15.0	15.0	30
DEFLECTION, MAX.		7 DEG UP 25 DEG DOWN (2)	135 DEG (3)	7 DEG UP 12.5 DEG DOWN (2)	30 DEG UP 60 DEG DOWN (4)	30 DEG (4)

(2) STREAMWISE
(3) NORMAL TO HINGE LINE (ROTATION ANGLE)
(4) NORMAL TO HINGE LINE

Figure 1-9. Study Conventional Configuration

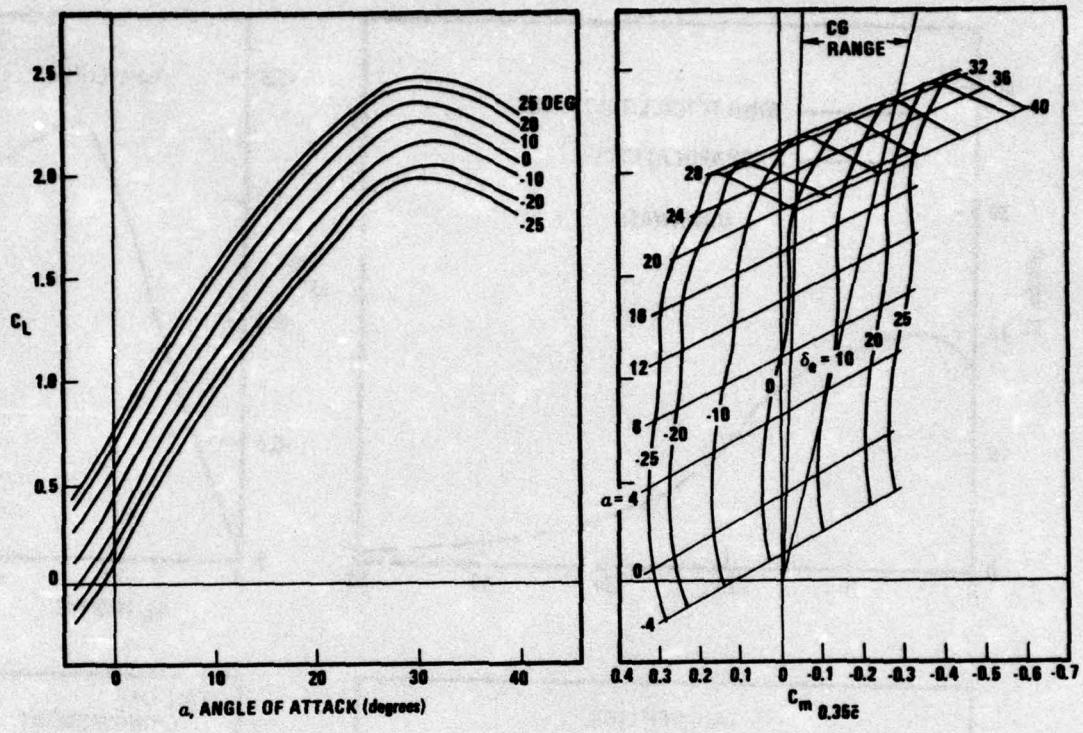

Figure 1-10. Conventional Configuration, Low-Speed Longitudinal Characteristics

1.2.1 CANARD CONFIGURATION. The flight control system for the canard configuration consists of sensors, flight control computer, canard, canard flap, right and left elevons, and a rudder. The control surfaces have the following characteristics:

Right and left elevon	±25 degrees maximum displacement
Right and left elevon	±75 deg/sec maximum rate
Canard	+15, -35 degrees, maximum displacement
Canard	±25 deg/sec maximum rate
Canard flap (geared to canard)	±25 degrees maximum displacement
Rudder	±25 degrees maximum displacement

Wing trailing edge elevons provide pitch control with symmetric motion and roll control with differential motion. Additional pitch control is obtained by controlling the canard through a washout circuit. For up-and-away flight, the canard steady-state position is parallel to the wing. Large leading-edge-down canard deflections are effective for relieving nose-up pitch at high lift coefficients. For a conventional tailed aircraft with static instability, progressively larger trailing-edge-down tail

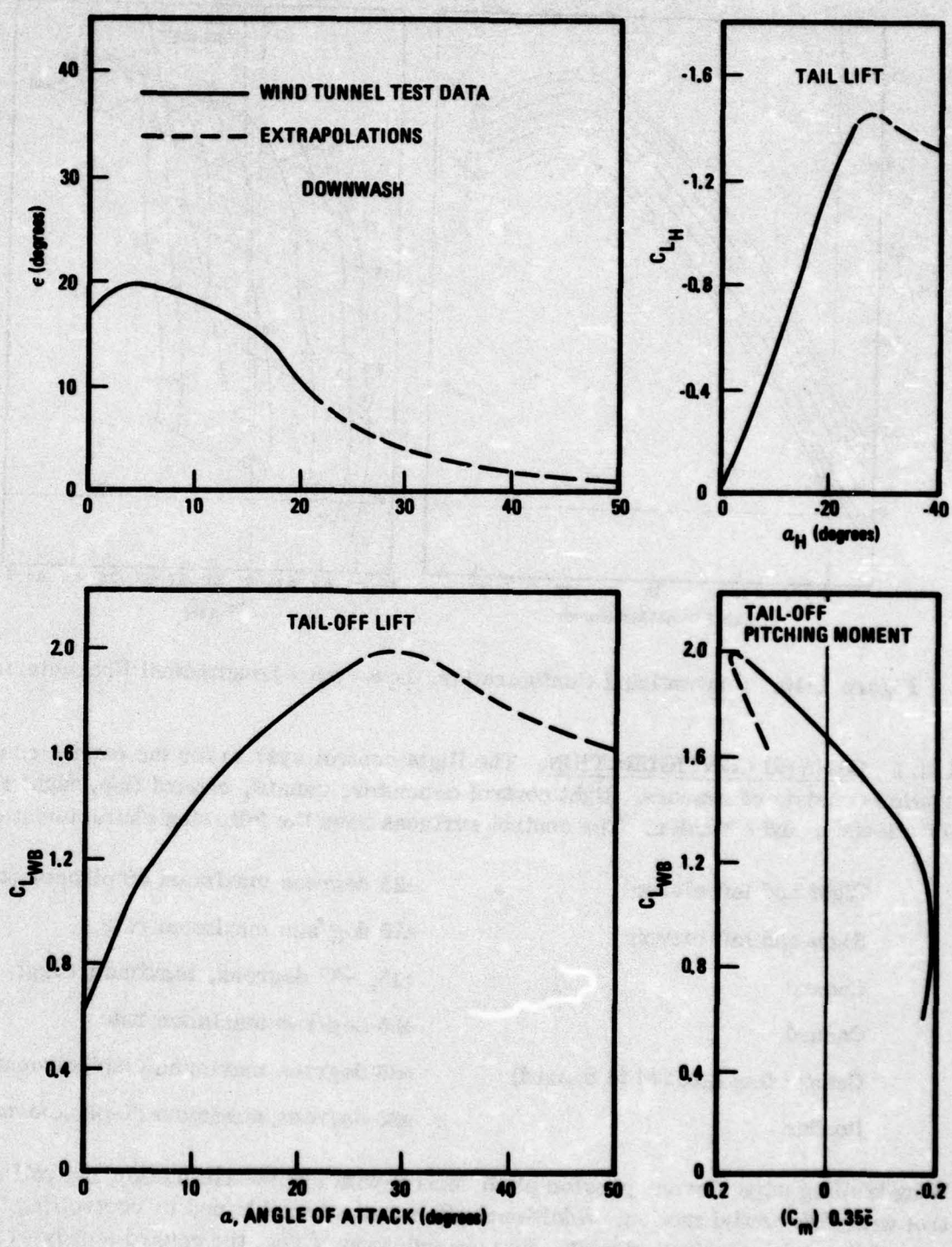

Figure 1-11. Conventional Configuration, High Angle of Attack Characteristics

deflections are required as the lift coefficient increases. If the tail deflection is limited by either hinge moment or surface travel, the tailed aircraft might pitch up out of control.

Low-speed high-lift is attained by engaging an antiservoed simple canard flap and deflecting the canard up. The resulting trim requires down elevon deflection. At zero-degree canard deflection, 10 degrees of canard flap is commanded.

The basic longitudinal control laws, Figure 1-12, use normal load factor (n_z), pitch rate ($\dot{\theta}$), and angle of attack (α) for feedback stabilization. By increasing the electrical angle of attack signal as angle of attack reaches 28 degrees, an effective angle of attack limiter is included in the control system. As the angle of attack approaches 28 degrees, the elevons and canard are deflected for increased nose-down moment. The canard is "washed out" unless set to a fixed position by the flap input or unless the elevon command is greater than +20 degrees. If the elevon command is greater than +20 degrees, the canard will deflect leading edge down to a maximum deflection of -10 degrees with the amplitude given by

$$\delta_{c_{com}} = -2\ (\delta_e - 20 \text{ degrees})$$

Two gains are scheduled with dynamic pressure as shown in the diagram.

The lateral/directional control system, Figure 1-13, used roll rate feedback for roll rate command system. The roll stick force gradient is as shown. At high speeds, lateral acceleration and yaw rates are used for minimizing side-slip and for providing good directional damping characteristics. An aileron-to-rudder interconnect is scheduled with angle of attack for coordinated turns.

1.2.2 CONVENTIONAL CONFIGURATION. The conventional configuration control system uses an all-movable, differential horizontal tail for pitch and roll control; wing mounted flaperons for roll control; and a conventional rudder for yaw control. Maneuver capability at high angles of attack is enhanced with a full-span, leading-edge flap positioned automatically after takeoff as a function of Mach number, angle of attack, and pitch rate. The control surfaces characteristics are:

Horizontal Tail	±25 degrees maximum displacement
Horizontal Tail	±60 deg/sec maximum rate
Flaperon	±20 degrees maximum displacement
Flaperon	±56 deg/sec maximum rate
Rudder	±30 degrees maximum displacement
Rudder	±120 deg/sec maximum rate

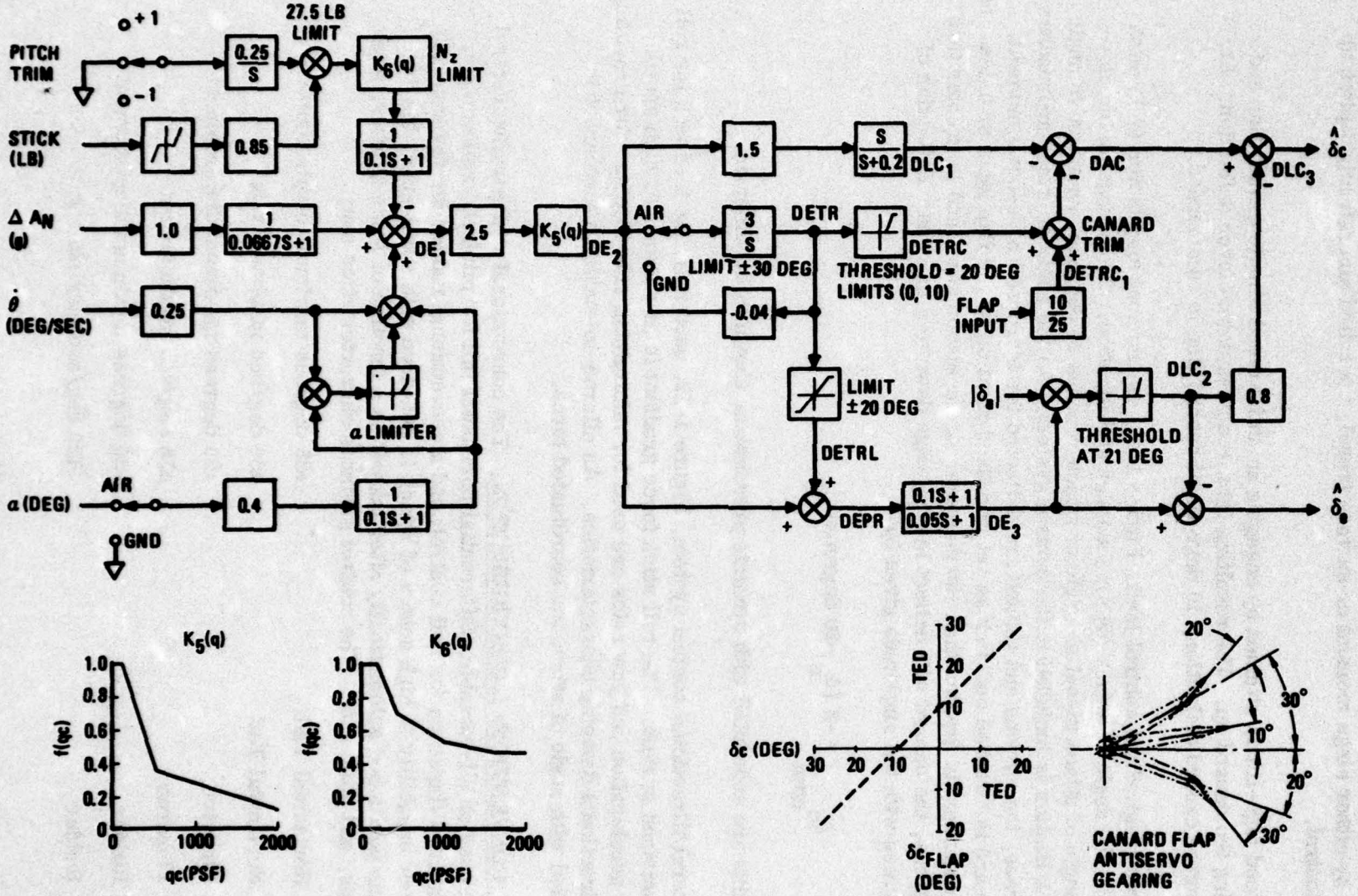

Figure 1-12. Canard Configuration, Longitudinal Control System

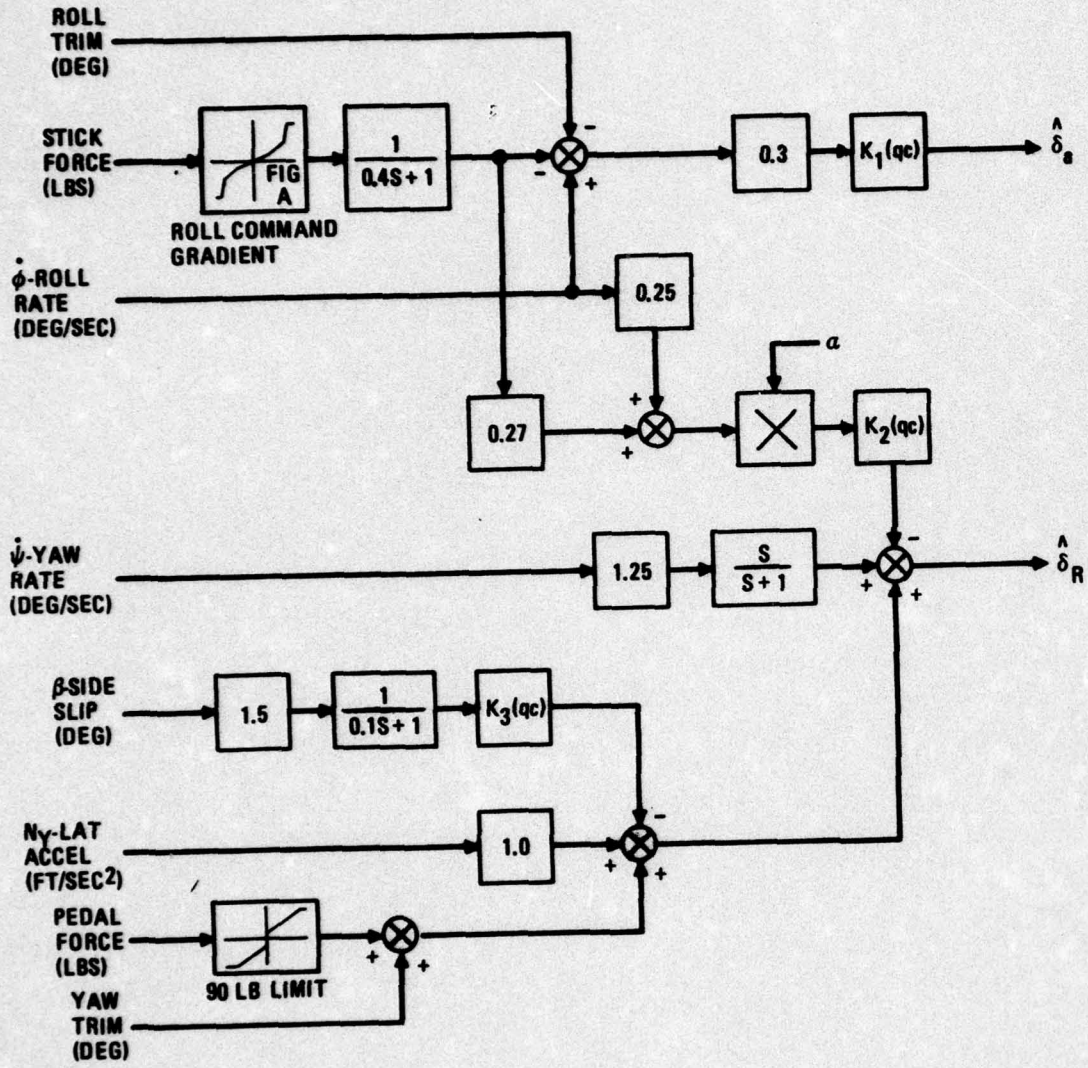

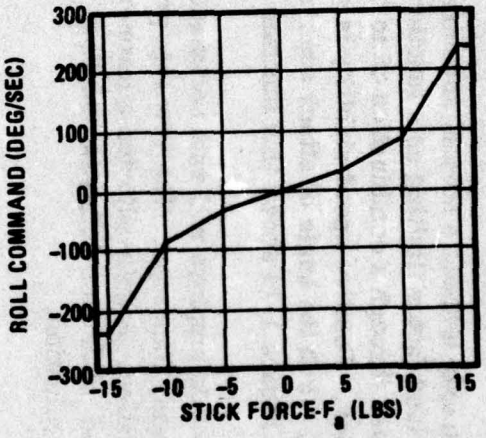

FIGURE A

Figure 1-13. Lateral/Directional Control System

The pitch axis utilizes a normal acceleration-referenced command system to provide positive load factor limiting as a function of flight condition. Neutral speed stability is achieved through a combination of normal acceleration command and forward loop integration. Positive speed stability is achieved through positive angle of attack limiting. Both the angle of attack sensor input and the feedback loops limit angle of attack. Figure 1-14 shows this function on the autopilot block diagram.

The roll axis employs roll rate command through both the differential horizontal tail and the wing flaperons. The yaw axis provides directional damping and stability augmentation. A gain-adjusted aileron-rudder interconnect and a roll rate-to-rudder crossfeed minimizes roll-yaw coupling, facilitates precise tracking, and provides turn coordination.

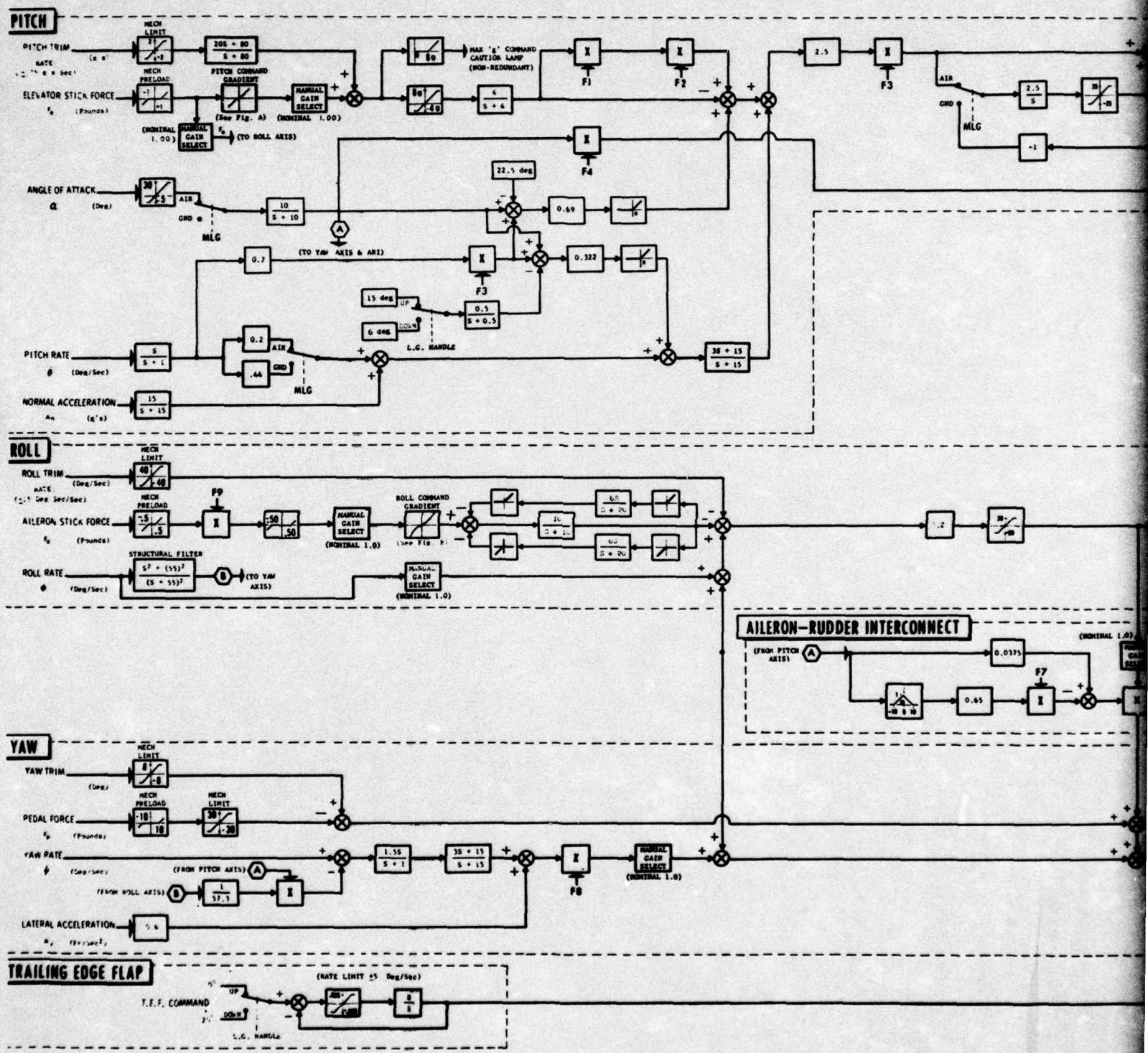
PITCH
PITCH TRIM
RATE
ELEVATOR STICK FORCE
(Pounds)
MECH LIMIT
MECH PRELOAD
PITCH COMMAND GRADIENT
(See Fig. A)
MANUAL GAIN SELECT
(NOMINAL 1.00)
(TO ROLL AXIS)
MAX 'g' COMMAND CAUTION LAMP (NON-REDUNDANT)
F1
F2
F3
F4
AIR
GND
MLG
ANGLE OF ATTACK
(Deg)
22.5 deg
0.69
(TO YAW AXIS & ARI)
0.322
15 deg
UP
6 deg
DOWN
L.G. HANDLE
PITCH RATE
(Deg/Sec)
NORMAL ACCELERATION
(g's)
ROLL
ROLL TRIM
(Deg/Sec)
AILERON STICK FORCE
F9
ROLL COMMAND GRADIENT
(See Fig. B)
(NOMINAL 1.0)
STRUCTURAL FILTER
ROLL RATE
(TO YAW AXIS)
AILERON-RUDDER INTERCONNECT
(FROM PITCH AXIS)
0.0375
F7
0.65
(NOMINAL 1.0)
YAW
YAW TRIM
PEDAL FORCE
YAW RATE
(FROM PITCH AXIS)
(FROM ROLL AXIS)
F8
LATERAL ACCELERATION
TRAILING EDGE FLAP
T.E.F. COMMAND
(RATE LIMIT ±5 Deg/Sec)
L.G. HANDLE

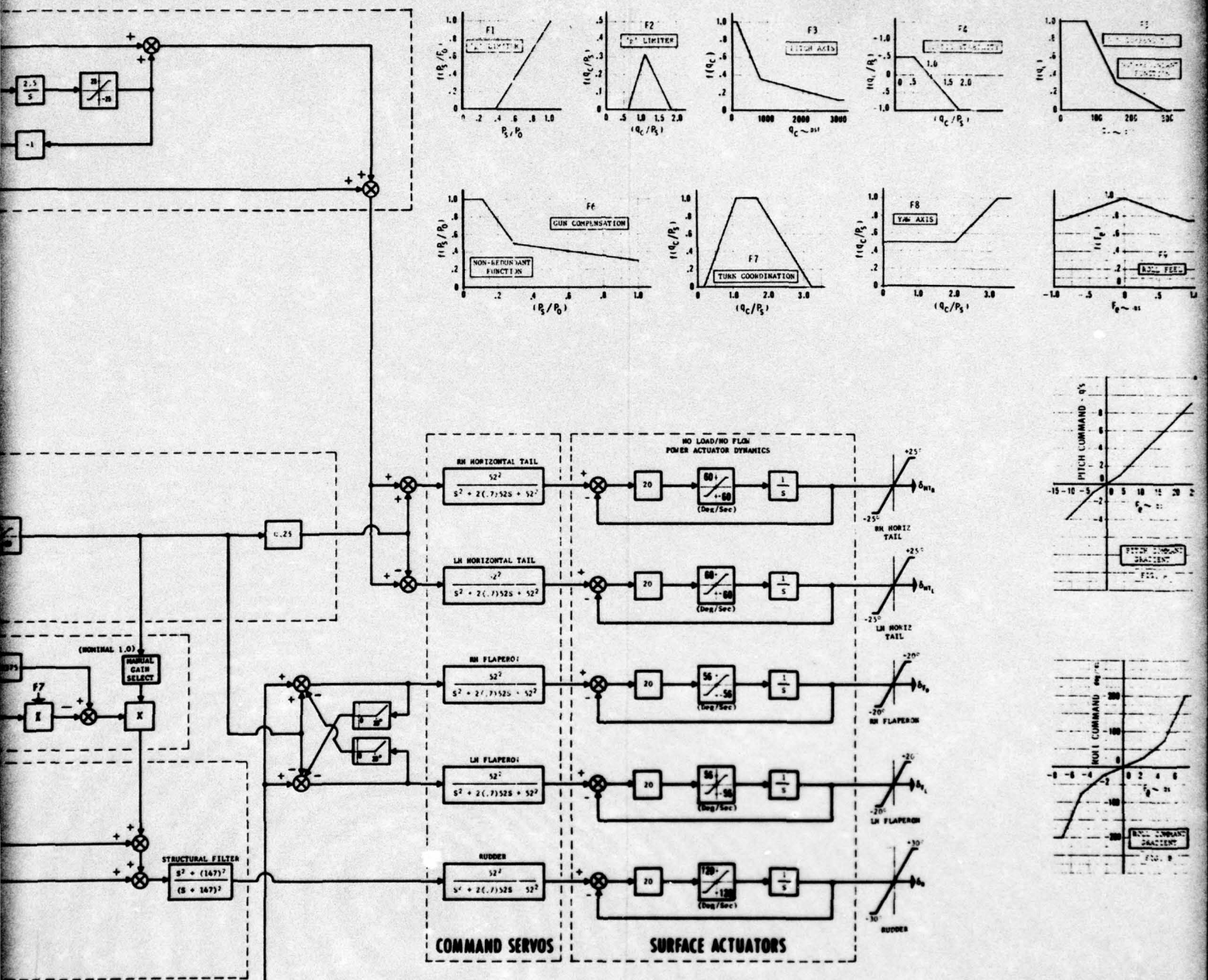

Figure 1-14. Autopilot Block Diagram

2

SECTION 2

LONGITUDINAL GUST RESPONSE

To evaluate the effects of flight conditions, gust amplitude, frequency, and shape, and various aircraft parameters on gust response, a detailed digital six-degree-of-freedom simulation was used. This simulation used nonlinear aerodynamic characteristics, inertial data, and a model of the control system described in Section 1. Prior to the application of the gust, the aircraft is trimmed to the specified flight conditions. For each simulation run, the following digital information is available:

a. Vehicle trim parameters.

b. Nonlinear aerodynamic input.

c. Linearized aerodynamic characteristics at the trim condition.

d. Gust time history plots.

The gust response for each configuration was analyzed at static margins from +4%$\bar{c}$ to -10% $\bar{c}$.

2.1 CRITICAL FLIGHT CONDITION

For use throughout this study it is desirable to select one flight condition for which the control power requirements are most critical and to examine the sensitivity of control power requirements to variations in aircraft parameters and input disturbance levels during this condition. It is anticipated that the most severe situations occur at low speeds where the gust velocity/airspeed ratio yields the largest incremental angle of attack changes as well as the largest change in dynamic pressure, resulting in greater ΔC_m. The control power requirements during gust response were investigated for:

a. High lift power approach.

b. Maximum sustained load factor.

c. Maximum instantaneous loud factor.

2.1.1 CONVENTIONAL CONFIGURATION. Because the conventional configuration showed different aerodynamic characteristics with external stores, and because the pitch inertia varied significantly between the minimum and maximum landing weights, four power approach conditions were examined:

a. With stores, minimum weight

b. With stores, maximum landing weight

c. Without stores, minimum weight

d. Without stores, maximum landing weight

Conditions representative of maximum sustained and instantaneous load factor were obtained from the performance capability curves for the aircraft. These indicated:

a. Maximum sustained load factor:
   7.5g at sea level, M = 0.64
   5.0g at 10,000 ft, M = 0.60

b. Maximum instantaneous load factor:
   7.5g at sea level, M = 0.48
   7.5g at 10,000 feet, M = 0.62

The disturbance function in each case was a (1-cos) type gust with an amplitude of 50 ft/sec at a frequency of 3.0 rad/sec. (The basic mode frequency of the aircraft at the power approach condition is also 3.0 rad/sec.)

The main results are presented in Figures 2-1 through 2-4. It is apparent that the control power requirements at power approach are most critical. It can further be said that for a given cg location the lightweight condition with stores is more critical than the maximum landing weight conditions or the lightweight condition without stores. (This is not to say that the design minimum landing weight condition is most critical because for the other design landing conditions the cg might be further aft such that more control power would be required. Since this study is to examine a range of cg, however, the most critical condition over the range of cg corresponding to $0.37\ \bar{c} < X_{cg} < 0.55\ \bar{c}$ is the lightweight condition with external stores. For this condition, the static margin (% $\bar{c}$) and ω_n^2 have been plotted versus cg location and are shown in Figure 2-5.

Using this configuration, a series of runs was made in which the frequency of the (1-cos) gust was varied from 1.5 to 7.5 rad/sec. It was found that the most severe case in terms of required control power occured at a gust frequency of 6.0 rad/sec. These results are shown in Figure 2-6.

The configuration for the conventional aircraft used for the remainder of the study was:

Flight Condition: Power Approach

Aircraft: Minimum Weight w/stores

Gust Frequency: 6.0 rad/sec

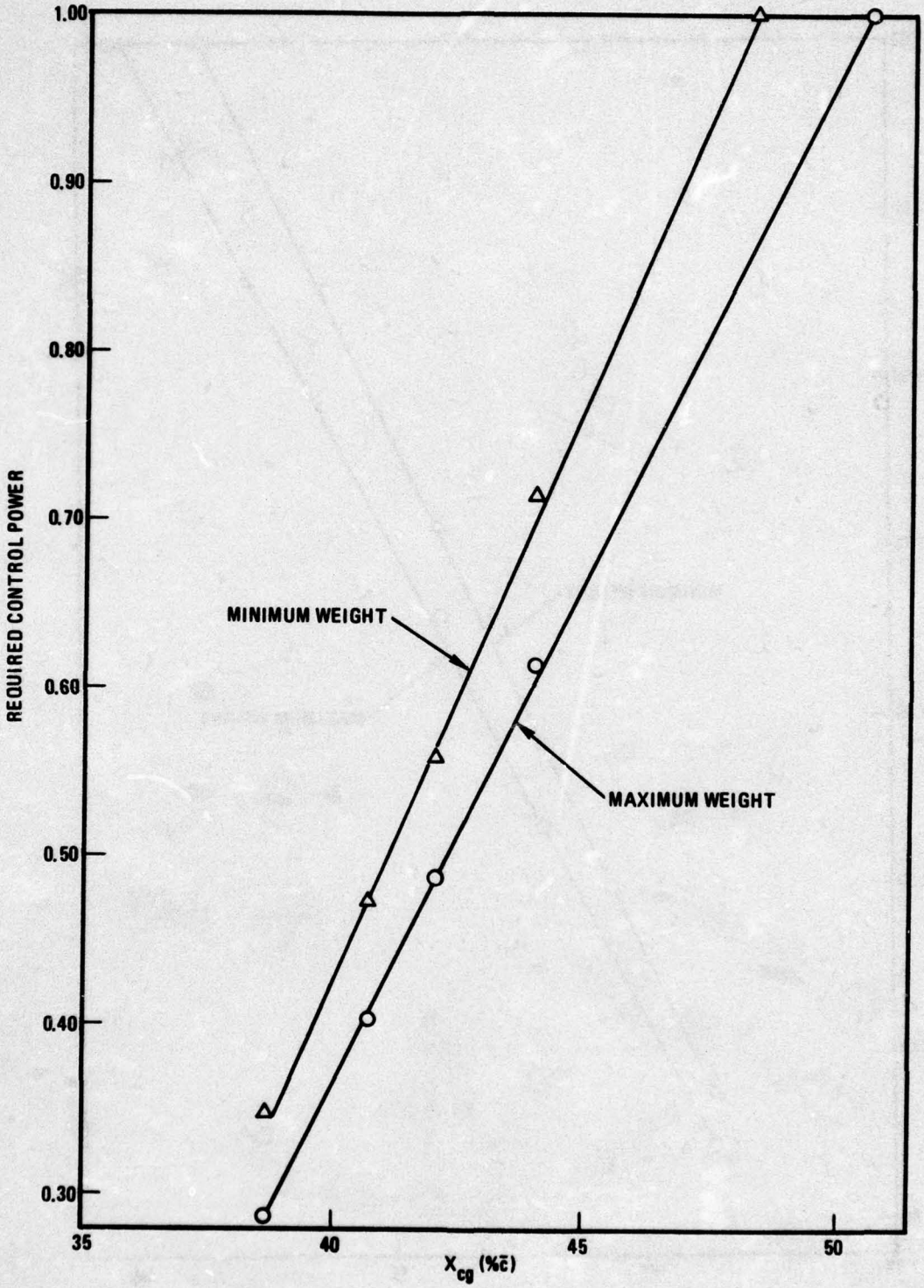

Figure 2-1. Conventional Configuration, Control Power Requirements, Power Approach Without Stores

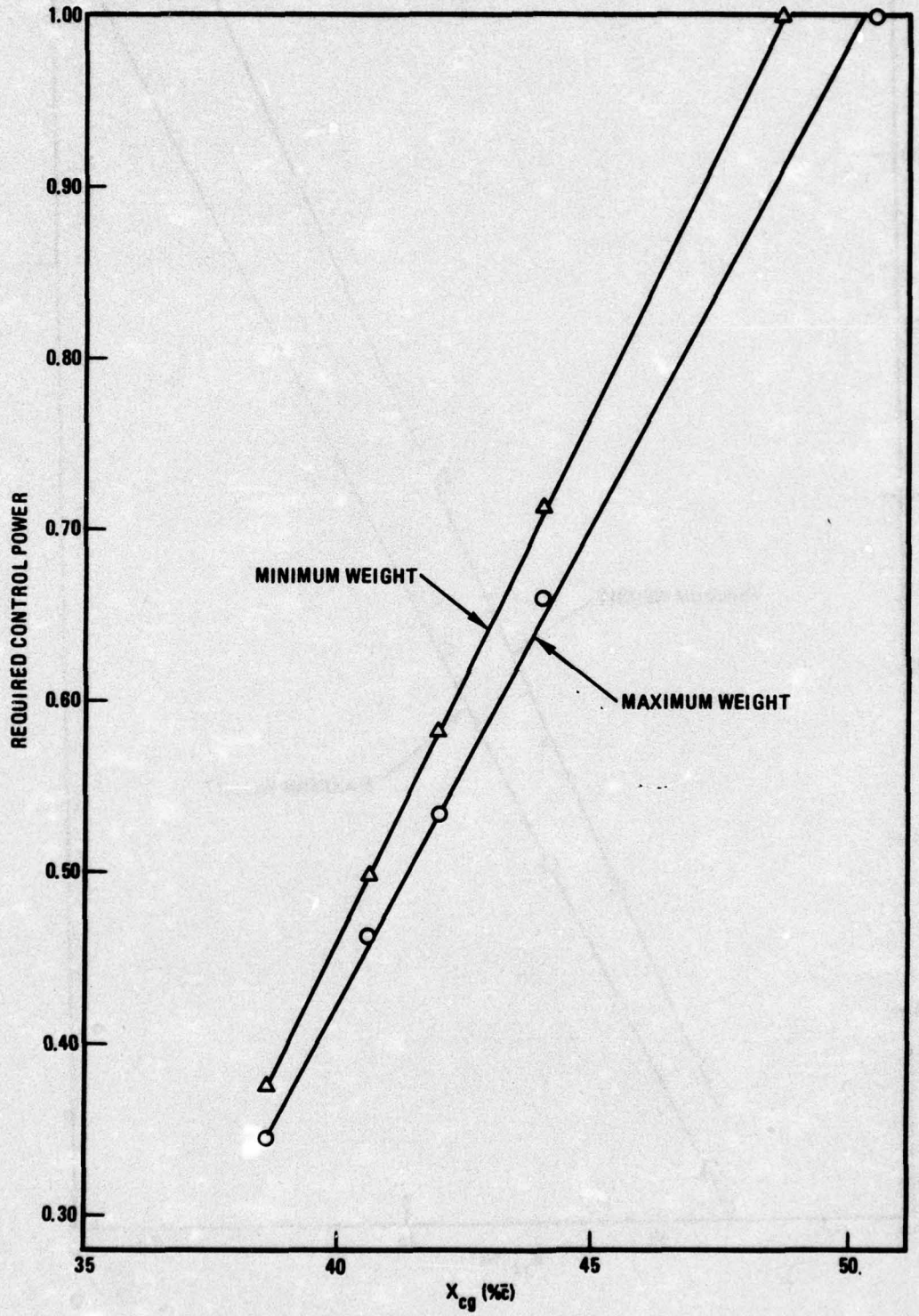

Figure 2-2. Conventional Configuration, Control Power Requirements, Power Approach With Stores

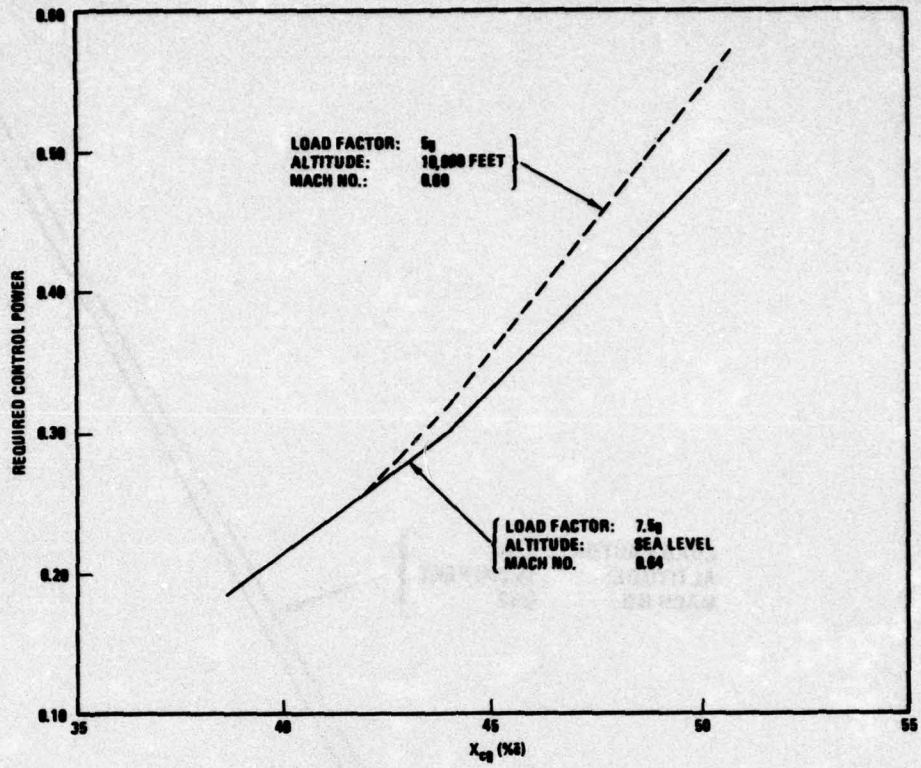

Figure 2-3. Conventional Configuration, Control Power Requirements, Maximum Sustained Load Factor

2.1.2 CANARD CONFIGURATION. The normal high-lift power approach configuration consists of the canard biased six degrees nose-up and the canard flap deflected to +16 degrees. The elevon is used to trim any unbalanced moment. Both the speed brake and the landing gear are in the extended position.

Two loading conditions were examined for the power approach configuration. The heavyweight condition is consistent with the Navy's 50-foot glide slope transfer requirement. The lightweight condition is a low-fuel, no-stores configuration. Various cg locations were examined between approximately +7 to -10% $\bar{c}$. A plot of static margin versus cg location is shown in Figure 2-7.

For all power approach cases, the aircraft was trimmed to 13.76 degrees body angle of attack, and the speed was varied to get the necessary lift for 1g flight. The elevon trimmed the moment due to a cg shift. For all cases, a (1-cos) gust was used with a magnitude of 50 ft/sec and a frequency of 2.0 rad/sec.

The results of the analysis for the power approach configuration are summarized in Figure 2-8. As for the conventional configuration, the lightweight condition is more critical for a given cg location.

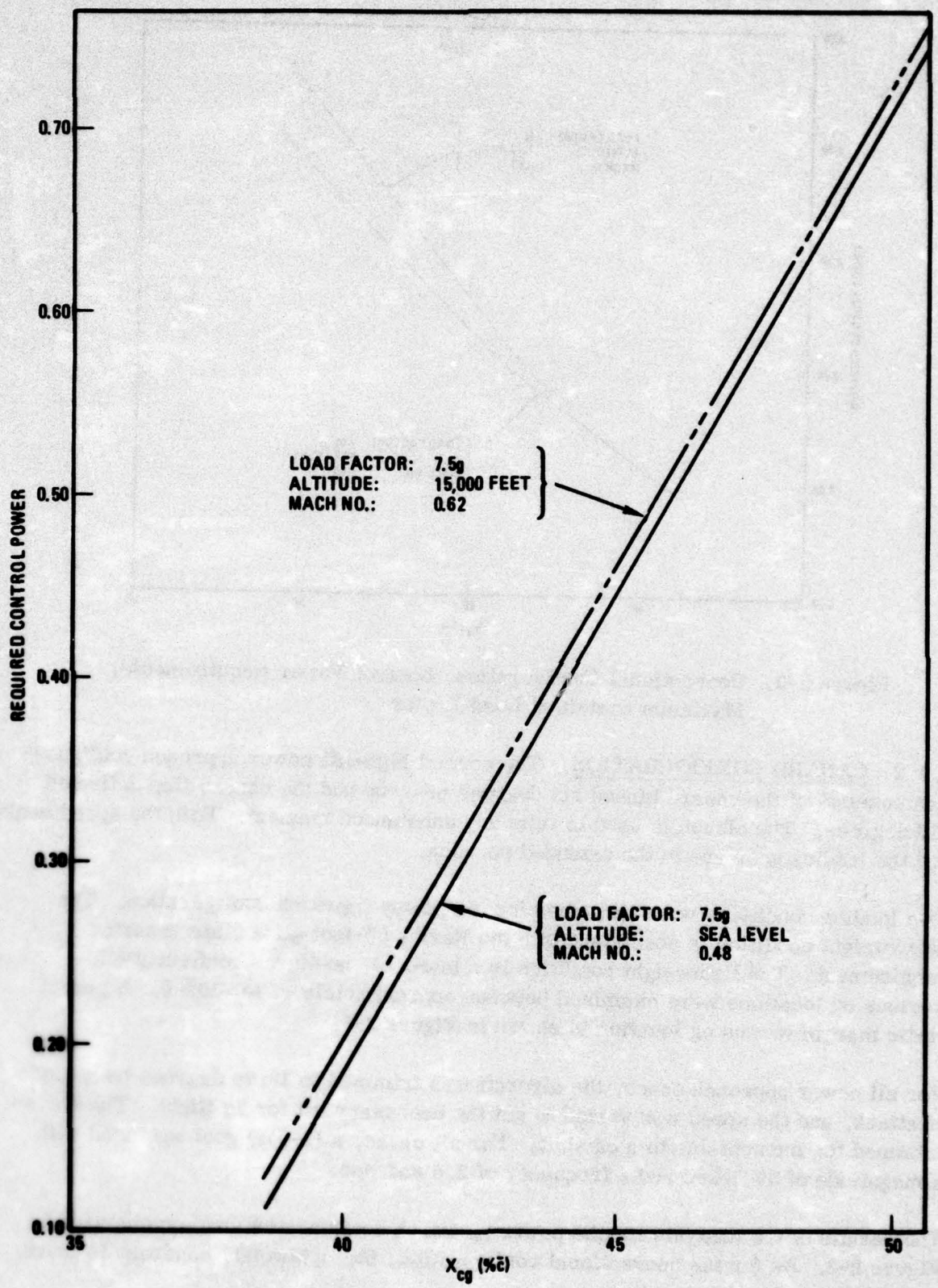

Figure 2-4. Conventional Configuration, Control Power Requirements, Maximum Instantaneous Load Factor

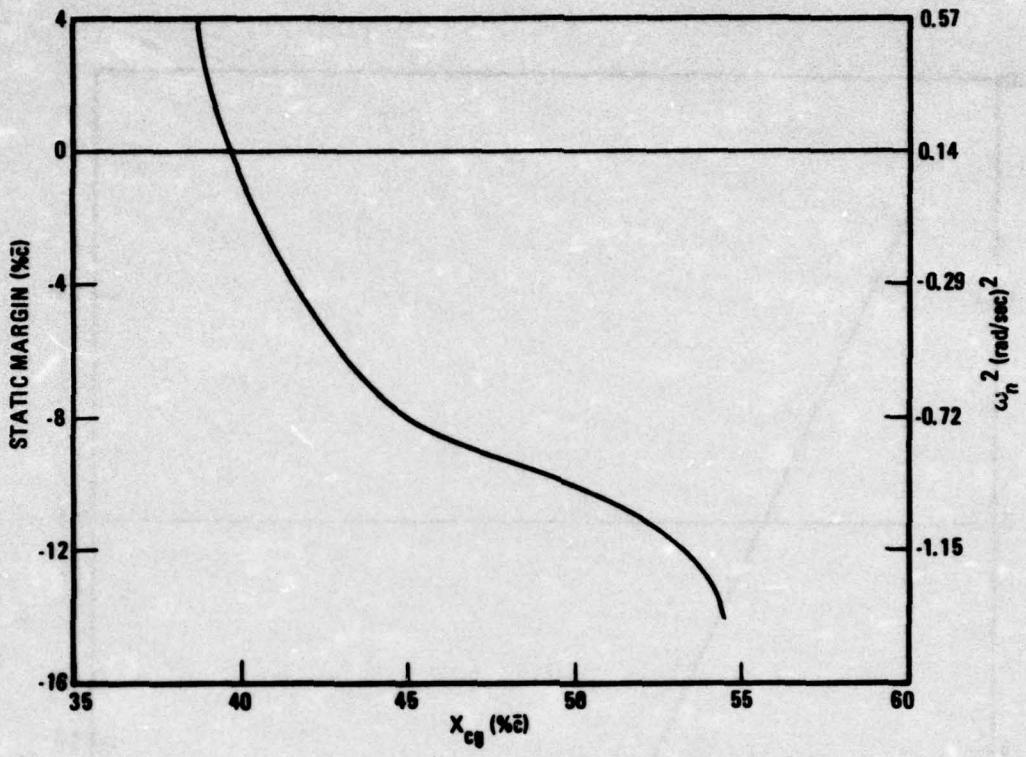

Figure 2-5. Conventional Configuration, Static Margin Versus cg Location, α_{TRIM} = 10 Degrees

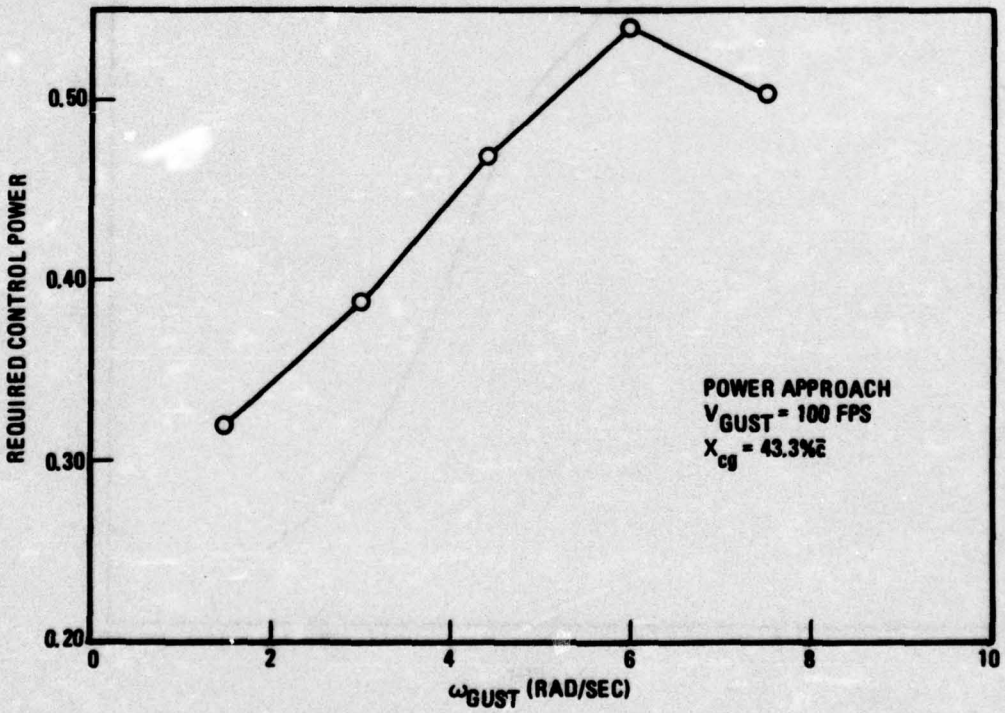

Figure 2-6. Conventional Configuration, Effect of Gust Frequency on Control Power Requirements

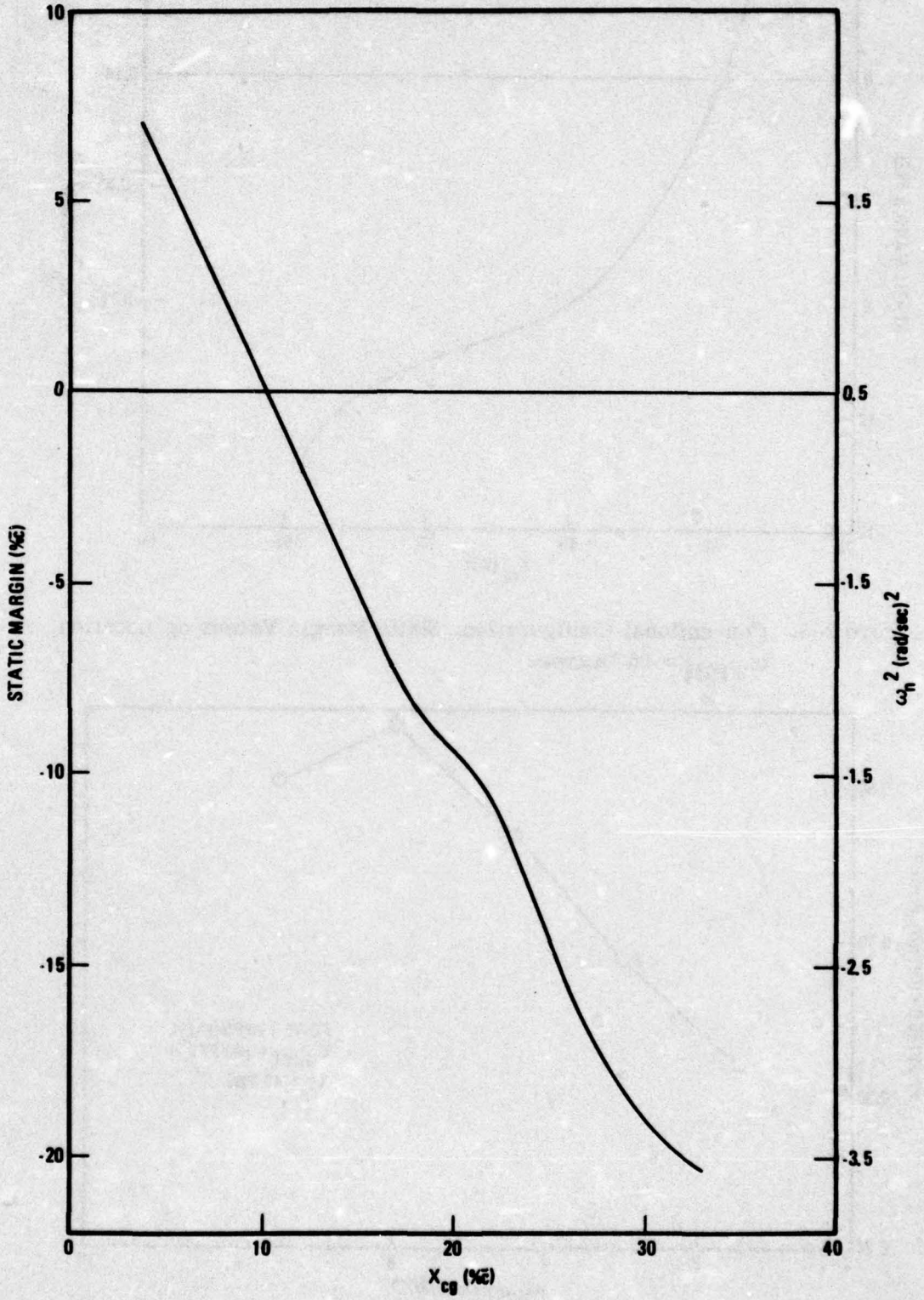

Figure 2-7. Canard Configuration, Static Margin Versus cg Location, Power Approach, α_{TRIM} = 13.76 Degrees

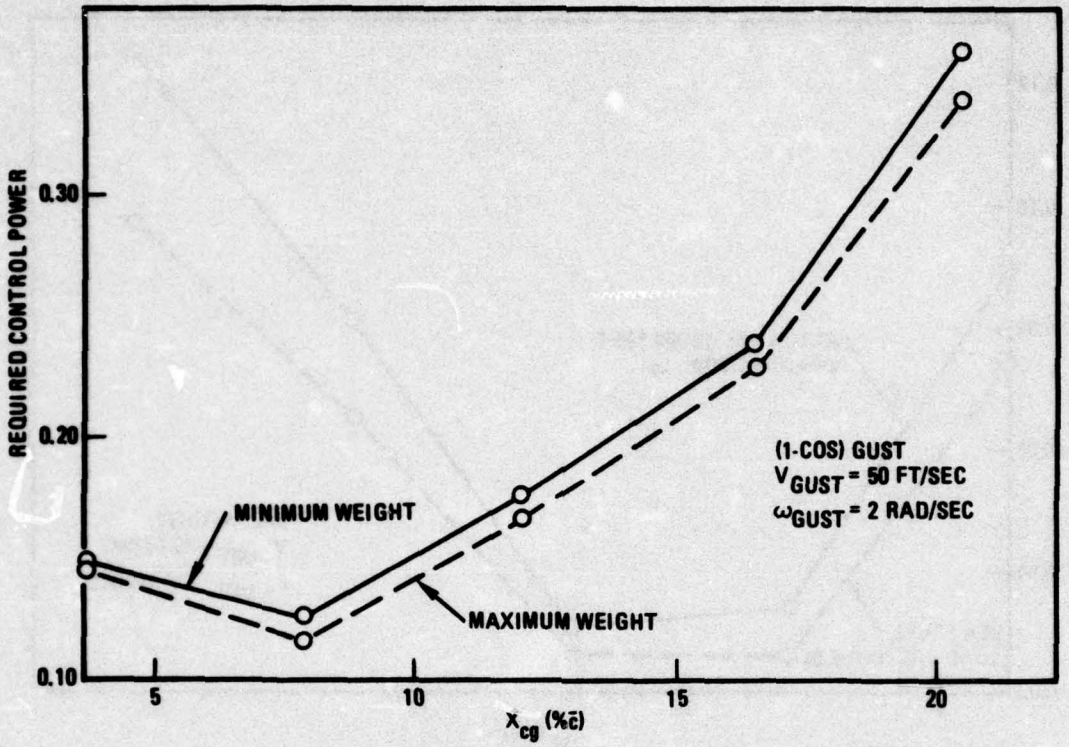

Figure 2-8. Canard Configuration, Control Power Requirements, Power Approach

The maximum sustained load factor for the canard configuration at sea level is 7.5g. This load factor is achieved at a velocity of 484 knots (M = 0.71) and at a weight of 24,188 pounds. The pitch moment of inertia was estimated to be 72,000 slug-ft^2. At an altitude of 10,000 feet, the maximum sustained load factor is 5.0g. The corresponding velocity is 421 knots (M = 0.64). The weight and inertia were the same as at sea level. Figure 2-9 shows the control power requirements versus cg location for both configurations. Again, a cg range from 3.7% to 20.5% $\bar{c}$ was examined.

It would appear from Figure 2-9 that the control power requirements are greater at altitude for the maximum sustained load factor. The differences in required control power could be due to differences in the relationship between the aircraft frequency/gust frequency at the two conditions. (For these conditions the gust frequency was not tuned to the aircraft.)

The maximum instantaneous load factor at both sea level and at 15,000 feet is 7.5g. At sea level, the corresponding velocity is 259 knots (M = 0.38) and at 15,000 feet, the velocity is 304 knots (M = 0.47). The weight used in both instances was 24,188 pounds and the pitch inertia was 72,000 slug-ft^2. Figure 2-10 shows the required control power versus cg location. Again, the control power requirements at altitude appear greater.

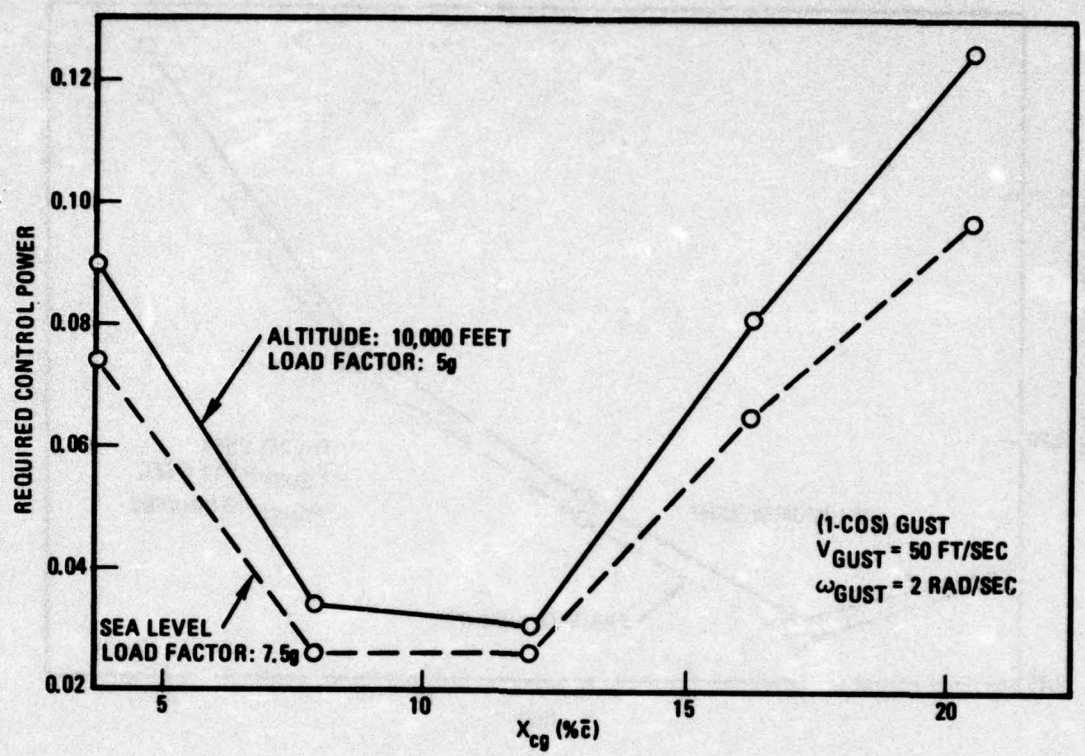

Figure 2-9. Canard Configuration, Control Power Requirements, Maximum Sustained Load Factor

From the data in Figure 2-10 it would appear that the control power requirements for the maximum instantaneous load factor case are more critical than for the power approach. The fact is, however, that for the forward cg locations, much of the control power requirements during the instantaneous g maneuver derives from the maneuver itself. (The figure shows total control power required including maneuver control.) The control power requirements for gust responses are of the same magnitude as for the sustained g maneuver - considerably less than for power approach. (The large normalized control power requirements for the instantaneous g maneuver are in the nose-up direction and the response to gust tends to unload the surfaces. Also, there is less total control power available in the nose-up direction for the canard configuration, which tends to amplify the normalized control power requirement in that direction.)

Figure 2-11 shows the control power required to trim during the power approach for the canard configuration. A representative computer-generated time history plot is shown in Figure 2-12. This represents the heavyweight configuration with the cg at 20.5% $\bar{c}$, corresponding to a static margin of -9.7% $\bar{c}$.

The effect of varying the gust frequency is shown in Figure 2-13. In terms of required control power, a gust frequency of 5 rad/sec is most critical. The basic mode

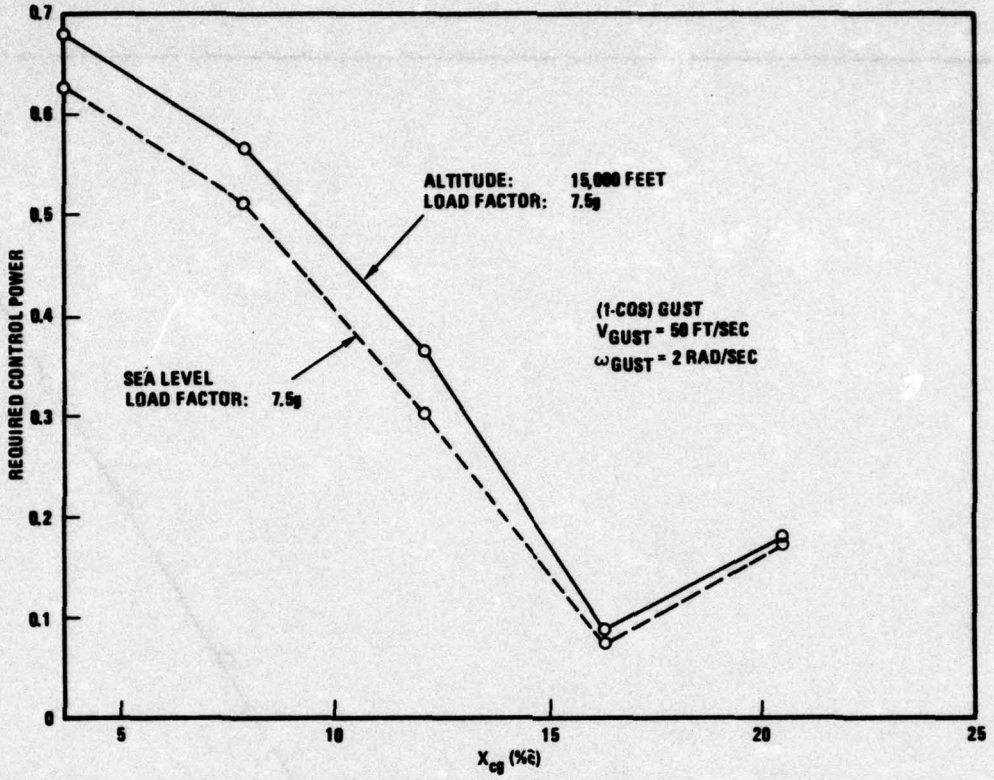

Figure 2-10. Canard Configuration, Control Power Requirements, Maximum Instantaneous Load Factor

frequency of the canard aircraft in the power approach configuration is 2.5 rad/sec. The maximum angle of attack increased with gust frequency to about 25 degrees at 5 rad/sec where it remained approximately constant as the frequency is increased further.

The canard configuration for the remainder of the study may now be summarized as follows:

Flight Condition:	Power Approach
Aircraft:	Minimum Weight (no stores)
Gust Frequency:	5 rad/sec

2.2 AIRCRAFT PARAMETER VARIATIONS

2.2.1 CONTROL SURFACE EFFECTIVENESS. Control surface effectiveness is a measure of the incremental change in C_m (or C_L) per (small) incremental change in the control surface deflection. To vary this parameter without incurring a variation in static margin, the relative distances between particular "constant" δ curves on the C_m - C_L plots were varied by "parallel displacement" to keep the C_m/C_L slopes

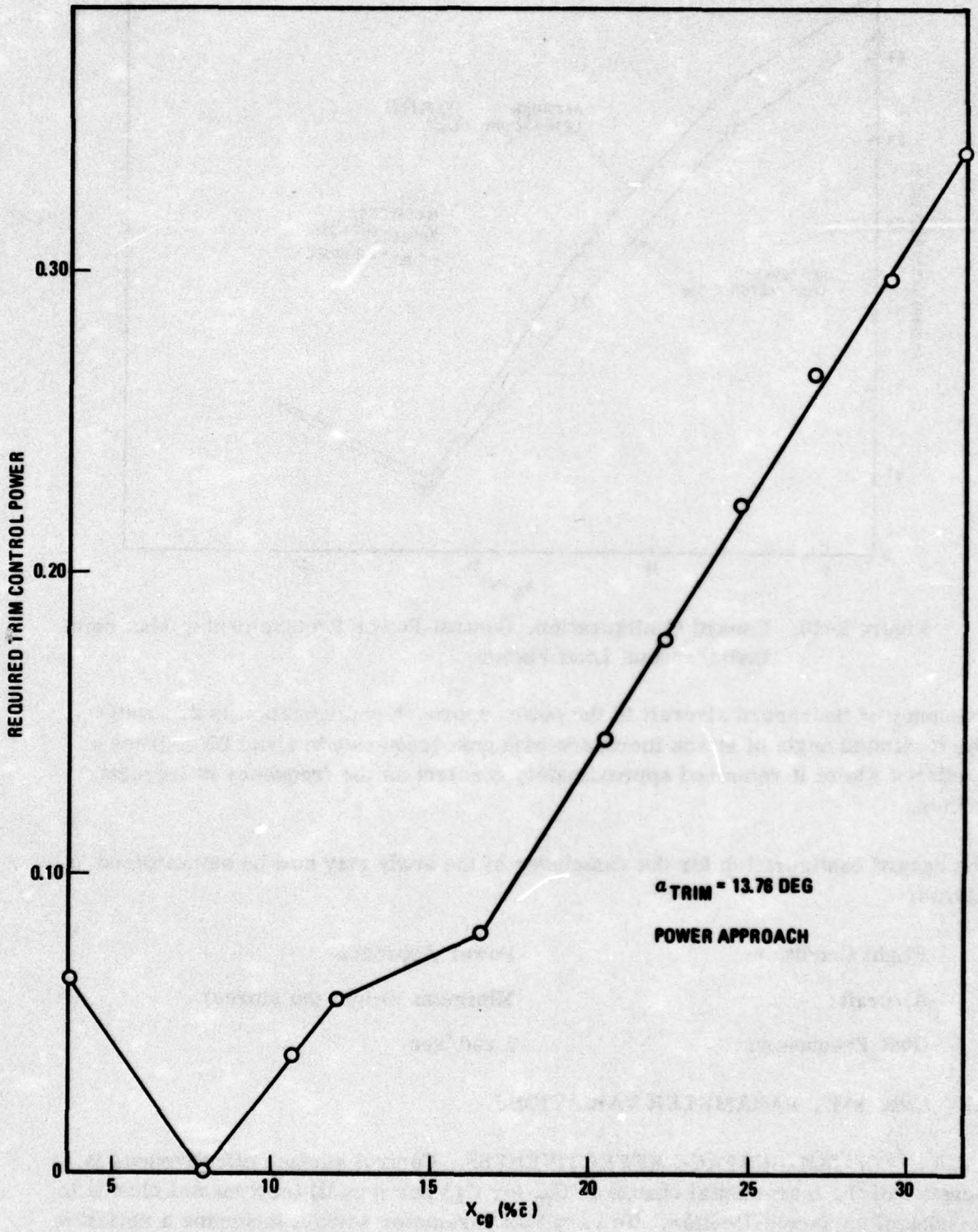

Figure 2-11. Canard Configuration, Control Power Required for Trim Versus cg Location

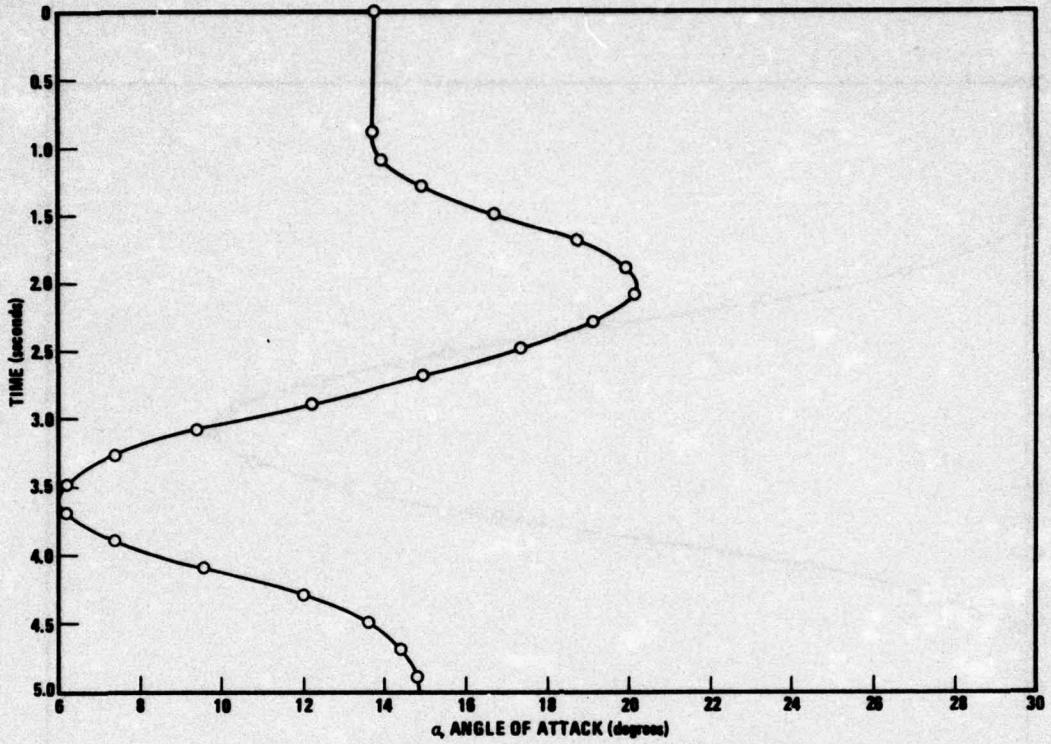

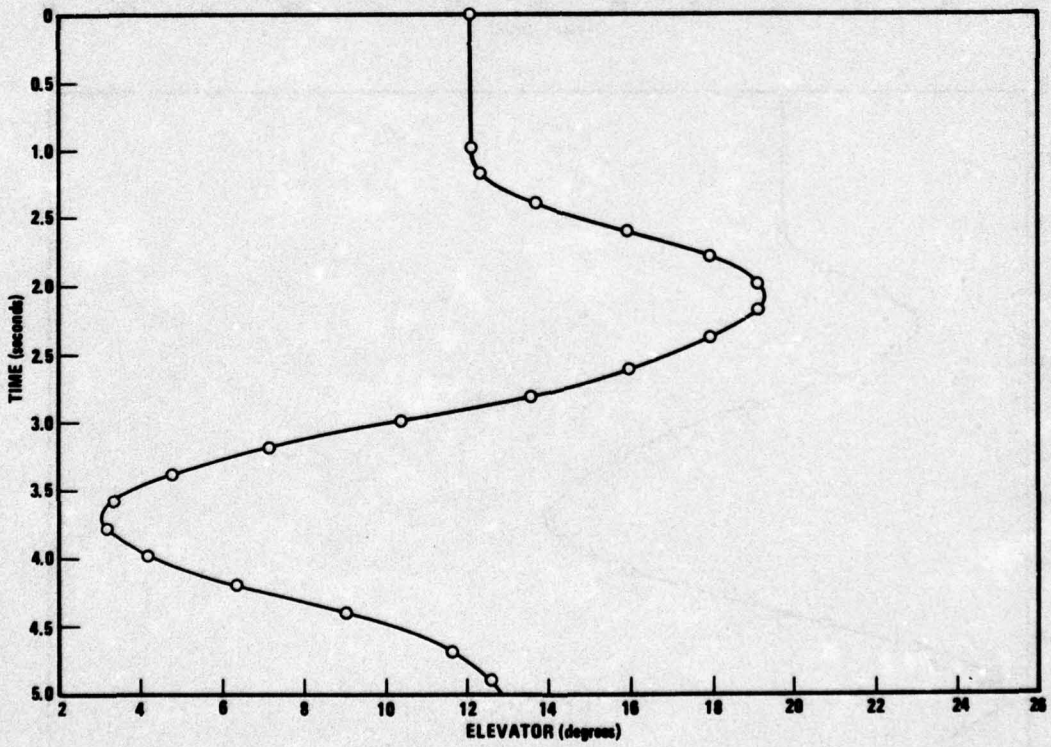

Figure 2-12. Canard Configuration, Computer-Generated Time History (Sheets 1 and 2 of 4)

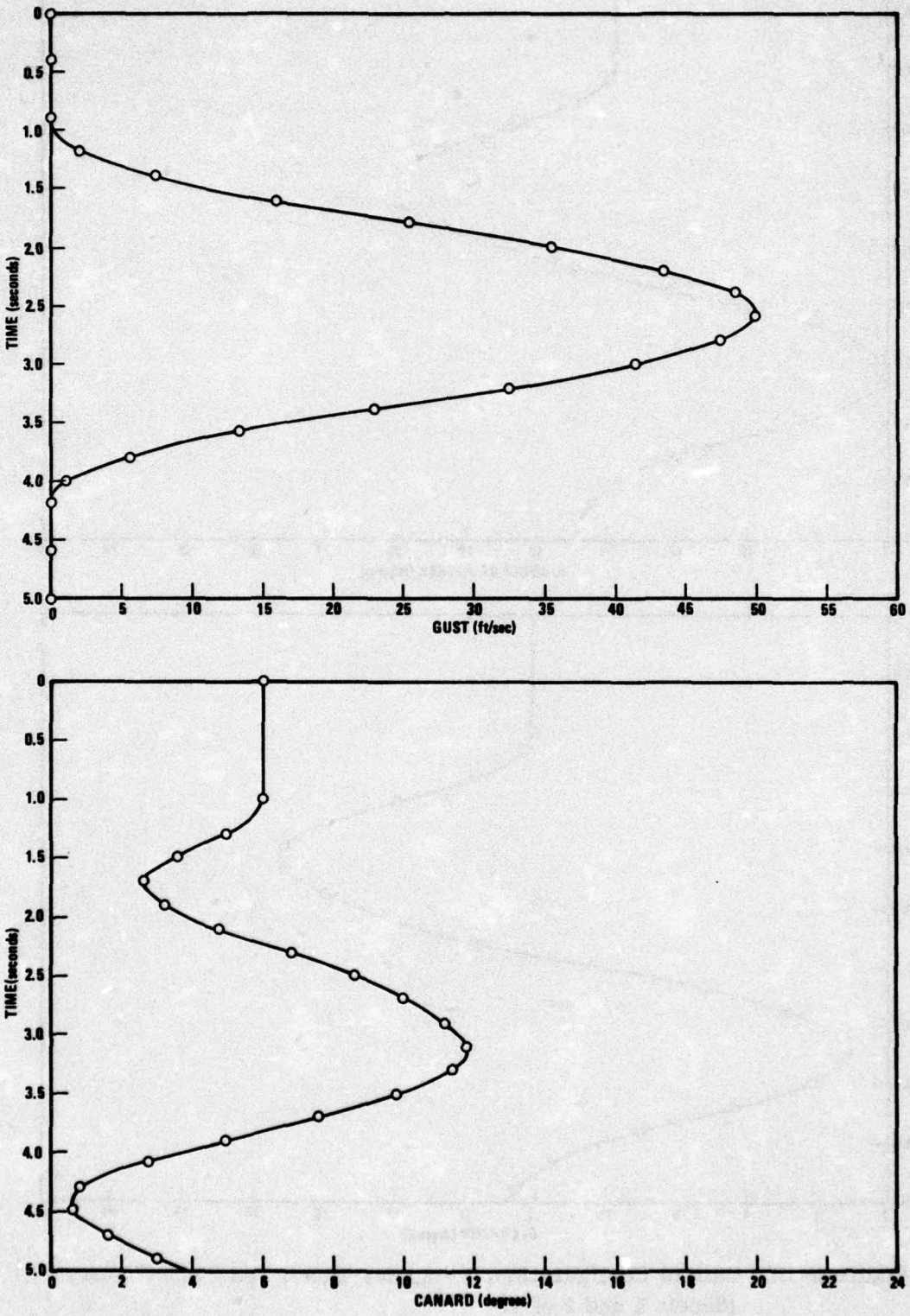

Figure 2-12. Canard Configuration, Computer-Generated Time History (Sheets 3 and 4 of 4)

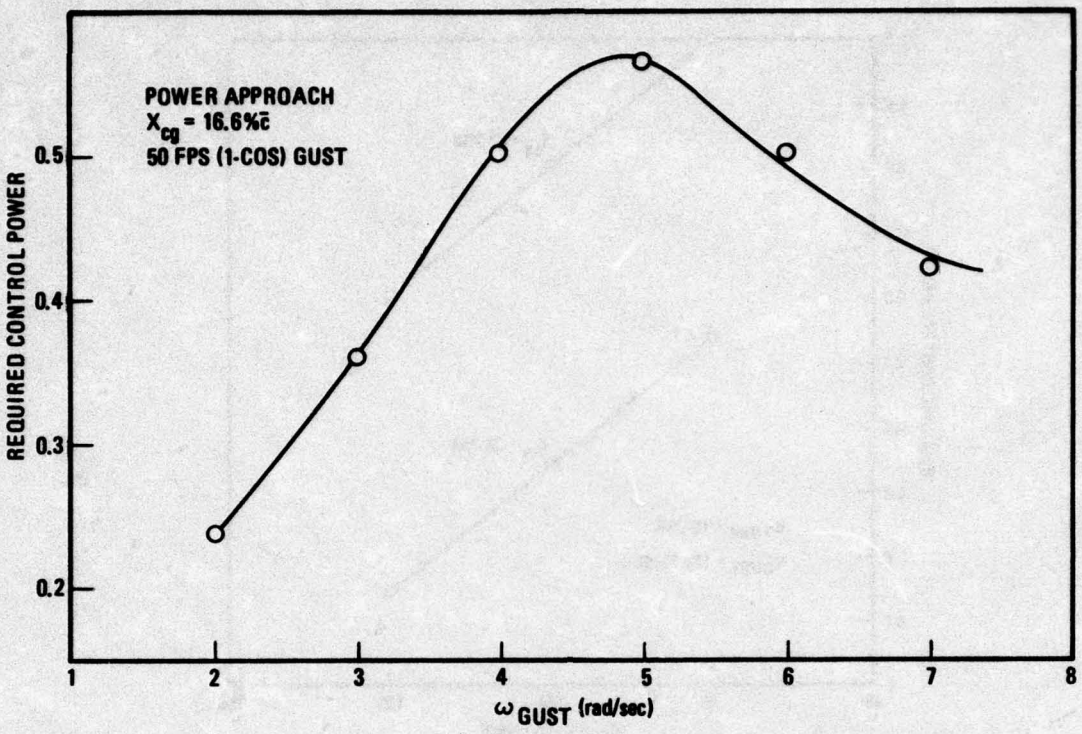

Figure 2-13. Canard Configuration, Effect of Gust Frequency on Control Power Requirements

(and hence the static margin) invariant. Some iteration was required to achieve a specified degree of variation.

Figures 2-14 and 2-15 summarize the changes in control power requirements versus control effectiveness for the conventional configuration and canard configuration respectively. These results are intuitively evident in the sense that as the control effectiveness is decreased, a corresponding increase in control deflection must occur if the vehicles are to respond to the same disturbance. What is not obvious is why the conventional configuration appears to be so much more sensitive to variations in control effectiveness or why the required control power varies linearly with control effectiveness.

The canard configuration appears less sensitive to variations in control effectiveness because the surfaces reach the rate limits for every case; whereas, in the conventional configuration this is not true. As a result, the response time histories vary much more for the canard configuration. (Another point that is not obvious is that for the canard configuration the more stable cg location required more normalized control power. This is because there is less control available in one direction than the other.)

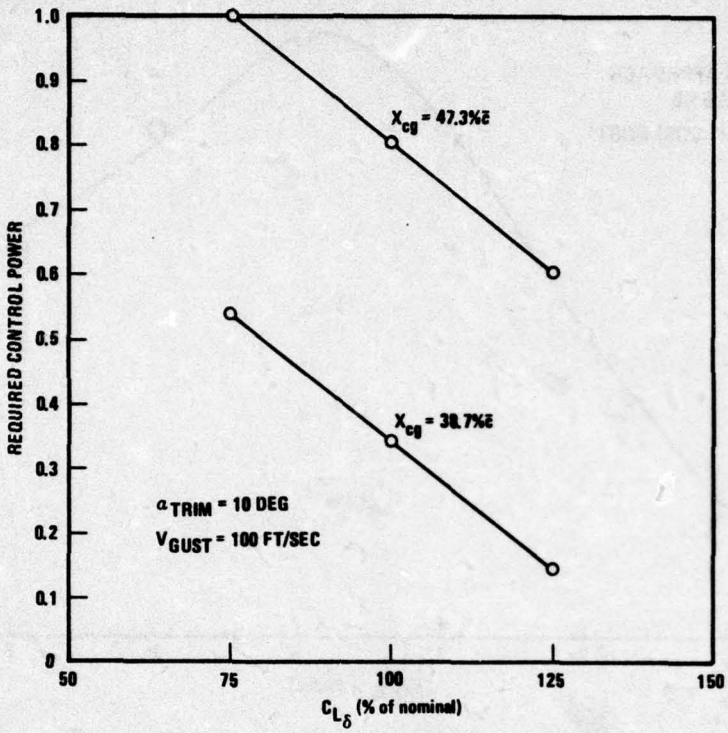

Figure 2-14. Canard Configuration, Required Control Power as a Function of Control Surface Effectiveness, α_{TRIM} = 10 Degrees

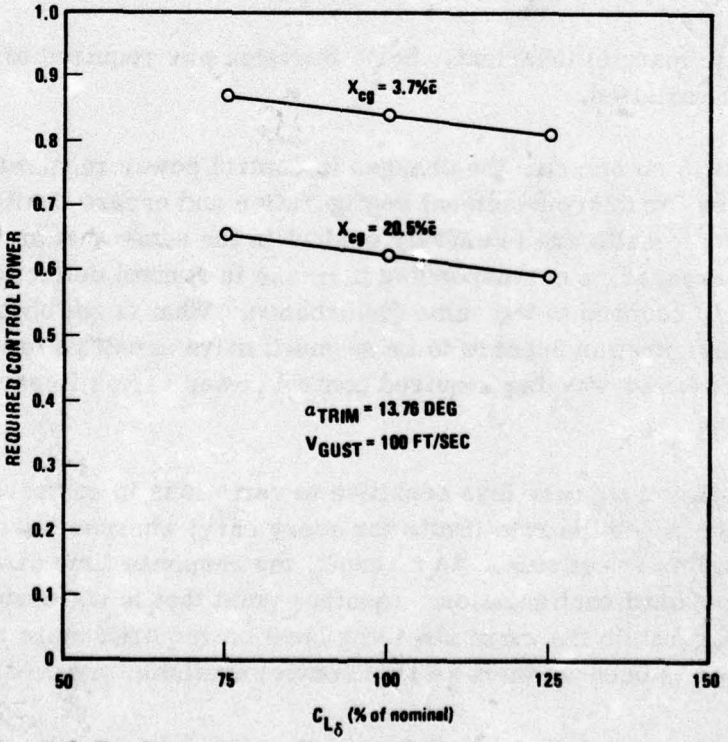

Figure 2-15. Canard Configuration, Required Control Power as a Function of Control Surface Effectiveness, α_{TRIM} = 13.76 Degrees

2.2.2 ZERO-LIFT PITCHING MOMENT. The sensitivity of required control power to variation in C_{m_o} for the conventional configuration is shown in Figure 2-16. Results for both a stable condition (X_{cg} = +38.7% $\bar{c}$) and an unstable condition (X_{cg} = 47.3% $\bar{c}$) are presented.

The fact that the total required (normalized) pitch control power exhibits contrasting trends as a function of

$$\Delta C_{m_o}/C_{m_o}$$

for the stable and unstable configurations is attributed to the fact that pitch control power is derived from a positive maximum value of control surface deflection for the statically unstable configuration and vice versa for the stable one.

Figure 2-17 shows the effects of variations in C_{m_o} on the required control power for the canard configuration. Again both a stable configuration (X_{cg} = +3.7% $\bar{c}$) and an unstable configuration (X_{cg} = 20.5% $\bar{c}$) were examined, corresponding to static margins of +7% $\bar{c}$ and -9.7% $\bar{c}$ respectively.

For the stable configuration, which requires nose-up control for trim, increasing the nose-up pitching moment results in a decrease in trim control power. For the unstable configuration, which requires nose-down trim, an increase in nose-up pitching moment requires an increase in trim control power (i.e., an increase in nose-down control).

The total control power requirements for gust response indicate that for the stable configuration, the required control power increases with an increase in nose-up pitching moment, and for the unstable cg location, the required control power increases with any change in C_{m_o} either positive or negative. For the stable configuration, the peak requirements are in the nose-up direction. For the unstable configuration, the peak requirements are in the nose-up direction for negative changes in C_{m_o} and in the nose-down direction for positive ΔC_{m_o}.

2.2.3 MAXIMUM USABLE C_L VERSUS CG. The maximum usable lift coefficient as used here corresponds to the maximum time angle of attack based on the gust upset boundary.

A gust boundary is that steady-state angle of attack beyond which a gust of specified amplitude causes a loss of control. Normally this boundary is obtained by incrementally increasing the steady-state angle of attack and observing that value at which loss of control occurs for the specified gust. As an arbitrary cutoff point, it was here assumed that if the aircraft recovered from the gust when the trim (steady-state) angle of attack was 30 degrees, this was taken to be the boundary point for purposes of establishing the maximum usable C_L.

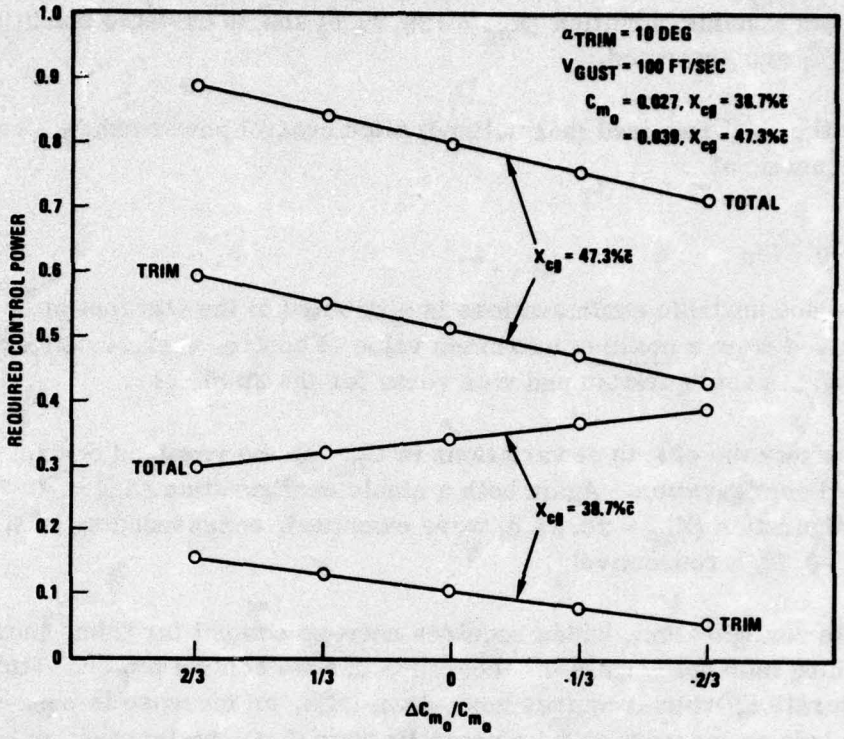

Figure 2-16. Conventional Configuration, Control Power Sensitivity to Variation in C_{m_o}

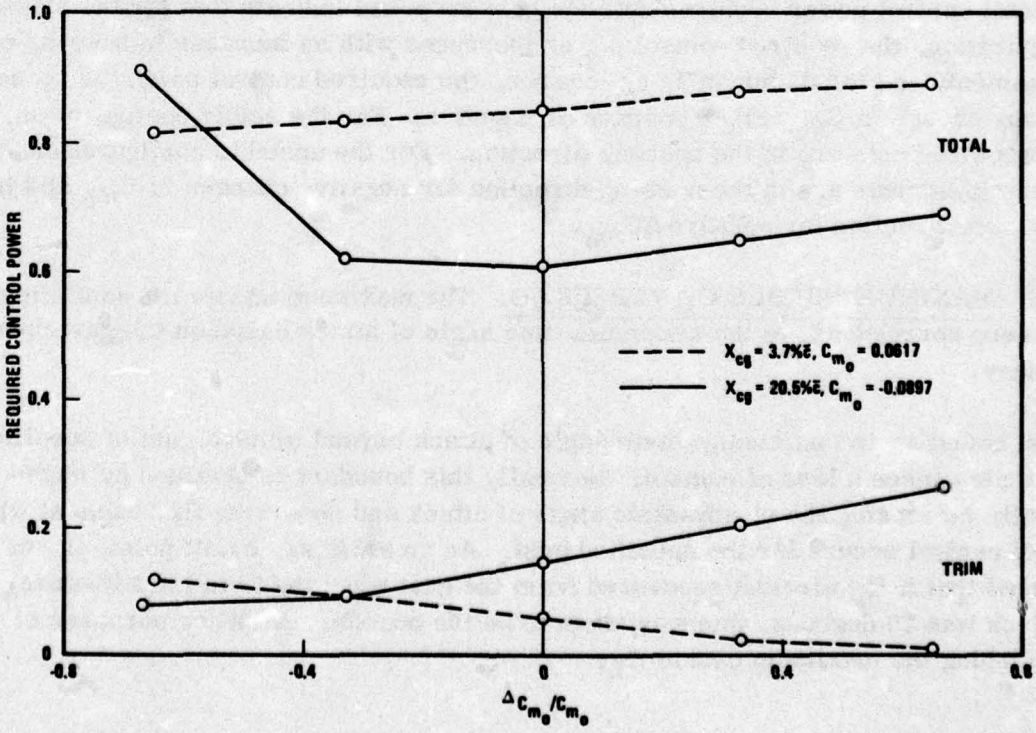

Figure 2-17. Canard Configuration, Control Power Sensitivity to Variation in C_{m_o}

While there is some flexibility in the choice of a specific value of cutoff point (why not 25 or 35 instead of 30 degrees?), there is a lesser inclination to dispute the need for establishing such a cutoff point. For any aircraft, there is usually some value of trim angle of attack beyond which it is highly imprudent to operate because of visibility, over-rotation, or similar considerations. The value used here, is, in the absence of relevant mission data, somewhat arbitrary.

For the conventional configuration it was found that at an initial angle of attack of 30 degrees, a 100 fps (1-cos) gust could not upset the aircraft. This indicated a stable break in the C_m/C_L curves at high angles of attack.

Attempts to reach an unstable configuration at α_{TRIM} = 30 degrees resulted in saturating the control surfaces trying to trim the aircraft. To circumvent the difficulties in dealing with saturated control situations, it was decided to examine the control power requirement versus cg location and gust intensity using a nominal power approach condition. Figure 2-18 shows the results of this investigation. It is interesting to note that doubling the gust intensity imposes rather minimal increases in the control power requirements. (This implies either the error signals in the flight control system are being limited or the surfaces are rate limited.) The effect of the trim control power requirements at the aft cg locations is evident.

Figure 2-19 shows the gust impact boundaries for the canard configuration for various magnitude (1-cos) type gusts. As can be seen, the angle of attack limit establishes the usable C_L for static margins as unstable as -14% $\bar{c}$. Thus for the conventional configuration, the maximum usable C_L is defined by the α_{TRIM} limit at a static margin of approximately -10% $\bar{c}$. For static margins less than -14% $\bar{c}$, the gust magnitude dictates the usable C_L.

2.3 EFFECTS OF CONTROL SYSTEM ON GUST RESPONSE

2.3.1 CONTROL SURFACE RATE LIMITS. Figures 2-20 and 2-21 show the sensitivity of control power requirements to reductions in surface rate limits for the conventional and canard configurations respectively. Very early in this study it became apparent that the conventional configuration seldom used more than 50% of its surface rate capability during gust response. This is clearly evident in Figure 2-20, which shows that the required control power is essentially unchanged for reductions in rate limits up to 70%.

Because the canard configuration has multiple control surfaces for pitch control, it was necessary to maintain a constant ratio of elevon rate limit to canard rate limit. A range of surface rate limits from 50% to 200% nominal was investigated. The nominal or design surface rate limits are 75 deg/sec for the elevon and 25 deg/sec for the canard.

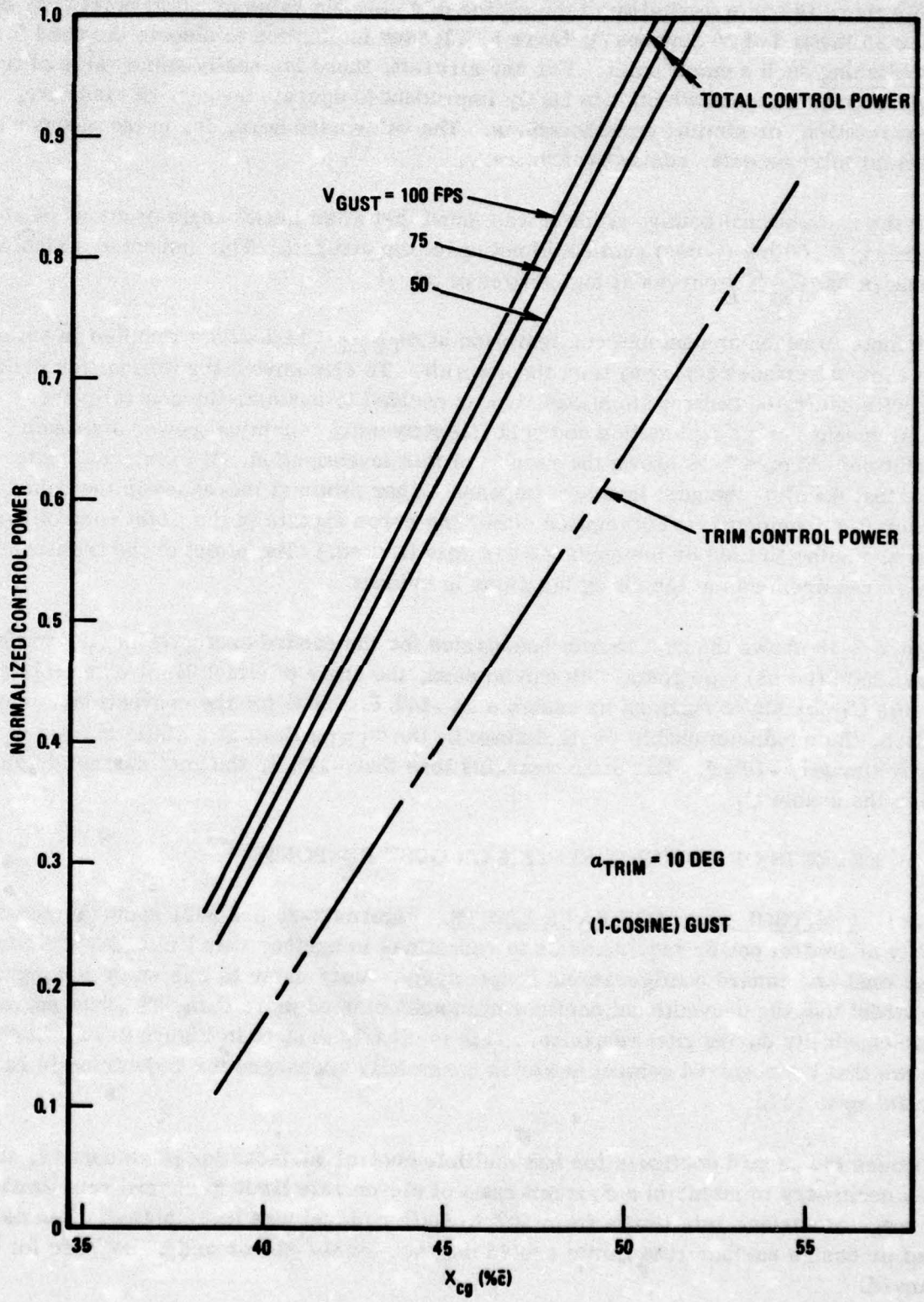

Figure 2-18. Conventional Configuration, Control Power Required Versus cg Location

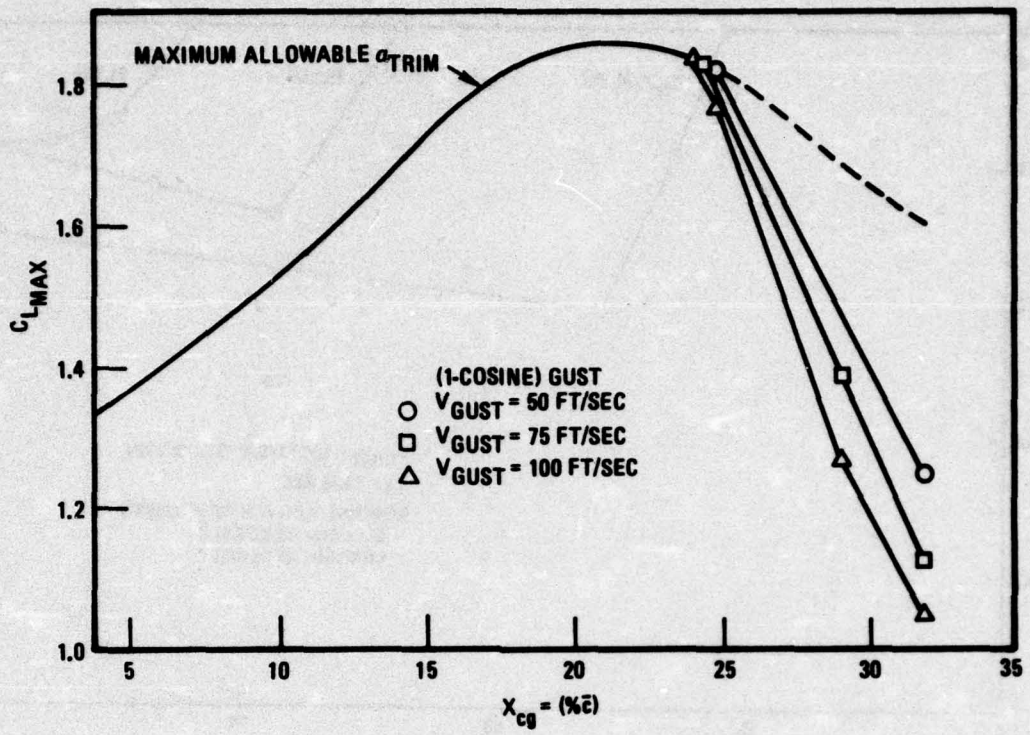

Figure 2-19. Canard Configuration, Maximum Usable C_L

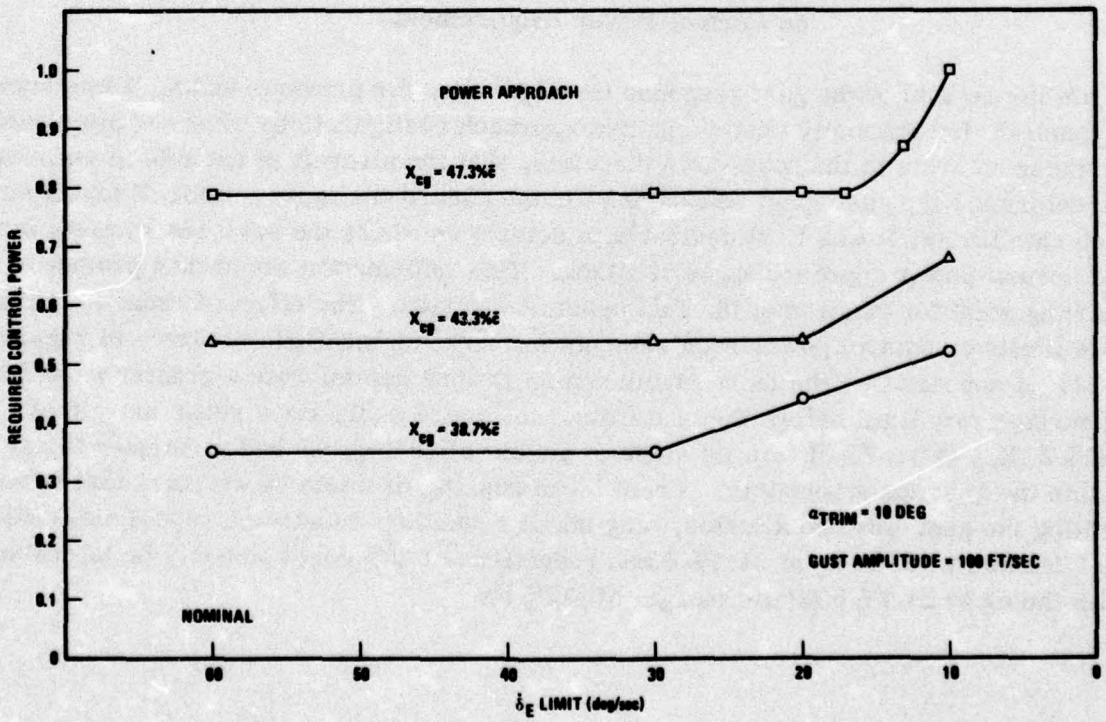

Figure 2-20. Conventional Configuration, Variation in Control Surface Rate Limit

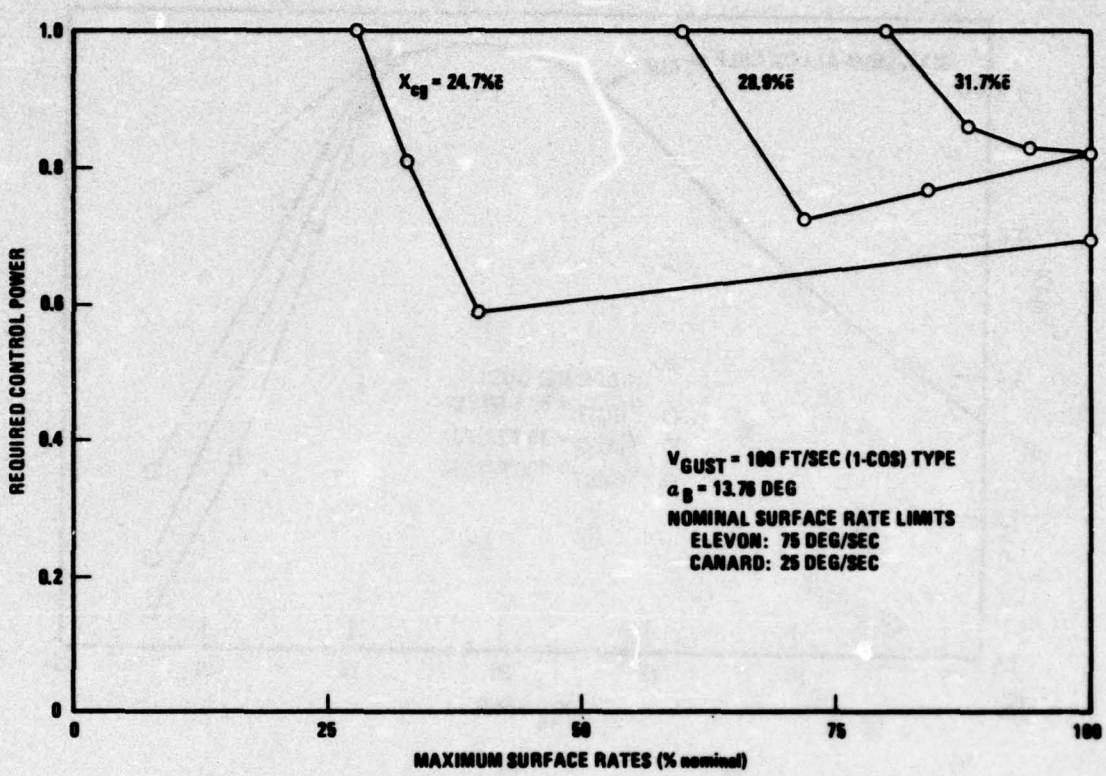

Figure 2-21. Canard Configuration, Effect of Surface Rate Limits on Control Power Requirements

From the results of the gust response time histories for previous tasks, it was known, in general, for statically unstable power approach configurations when the pitch control surfaces saturate in the nose-down direction, that the aircraft is not able to recover. To determine the gust upset boundaries for the canard configuration for different surface rate limits, it was first desirable to determine where the surfaces saturate for the normal power approach angle of attack. This information would then provide a starting point for generating the gust upset boundaries. The effect of reduced surface rate limits on control power requirements for three cg locations is shown in Figure 2-21. It appears that the more stable configurations can tolerate a greater reduction in surface rate limit before they saturate. In Figure 2-21, for a static margin of -20% $\bar{c}$ (X_{cg} at 31.7% $\bar{c}$), a trim angle of attack of 10 degrees had to be used to get within the gust upset boundary. From these results, it would be expected that in generating the gust upset boundaries, only small reductions in surface rate limits could be tolerated with the cg at 31.7% $\bar{c}$ and reductions of 50% could possibly be tolerated with the cg at 24.7% $\bar{c}$ (static margin of -14% $\bar{c}$).

Figure 2-22 shows the gust upset boundaries for nominal surface rate limits, and for 50%, 75%, and 200% nominal limits. Recovery from a 100 ft/sec (1-cos) type gust was possible for a 50% reduction in rate limits with the cg at 24.7% $\bar{c}$, but not with a more aft cg. With a 25% reduction in surface rate limits, recovery was clearly possible with the cg as far aft as 28.9% $\bar{c}$. It was not clear that a recovery was possible at a cg at 31.7% $\bar{c}$ (hence, the broken line). Doubling the surface rate limits increased the maximum usable C_L slightly. The most significant result here is that the control surface rate limits appear to be more critical in defining an aft limit on the cg than in defining an upper limit on C_L.

The investigation of the effect of variations in control surface rate limits for the two configurations has yielded some puzzling results. To begin with, one must conclude from the plot in Figure 2-21 that a decrease in the control rate limits is, in some instances, less demanding on control power. This apparent anomaly can be explained as follows. When the elevon is position saturated, and the canard is rate saturated in a nose-down control effort, the maximum excursion of the canard is indeed controlled by how fast that maximum can be reached. In other words, when a recovery situation prevails, the decreased rate limit on the control surface may actually limit the maximum deflection of the canard whenever the disturbance (gust) induces a maximum flow rate.

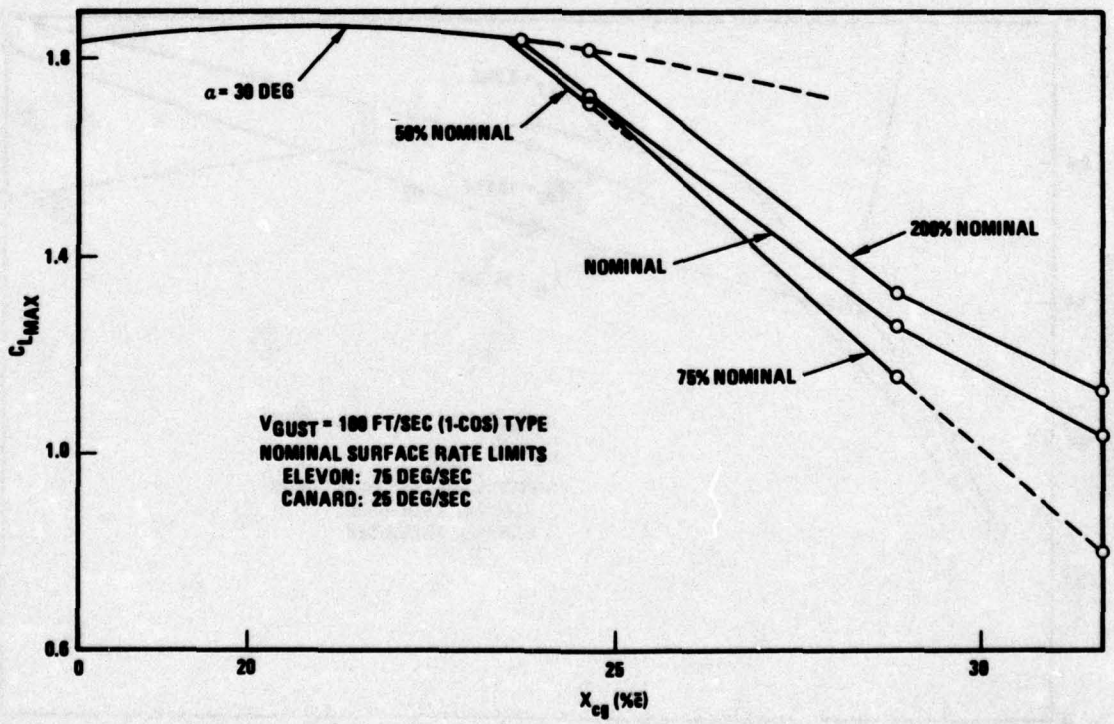

Figure 2-22. Canard Configuration, Sensitivity of Gust Upset Boundary to Variation in Surface Rate Limits

The other seemingly anomalous result is that for configurations with increasingly unstable configurations, the conventional configuration is less demanding on control power as rate limits are decreased, while the reverse is true for the canard configuration.

For the plots shown in Figure 2-21, the control surface rate limit was always at the maximum. To study control power requirements that are presumably less demanding on control surface rate (for the same gust disturbance), a stable (X_{cg} = 3.7% $\bar{c}$) and two unstable (X_{cg} = 16.6% $\bar{c}$ and 24.7% $\bar{c}$) configurations were selected, with the surface rate limits increased to 200% nominal. The results are shown in Figure 2-23. For the unstable configurations, a rate saturation occurred even with the rate limits raised to 200% of nominal.

2.3.2 CONTROL SURFACE GEARING. An investigation of the effect of variations in control surface gearing is limited to the canard configuration since the conventional configuration does not incorporate multiple control surfaces in pitch. The canard configuration incorporates a canard, canard flap, and an elevon for longitudinal control. Again, because it was desirable to look at both a stable configuration and an unstable configuration, the nominal power approach angle of attack was used, and changes in control power requirements were investigated.

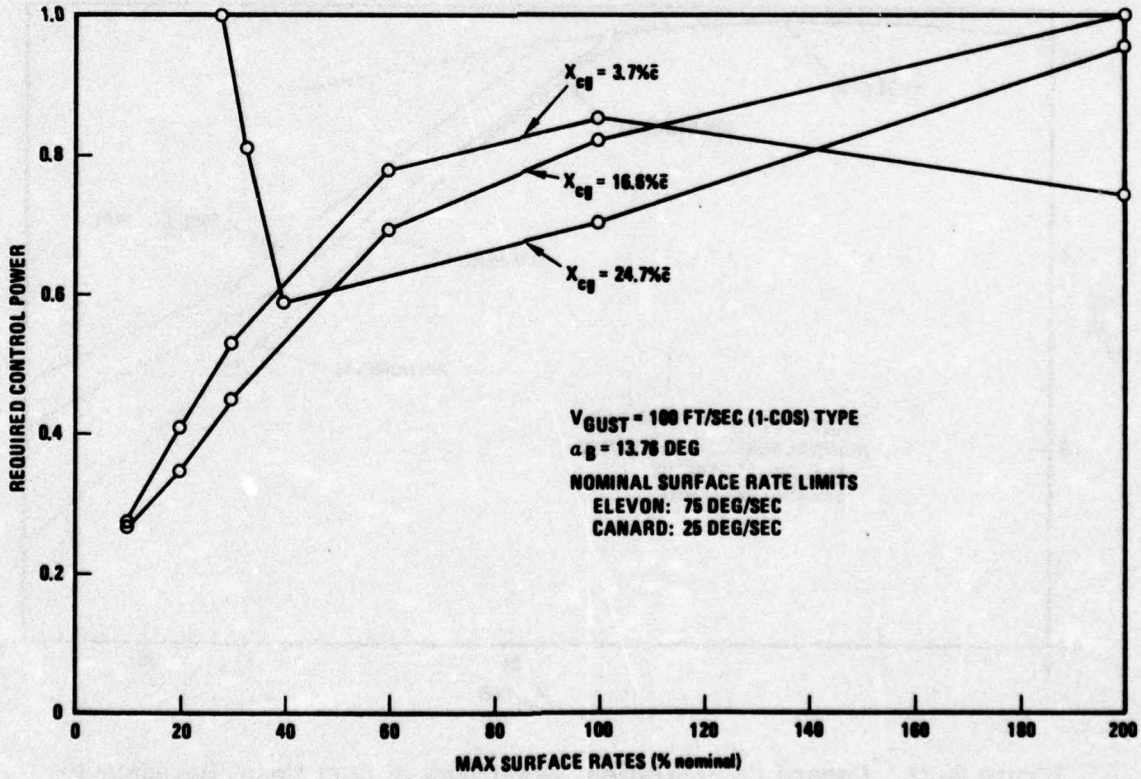

Figure 2-23. Canard Configuration, Effect of Surface Rate Limits on Control Power Requirements

The baseline canard configuration incorporates a flap on the canard with antiservo gearing. For this analysis, the effects of varying the gearing ratio from 0 to 2 were examined. The baseline gearing ratio is 1. A ratio of 0 would, in effect, be a canard with no flap and a ratio of 2 would be a flap that deflects two degrees for each degree of canard deflection. In actuality, a ratio of 2 would probably result in a complete loss of flap effectiveness at large canard deflection, but these effects were not included in this analysis.

Figure 2-24 shows the effect of varying this gearing ratio on the required control power. The canard/canard flap gearing ratio has little effect on the control power requirements. This result was predictable because of the area differences between the canard flap and the other pitch control surfaces.

Another reason for using the normal power approach angle of attack for this portion of the analysis is that the aerodynamic data is fairly linear and well defined in this region, and changes in canard/elevon "gearing" can be approximated by simply changing the relative effectiveness of the surfaces. (It should be remembered, however, that changing the control surface effectiveness also causes a shift in static margin.) A plot of static margin versus canard/elevon effectiveness ratio is shown in Figure 2-25. The static margin changes primarily with canard effectiveness and very little with elevon effectiveness.

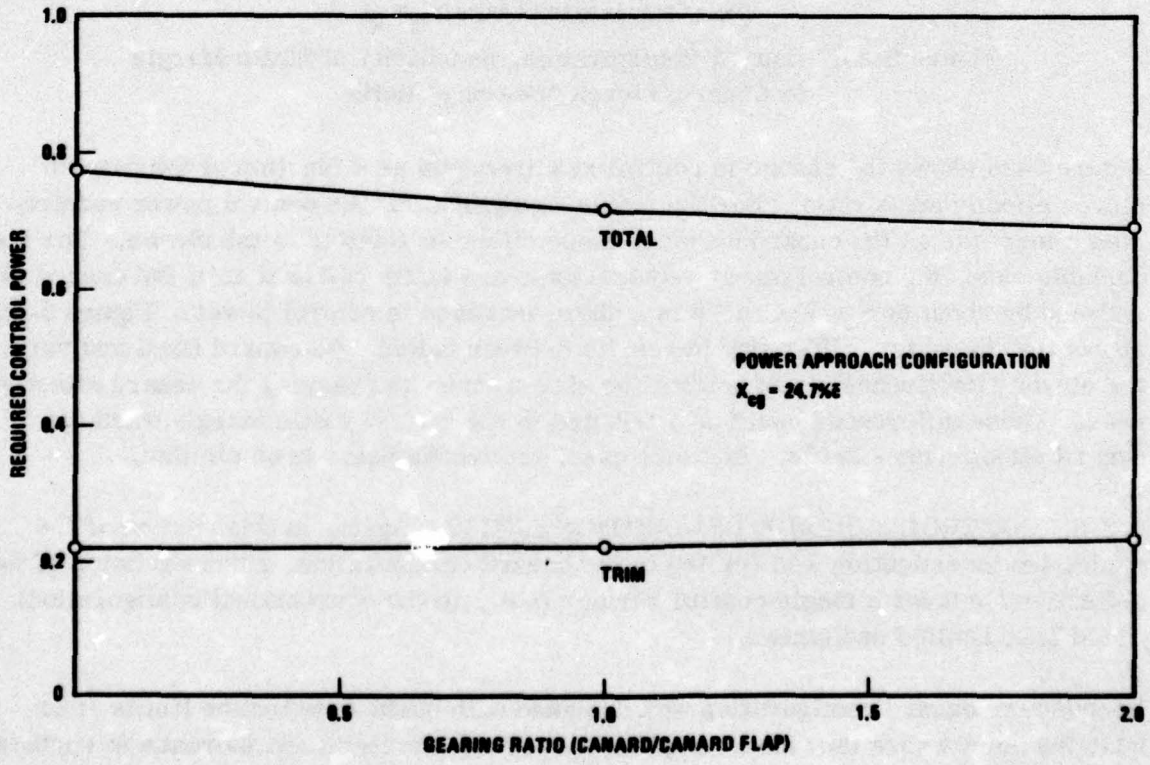

Figure 2-24. Canard Configuration, Sensitivity of Control Power Requirements to Canard/Canard Flap "Gearing" Ratio

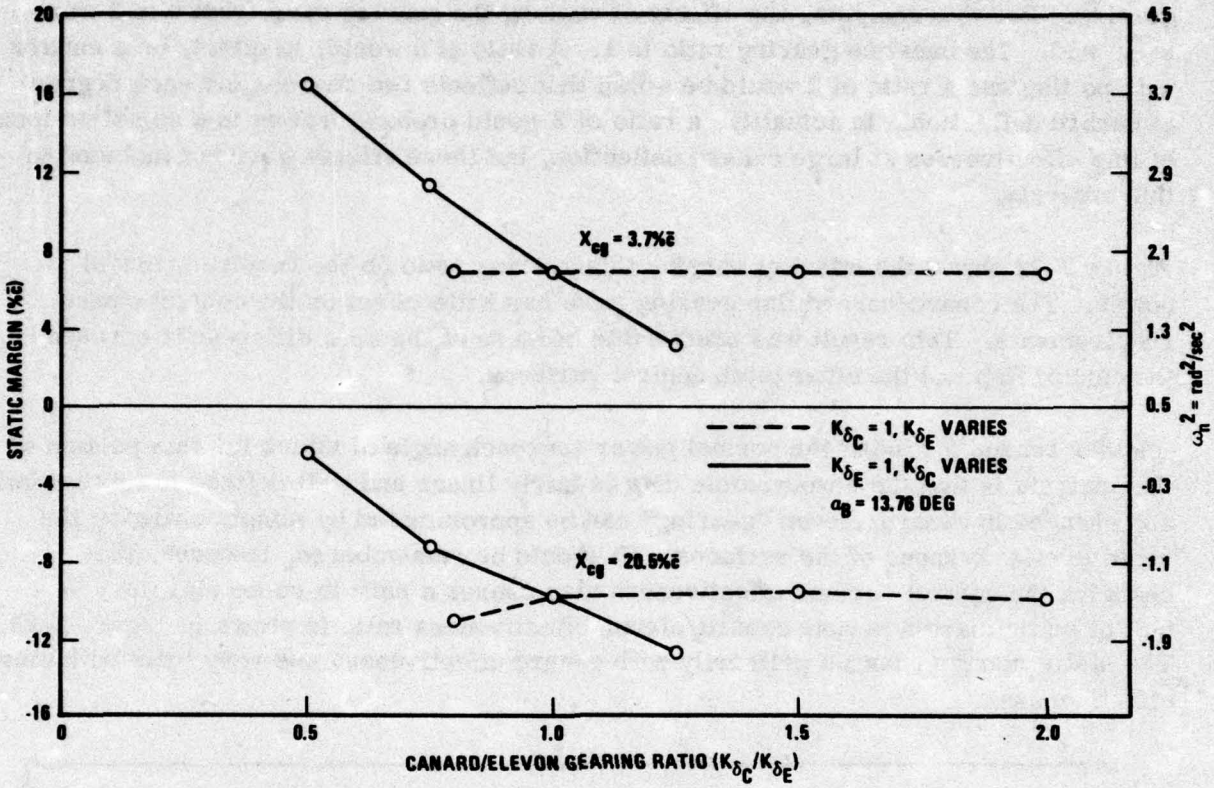

Figure 2-25. Canard Configuration, Sensitivity of Static Margin to Canard/Elevon "Gearing" Ratio

Figure 2-26 shows the change in control requirements as a function of the canard/elevon effectiveness ratio. For the stable configuration, the control power requirements increase as the canard becomes more effective relative to the elevon. For the unstable case, the control power requirements are fairly constant until the canard is reduced by about 50% where there is a sharp increase in control power. Figure 2-26 shows that there is a difference in results between holding the canard fixed and varying the elevon effectiveness, and holding the elevon vixed and varying the canard effectiveness. These differences could be attributed to the shift in static margin when the canard effectiveness shifts. In either case, the trends seem to be similar.

2.3.3 CONTROL SURFACE DEFLECTION LIMITS. Again, in this portion of the study, the investigation was limited to the canard configuration, since variation of the deflection limit for a single control surface (i.e., in the conventional configuration) would have limited usefulness.

Because the canard configuration was designed with surface deflection limits at or near the point where they have complete loss of effectiveness, no increase in surface deflection limits was examined. Deflection limits of 50% and 75% of design were investigated. The design deflection limits were +15, -35 degrees for the canard and +21, -30 degrees for the elevon, where a positive sign indicates trailing-edge down.

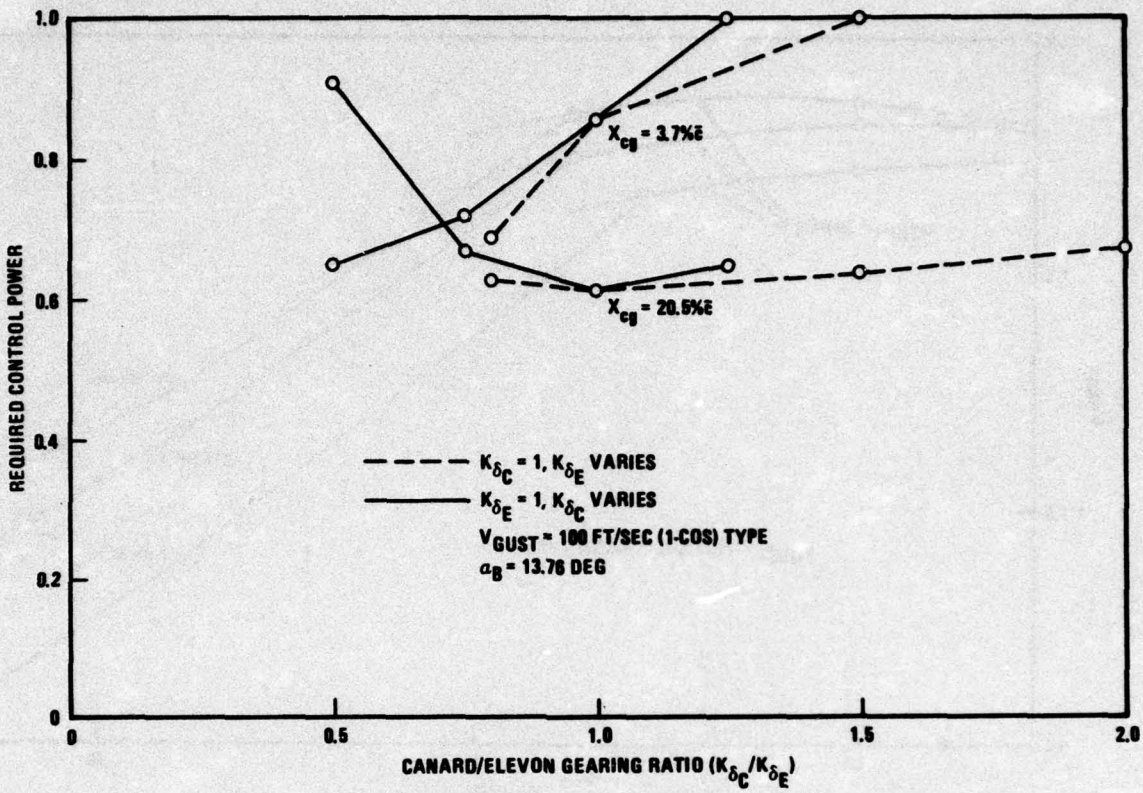

Figure 2-26. Canard Configuration, Sensitivity of Control Power Requirements to Canard/Elevon "Gearing" Ratio

The results of decreasing the deflection limits are presented in Figure 2-27. As expected, a decrease in the deflection limits results in a decrease in maximum C_L. For the cg as far aft as 31.7% $\bar{c}$, recovery is still possible with only 50% of the design deflection limits. The trim C_L curves at α = 30 degrees would eventually merge as the cg moved forward and the trim δ_c became less than the limit δ_c.

2.4 INFLUENCE OF GUST SHAPE

The (1-cos) shape is the type most commonly used for purposes of simulating a discrete gust. To compare the control power requirements for different gust shapes, the five shown in Figure 2-28 were used.

2.4.1 CONVENTIONAL CONFIGURATION. Maximum gust intensity was set at 100 ft/sec at a period of T = 1.05 seconds (corresponding to an ω_{GUST} = 6 rad/sec). Results are displayed in Figure 2-29 for an α_{TRIM} = 10 degrees, in which static margin was the parameter varied. It is evident that the (1-cos) gust shape is critical insofar as control power requirements are concerned. Intuitively, one would expect that the sharp-edged sawtooth or rectangular gust shape would be more demanding on

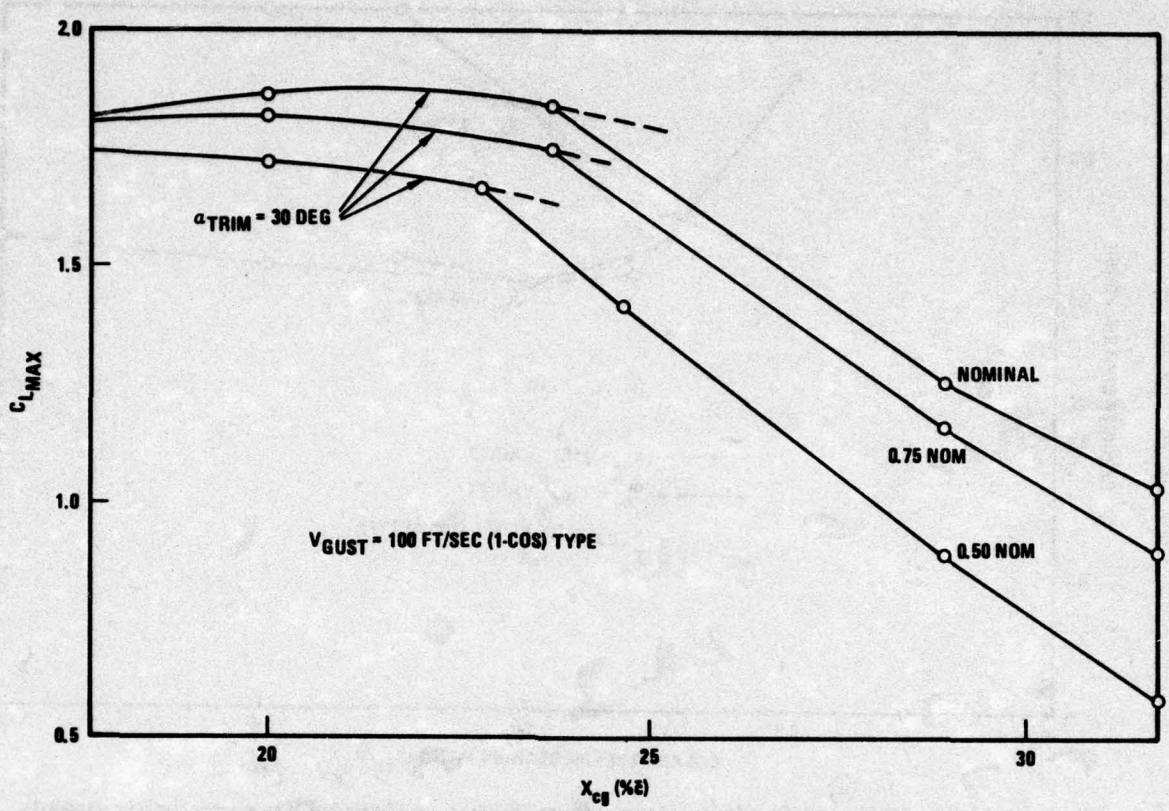

Figure 2-27. Canard Configuration, Gust Upset Boundary Sensitivity to Surface Deflection Limits

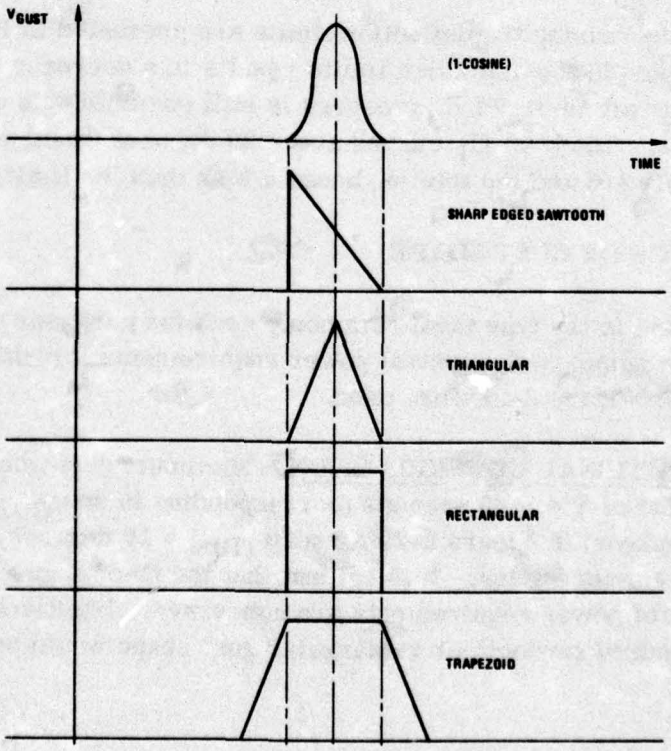

Figure 2-28. Gust Mode Shapes

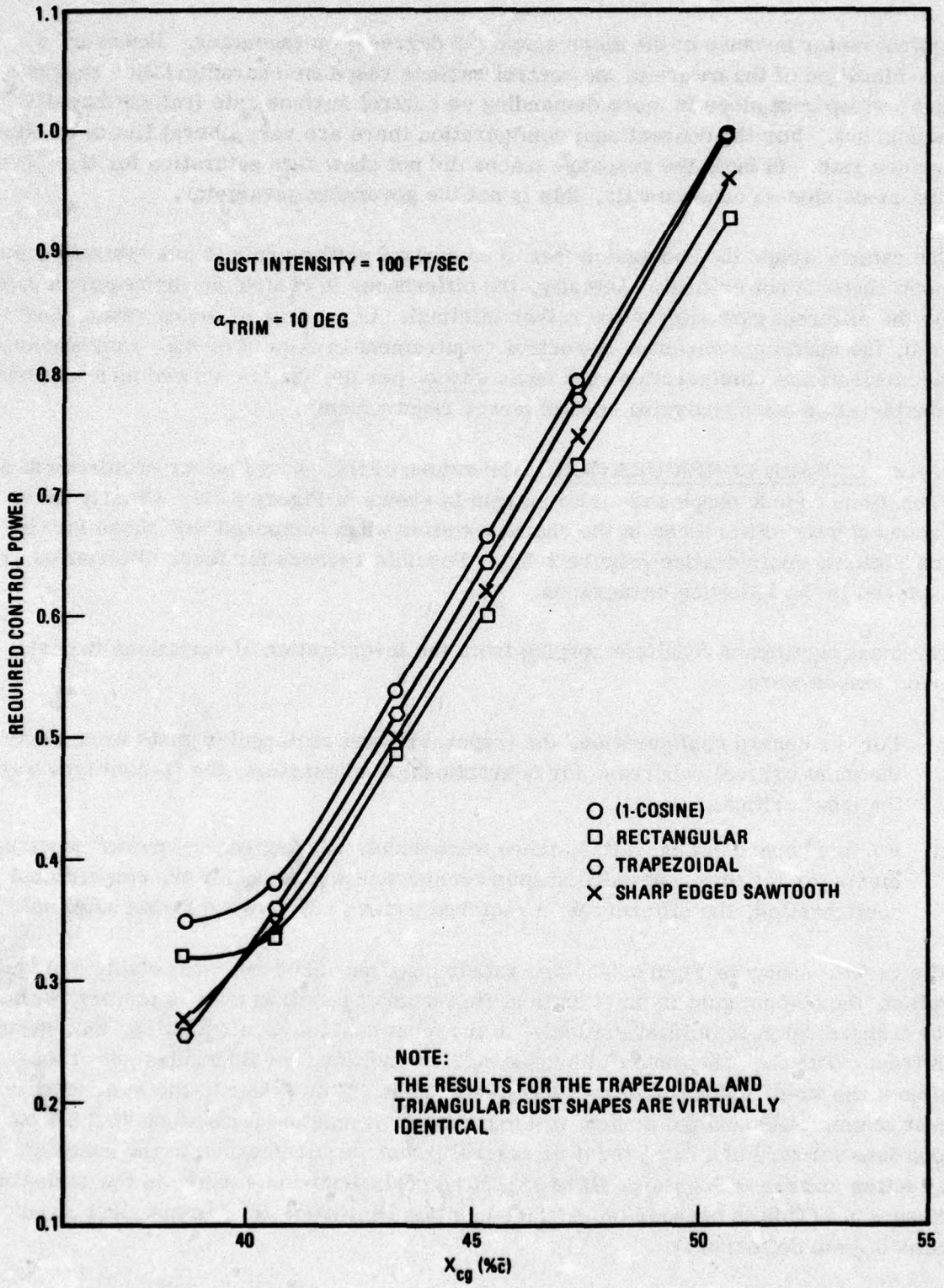

Figure 2-29. Conventional Configuration, Effect of Gust Mode Shape

control power because of the slope shape (90 degrees) on encounter. However, a consideration of the nature of the control surface response characteristics suggests that a steep gust slope is more demanding on control surface rate (rather than displacement). For the conventional configuration there are very liberal limits on control surface rate. In fact, the response traces did not show rate saturation for the steep gust mode slopes; consequently, this is not the governing parameter.

One cannot escape the conclusion that when control surface rate is not saturated, gust mode shape is not critical. Actually, the differences in control power requirements for the different gust shapes are rather minimal. Over most of the cg range considered, the maximum variation in control requirement is about 7 or 8%. Consequently, the conventional configuration gust mode shape, per se, may be viewed as a secondary consideration when analyzing control power requirements.

2.4.2 CANARD CONFIGURATION. The nature of the control power requirement as a function of mode shape and static margin is shown in Figure 2-30. Clearly there are substantial differences in the characteristics when compared with those for the conventional configuration (Figure 2-29). Possible reasons for these differences are explored in the following paragraphs.

The most significant results emerging from the investigation of variations in gust mode shapes were:

a. For the canard configuration, the trapezoidal and rectangular gusts were clearly the most critical; whereas, for conventional configuration, the (1-cos) type was the most critical.

b. For the canard configuration, there were widely varying control power requirements for the different mode shapes considered; whereas, for the conventional configuration, the differences in required control power were rather minimal.

The results shown in Figure 2-30 are rather puzzling. For the most stable configuration, the (1-cos) gust is most critical (in terms of required control power), while the trapezoidal gust is least critical. In the most unstable configuration, the reverse is true. With the exception of the most stable condition, the triangular gust requires almost the same control power as the (1-cos) gust. This is due to the similarity in gust shape. Although not evident in Figure 2-30, it must be pointed out that for cg locations forward of 18% $\bar{c}$, the peak control power requirement is in the nose-up direction and for cg locations aft of 18% $\bar{c}$ the peak requirements are in the nose-down direction. (This is because the surface position limits are not symmetrical about zero-degree deflection.)

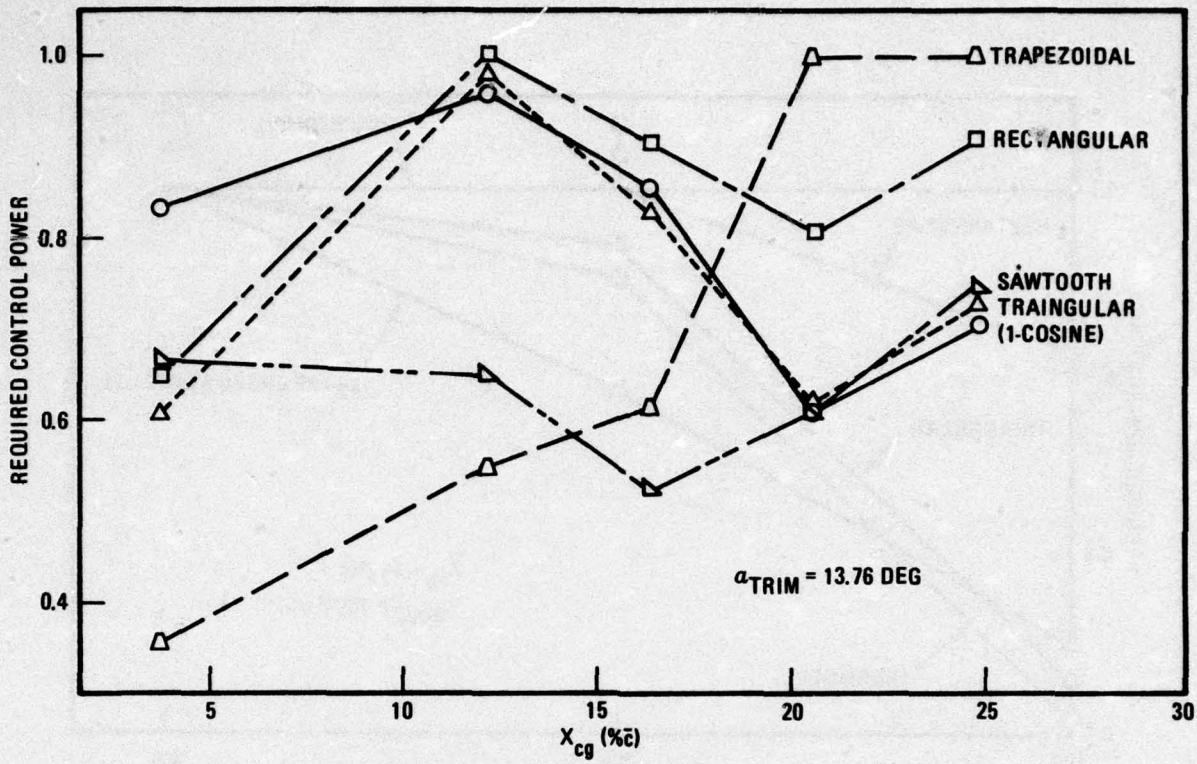

Figure 2-30. Canard Configuration, Effect of Gust Mode Shape

The time histories for the canard configuration showed that for the most unstable configuration, the elevon was position limited during trim and the only nose-down control moment had to come from the canard. (For the power approach configuration the canard is biased to six degrees nose-up deflection and the elevon trims any unbalanced pitch moment. If the elevon limits before reaching a trim condition, the canard is then used to trim.) For all of the gust shapes, the canard saturated in rate at some point in the response in the unstable configuration.

The required control power then was a direct function of how long the canard remained rate limited. Since the rectangular and trapezoidal gust shapes are at the maximum gust level of 100 fps longer than the other three gust shapes (Figure 2-28), it stands to reason that the canard would be rate limited longer in response to those two gusts. Consequently, the required control powers would be greater for the rectangular and trapezoidal gust shapes. This argument would imply that varying the canard rate limits would have a significant effect on the required control powers. Figure 2-31 illustrates the effect on required control power when the canard surface rate limit is doubled and tripled. As expected, the increase in rate limit allows the canard to deflect further in the given period of time, so that with the canard rate limit set to triple its nominal value, it will completely saturate for all gust shapes.

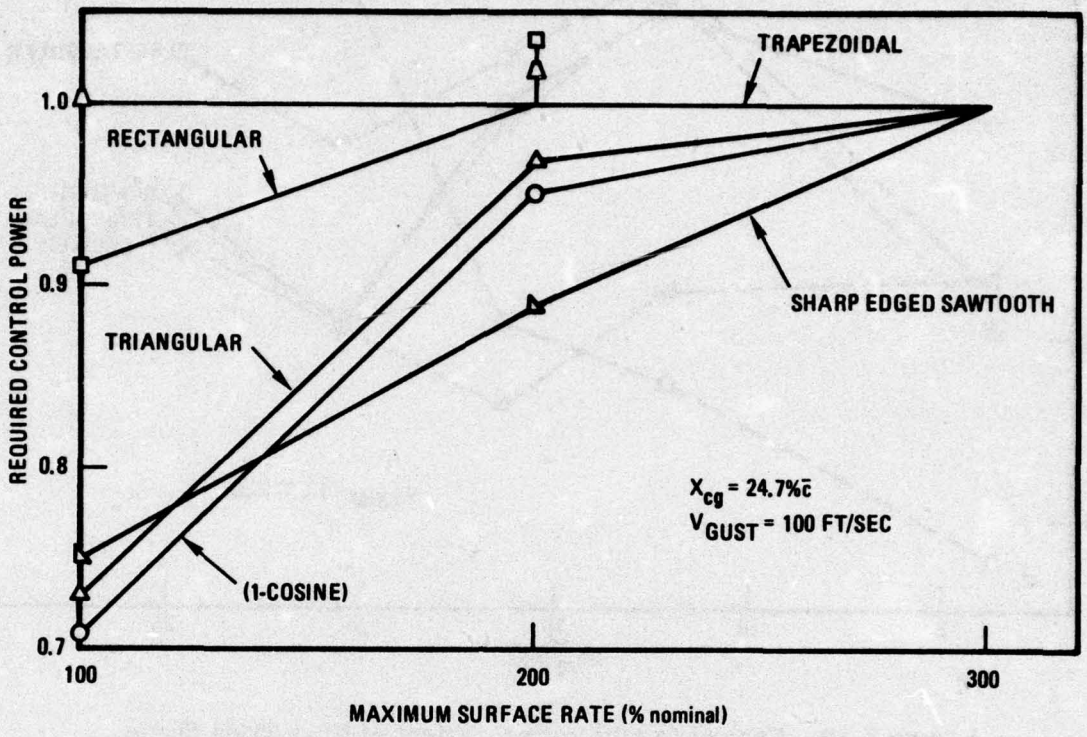

Figure 2-31. Canard Configuration, Variation in Control Surface Rate Limit

These results would seem to indicate that if the "period" of the rectangular and trapezoidal gusts were reduced, the control power requirements should also be reduced. Runs were made with the period for each of these two gust shapes cut in half. Thus, for the trapezoid, the "period" became the same as the (1-cos) gust; the ratio of the bases remained constant at 2:1. The results show that the peak required control power for the rectangular gust was 0.600, well below that shown in Figure 2-30. For the trapezoidal gust, the control power was 0.810, again below that shown in Figure 2-30, but more than that for the (1-cos) gust. Again, this is reasonable since the peak gust is reached sooner, and held longer, than in the (1-cos) gust.

Figure 2-32 shows the gust upset boundaries for the various discrete models of Figure 2-28, all with a gust amplitude of 100 ft/sec. Only that portion of the cg range is shown where the gust upset determines the maximum usable C_L. As can be seen, the only gust shape less critical than the (1-cos) gust is the triangular sawtooth. For cg locations forward of 23.8% $\bar{c}$, the trapezoidal gust is most critical, and aft of 23.8% $\bar{c}$, the rectangular gust is most critical.

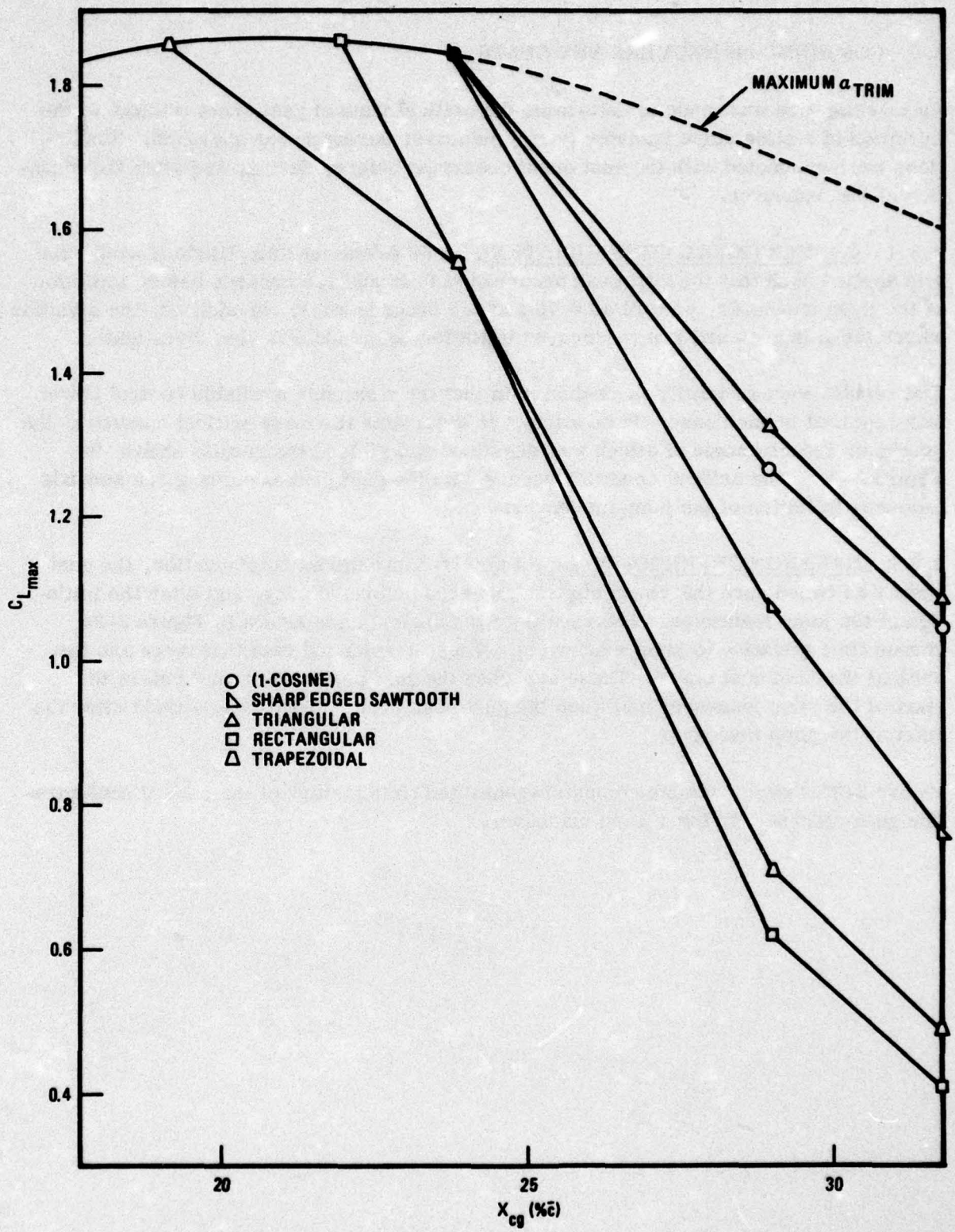

Figure 2-32. Canard Configuration, Maximum Usable C_L for Five Discrete Gust Models

2.5 COMBINED MANEUVERS AND GUSTS

An investigation was made to determine the critical time of gust onset relative to the initiation of a glide slope transfer (jump) maneuver during power approach. Simulations were conducted with the gust onset occurring before, during, and after the initiation of the maneuver.

2.5.1 CONVENTIONAL CONFIGURATION. A 50 ft/sec max amplitude (1-cos) gust was applied such that the gust peak occurred at 0.75 and 1.5 seconds before initiation of the jump maneuver, as well as 0.75 and 1.5 seconds after. In addition, the situation where the gust peak and jump maneuver initiation coincided was also investigated.

The results were generally inconclusive in that the maximum available control power was required in each case. In an attempt to determine the most critical condition, the maximum induced angle of attack was examined and yielded the results shown in Figure 2-33. The critical condition occurs with the gust peak occurring 1.5 seconds following initiation of the jump maneuver.

2.5.2 CANARD CONFIGURATION. As for the conventional configuration, the gust onset was timed such that the gust peak occurred before, during, and after the initiation of the jump maneuver. The results of the analysis are shown in Figure 2-34 versus time (relative to jump maneuver). These results indicate that there are two critical times of gust onset. These are when the gust peak occurs just before the start of the jump maneuver and when the gust peak occurs about 1.5 seconds after the start of the jump maneuver.

Figure 2-35 shows a sample computer-generated time history of the canard configuration gust response during a jump maneuver.

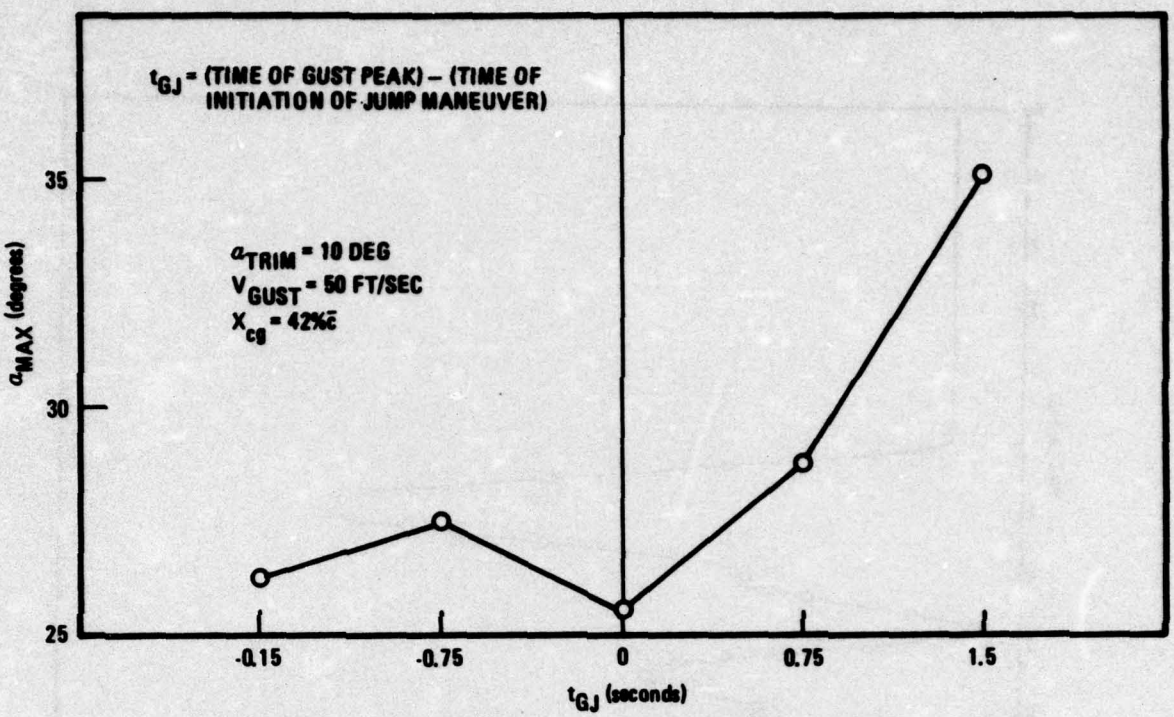

Figure 2-33. Conventional Configuration, Maximum Induced Angle of Attack From a Gust Superimposed on a Jump Maneuver

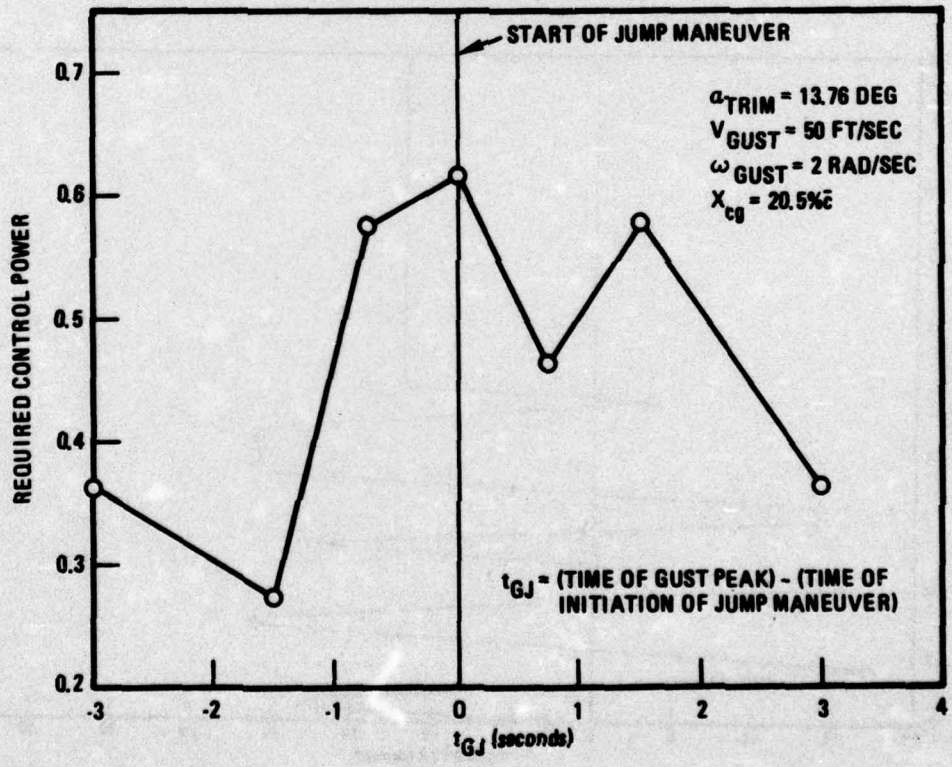

Figure 2-34. Canard Configuration, Control Power Requirements as a Function of Jump Maneuver Timing

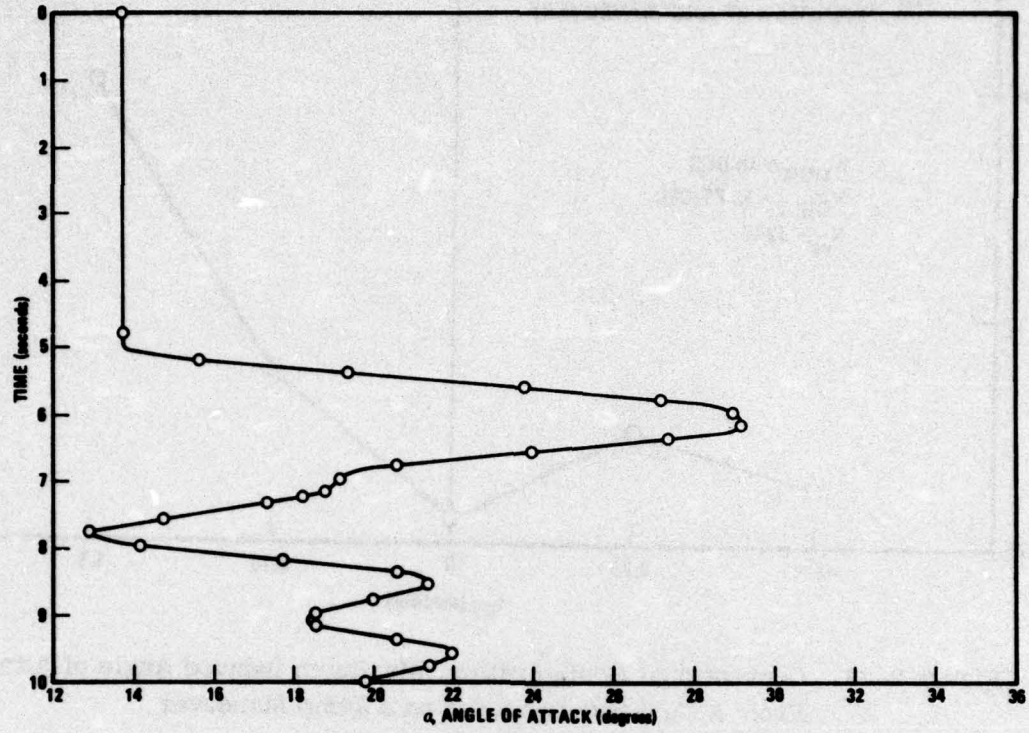

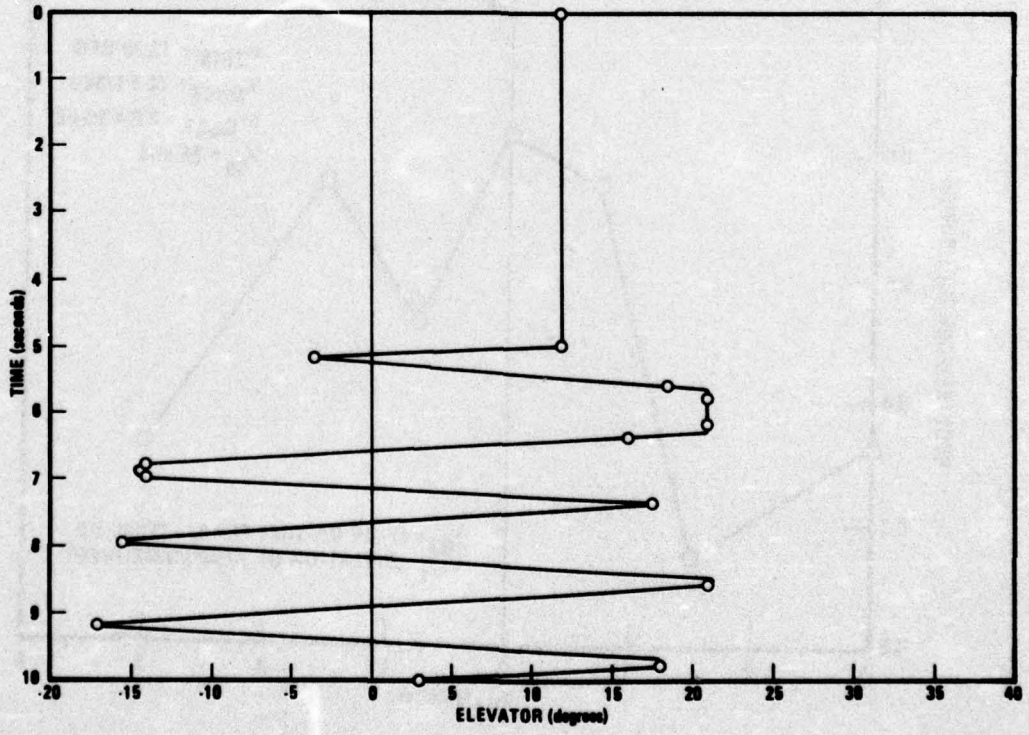

Figure 2-35. Canard Configuration, Time Response for Combined Gust/Jump Maneuver (Sheets 1 and 2 of 3)

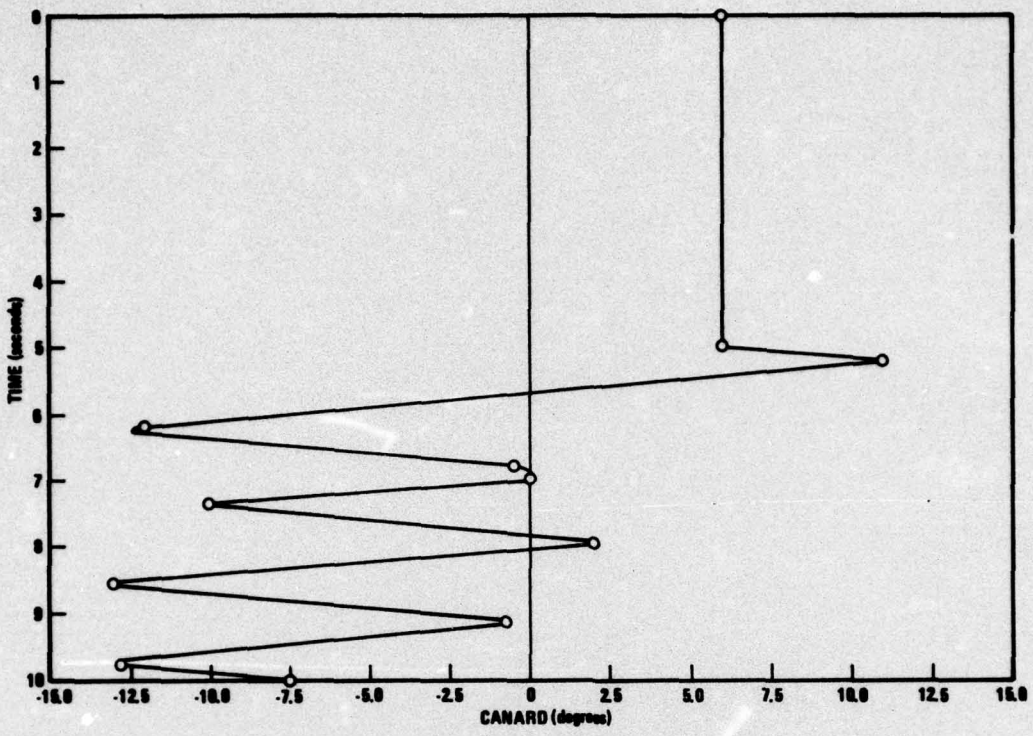

Figure 2-35. Canard Configuration, Time Response for Combined Gust/Jump Maneuver (Sheet 3 of 3)

SECTION 3

LATERAL GUST RESPONSE

3.1 EFFECTS OF RANDOM LATERAL GUST DURING DISCRETE LONGITUDINAL GUST

A critical gust condition occurs when a longitudinal gust acts in conjunction with a lateral gust excitation. To simulate this condition, a lateral random gust was applied to the aircraft. A Dryden type power spectrum was assumed for the gust, with parameters corresponding to a clear air turbulence (CAT) condition as recommended by MIL-8785-B. In this environment, the longitudinal gusts were applied. The five shapes shown in Figure 2-28 were used, with the aircraft in a power approach condition: first with a maximum C_L configuration, and then for a nominal power approach.

The quantities of interest in this phase of the study are the angle of attack, angle of sideslip, and the bank angle.

3.1.1 CONVENTIONAL CONFIGURATION. A nominal power approach configuration (α_{TRIM} = 10 degrees) was used in the simulation with a gust amplitude of 100 ft/sec. A maximum C_L condition (α_{TRIM} = 30 degrees) was also used with a gust amplitude of 75 ft/sec. The gust amplitude was lowered in the latter case in an attempt to maintain recovery capability while still exciting the maximum excursions. In both cases a cg at 47.3% $\bar{c}$ corresponding to -6.3% $\bar{c}$ static stability was used. The results are sumarized in Table 3-1.

The noteworthy result for the maximum C_L condition is that the motion is stable for all gust shapes considered except the trapezoidal and rectangular. For the latter two, there is a divergent motion in roll. The explanation for this rather unexpected result is that the maximum gust value acts for the longest time period as compared to the other three gust shapes. In the high α environment, the duration of the maximum gust intensity is the prime agent for generating roll rate, which could lead to divergence in roll. Furthermore, the cross coupling effects account for the higher control power requirement that is evident for the trapezoidal and rectangular gust shapes. In fact, the divergent motion in roll would ultimately lead to saturation of all control surfaces; the value of required control power less than unity reflects merely that longitudinal divergence had not yet occurred when the simulation was terminated.

For the nominal approach condition (α_{TRIM} = 10 degrees), all motions are stable for all mode shapes even though the gust intensity was increased to 100 ft/sec. Lateral/directional stability is greatly enhanded at the lower angles of attack.

Table 3-1. Conventional Configuration Response Characteristics, $X_{cg} = 47.3\% \bar{c}$

Gust Shape	Required Control Power	α (deg) (min	trim	max)	β (deg) (min	max)	ϕ (deg) (min	max)	V_{gust} (ft/sec)
(1-cos)	0.754	15.1	30.0	57.4	-11.9	10.5	-11.0	35.1	75
Trapezoid	0.960	6.7	30.0	58.1	-25.0	4.2	-19.9	174.5(1)	75
Rectangle	0.936	3.1	30.0	58.1	-26.9	4.3	-21.2	109.0(1)	75
Sawtooth	0.735	15.9	30.0	57.6	-11.4	11.8	-10.6	38.5	75
Triangle	0.755	15.5	30.0	55.8	-11.0	8.9	-9.1	34.0	75
(1-cos)	0.805	1.6	10.0	37.1	0.50	2.3	-0.92	21.3	100
Trapezoid	0.807	-9.1	10.0	38.0	-13.3	0	0	79.3	100
Rectangle	0.753	-6.9	10.0	37.6	-12.8	0	0	81.1	100
Sawtooth	0.773	2.0	10.0	37.6	-1.4	1.9	-0.49	13.1	100
Triangle	0.807	2.0	10.0	36.1	-1.5	1.3	0	13.2	100

(1) Divergent Motion

3.1.2 CANARD CONFIGURATION. The lateral stability at high angles of attack was investigated for the canard configuration in a manner identical to that for the conventional configuration. The results are summarized in Table 3-2. The lateral/dirctional stability of the canard configuration is greater than that of the conventional aircraft. No divergent motion occurred for excitations that induced a roll instability in the conventional configuration. The excursions in roll and sideslip were significantly less for the same excitations. These comparisons are valid in the sense that the cg locations on both aircraft were such as to give nearly identical static margin.

3.2 RESPONSE TO OBLIQUE GUSTS

When a gust is oblique, in the sense that it acts at some angle to the local vertical, there is induced in the aircraft a combination of longitudinal and lateral motions. In general, it is extremely difficult to predict the nature of such motions by purely analytical means because of the gross nonlinearity of the relevant aerodynamics and inertial cross-coupling of the aircraft. For purposes of the present study, this alone would constitute sufficient motivation for investigating the response to oblique gusts with a view to noting if there are any "surprises."

3.2.1 CONVENTIONAL CONFIGURATION. To induce lateral and longitudinal motions of moderate magnitude, a (1-cos) gust of 75 ft/sec maximum amplitude was applied to the aircraft. The results are shown in Figures 3-1 through 3-6 for the basic response parameters of interest; namely, angle of attack, angle of sideslip, bank angle, together with the tail, rudder, and flaperon deflections, δ_E, δ_R, and δ_A respectively. To obtain the curves shown, the gust was applied vertically and thereafter in angles with respect to the vertical in increments of five degrees, ending with a gust vertically downward (gust angle = 180 degrees). In each case the maximum and minimum value of the respective parameters were noted, thereby giving the two points shown for each value of gust angle.

In general, the overall nature of the curves is what one would expect. Lateral motions predominate when the gust angle is close to 90 degrees, and longitudinal motions predominate when the gust is near vertical. Also, a "vertical-up" gust excites the lateral motions whereas a "vertical-down" does not. This would appear traceable to the fact that an "up" gust induces an angle of attack in excess of 40 degrees, such that the usual assumptions for decoupling of the longitudinal and lateral motions are not satisfied.

Table 3-2. Canard Configuration Response Characteristics X_{cg} = 16.6% $\bar{c}$

Gust Shape	Required Control Power	α (deg) (min	trim	max)	β (deg) (min	max)	ϕ (deg) (min	max)	V_{gust} (ft/sec)
(1-cos)	0.565	1.0	13.76	33.5	-0.20	0.45	-0.55	1.5	75
Trapezoid	0.795	-3.0	13.76	35.0	-0.33	0.78	-2.1	1.6	75
Rectangle	0.890	-8.0	13.76	35.0	-0.55	1.10	-7.0	2.0	75
Sawtooth	0.496	3.0	13.76	32.5	-0.26	0.65	-2.0	1.7	75
Triangle	0.650	0.0	13.76	33.0	-0.17	0.32	0.0	1.5	75
(1-cos)	0.610	18.0	28.0	60.0	-1.25	1.50	-3.0	2.1	75
Trapezoid	0.740	11.5	28.0	61.0	-3.0	8.2	-2.0	22.0	75
Rectangle	0.865	4.5	28.0	58.0	-2.0	10.0	-3.0	12.0	75
Sawtooth	0.580	20.0	28.0	55.0	-2.0	7.0	-3.4	12.6	75
Triangle	0.612	18.0	28.0	59.0	-1.4	1.2	-3.3	1.7	75

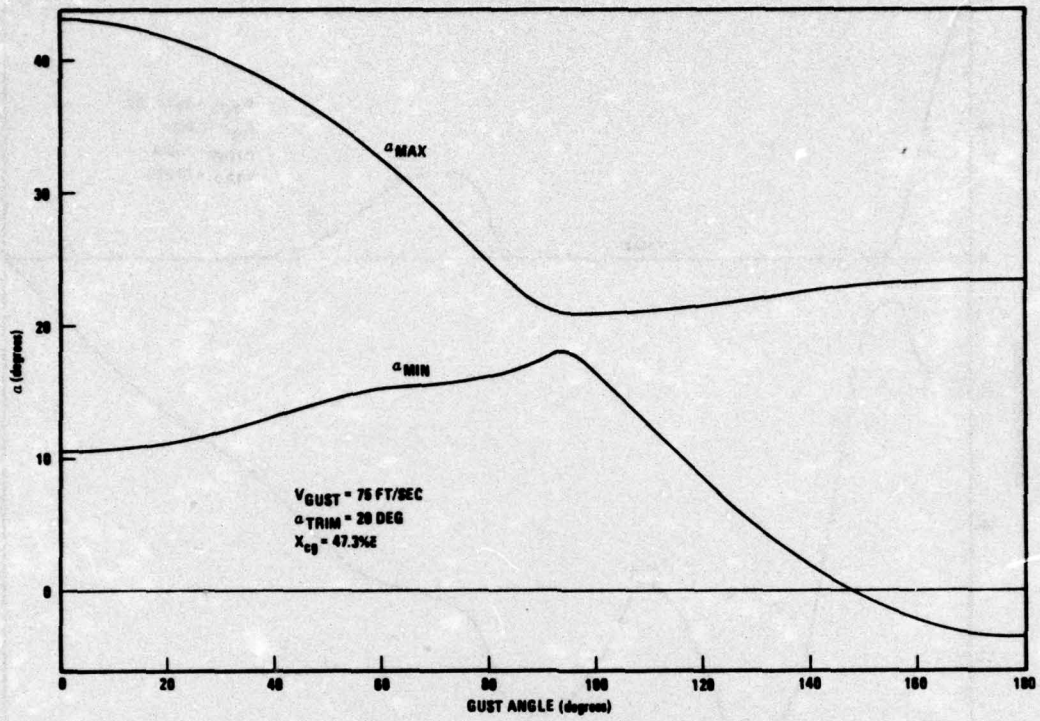

Figure 3-1. Conventional Configuration, Angle of Attack Response to Oblique Gusts

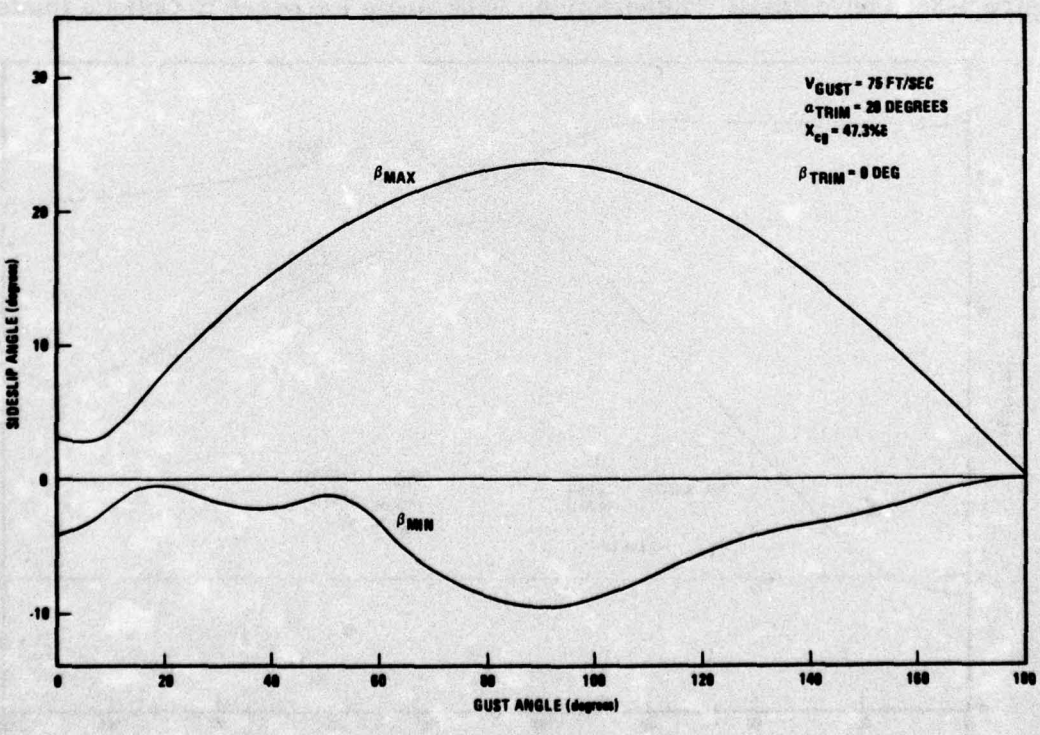

Figure 3-2. Conventional Configuration, Sideslip Angle Response to Oblique Gusts

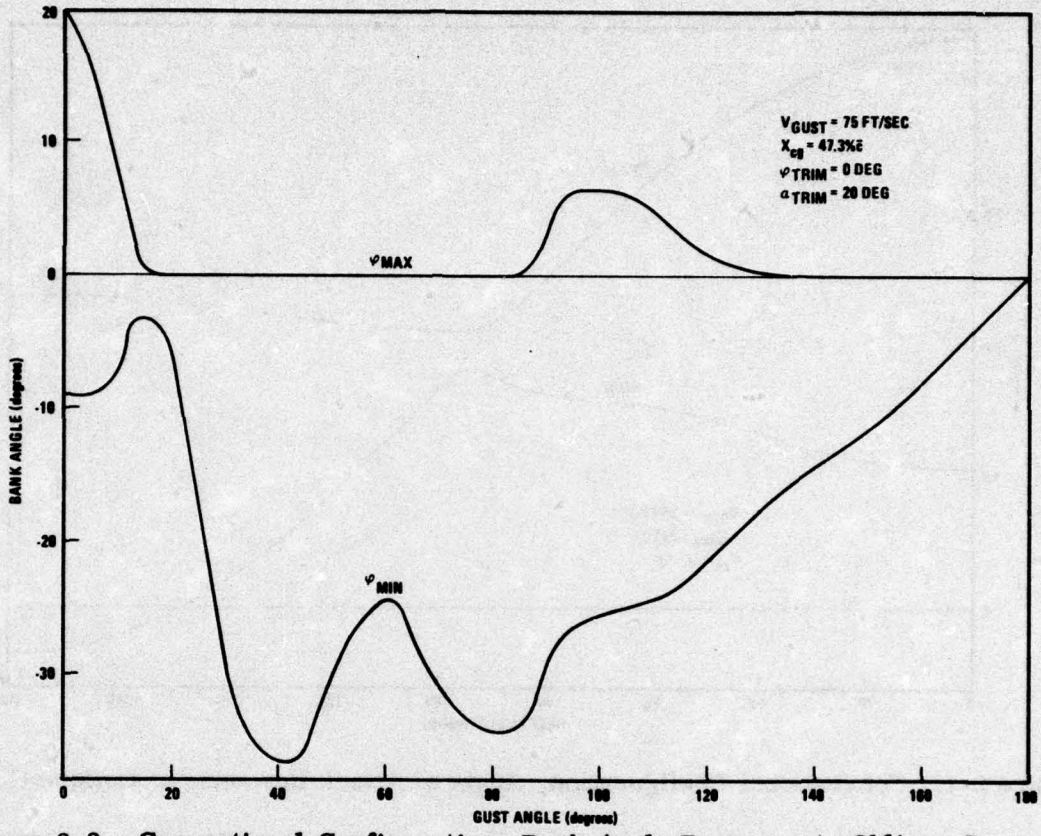

Figure 3-3. Conventional Configuration, Bank Angle Response to Oblique Gusts

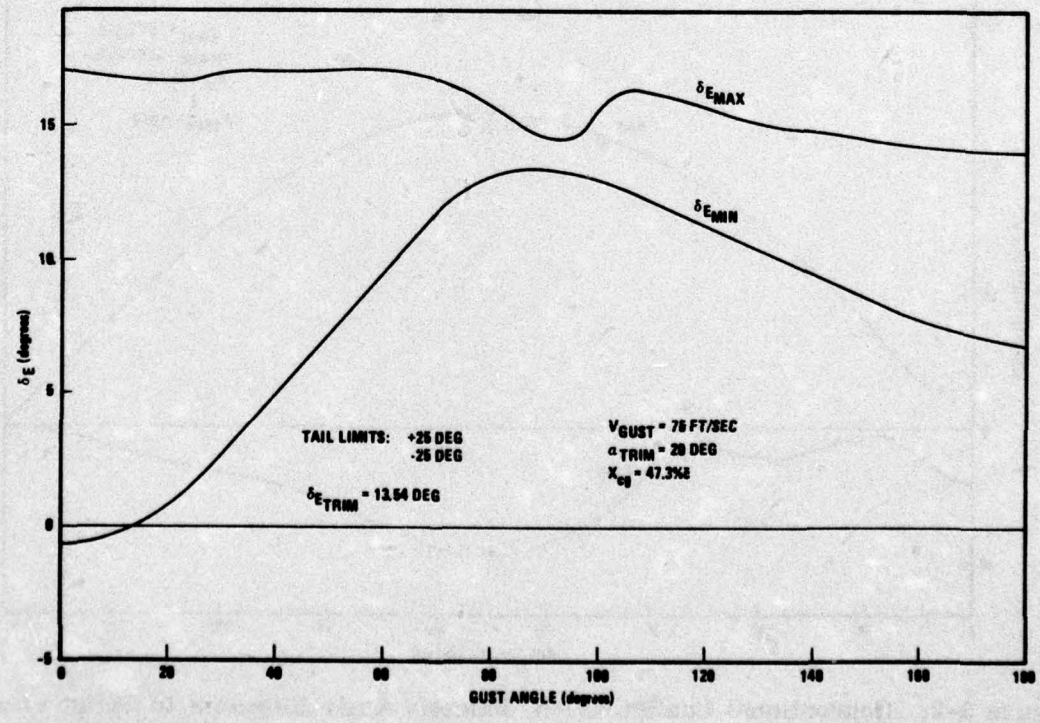

Figure 3-4. Conventional Configuration, Response of Tail to Oblique Gusts

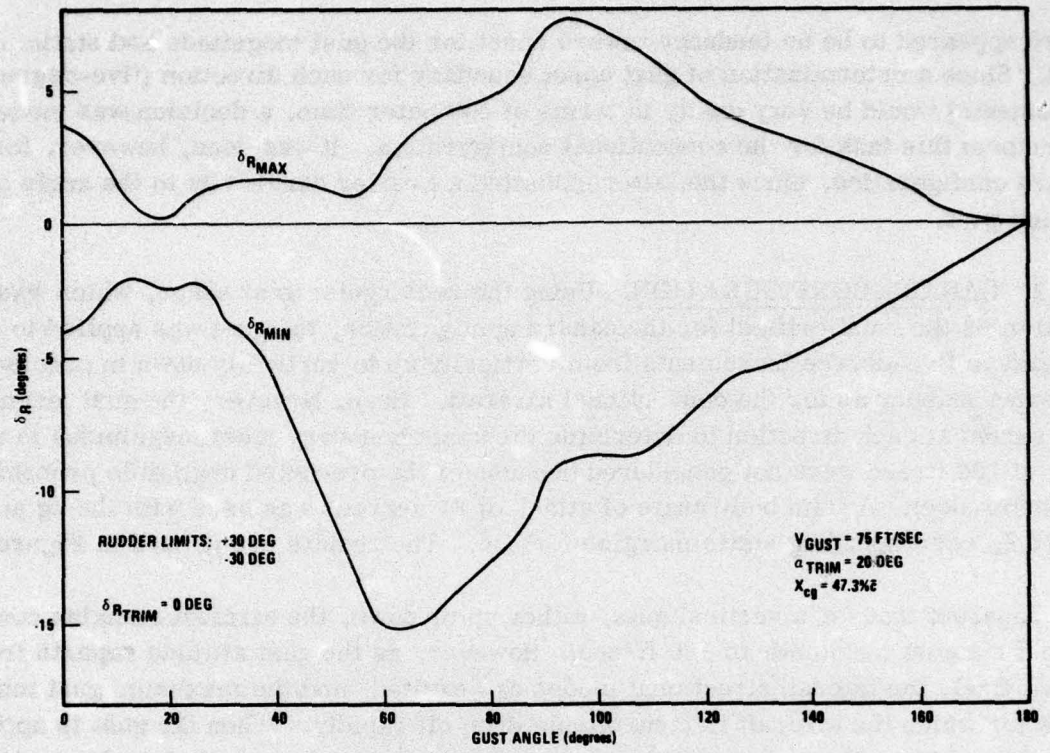

Figure 3-5. Conventional Configuration, Response of Rudder to Oblique Gusts

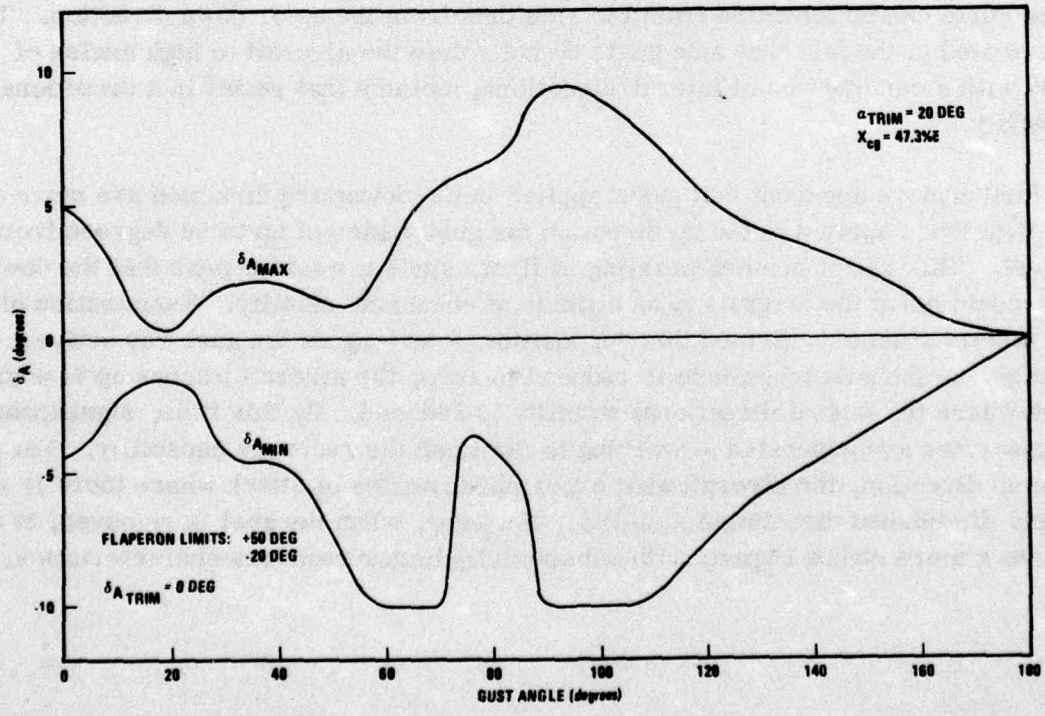

Figure 3-6. Conventional Configuration, Response of Flaperon to Oblique Gusts

There appeared to be no tendency toward upset for the gust magnitude and static margin used. Since a determination of gust upset boundary for each direction (five-degree increments) would be very costly in terms of computer time, a decision was made not to perform this task for the conventional configuration. It was done, however, for the canard configuration, since the latter exhibited a greater sensitivity to the angle of the applied gust.

3.2.2 CANARD CONFIGURATION. Using the rectangular gust shape, which was found to be the most critical for the canard configuration, the gust was applied to the aircraft in five-degree increments from vertically up to vertically down in precisely the same manner as for the conventional aircraft. Here, however, the gust magnitude was varied at each direction to determine the upset boundary (gust magnitudes in excess of 100 ft/sec were not considered because of the presumed negligible probability of occurrence). A trim body angle of attack of 21 degrees was used with the cg at 16.6% $\bar{c}$, corresponding static margin of -8% $\bar{c}$. The results are plotted in Figure 3-7.

It is apparent that for a vertical gust, either up or down, the aircraft remains controllable for a gust magnitude of 100 ft/sec. However, as the gust attitude departs from the vertical, the lateral/directional modes are excited, and the maximum gust magnitudes for which the aircraft is controllable drop off rapidly. When the gust is applied at angles of 30 to 60 degrees from the up or down direction, magnitudes of only 40 to 50 ft/sec can be tolerated. At a gust angle of 90 degrees, the canard configuration is again controllable for gust magnitudes of 100 ft/sec. In fact, Figure 3-7 indicates that higher gusts can be tolerated from the side than from the up or down direction. This is attributed to the fact that side gusts do not rotate the aircraft to high angles of attack with a combination of lateral/directional motions that result in a directional instability.

It is furthermore apparent that gusts applied in the downward direction are more critical than those applied in the up direction for gust angles of up to 60 degrees from the vertical. This result seemed puzzling at first, since it would appear that the down gusts would drive the aircraft to an attitude of enhanced stability. Examination of the time history traces confirmed this supposition — as long as the gust was active. However, as the gust magnitude is reduced to zero, the aircraft pitches up to angles of attack where the lateral directional stability is reduced. By this time, significant roll and yaw rates are generated — working to diminish the recovery capability. For gusts in the up direction, the aircraft also experiences angles of attack where there is a sharply diminished directional stability. However, when the gust is removed, it returns to a more stable region, with substantially better recovery characteristics.

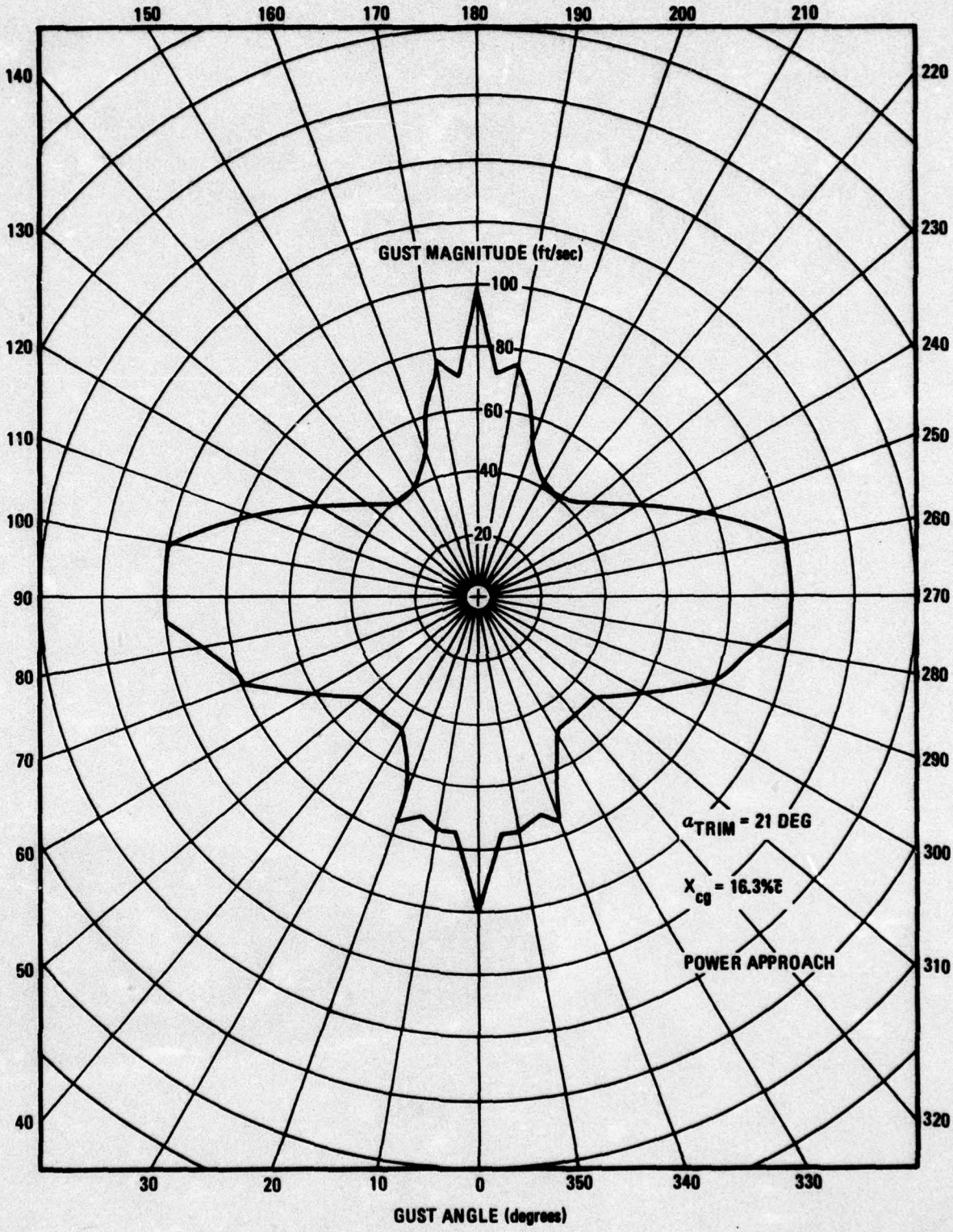

Figure 3-7. Canard Configuration, Oblique Gust Boundary: Maximum Gust Amplitude Versus Gust Angle, (1-cosine) Gust

SECTION 4

CONCLUSIONS

The primary aim of the investigation was to determine the sensitivity of control power requirements to variations in aircraft parameters and input disturbance levels for statically unstable aircraft. The significant conclusions that emerge as a result of the study may be summarized as:

a. The low-speed power approach conditions were more critical for both configurations. This is due to the larger incremental changes in angle of attack and dynamic pressure for a given gust magnitude. This results in larger incremental changes in the vehicle pitching moment.

b. The critical gust frequency for the (1-cos) gust was found to be approximately twice ω_n for each configuration.

c. Static margin is the primary quantity influencing the control power requirement. For the conventional configuration where surface rate saturation during a gust response was rare, the control power requirements varied linearly with cg position — which is a result of the linear relationship between cg location and trim control power requirements.

d. The sensitivity of control power requirements to variations in control effectiveness, C_{m_o}, and multiple control surface gearing is predictable by the manner in which these variations in the particular parameter alter the static margin.

e. The sensitivity of control power requirements to gust mode shape was found to be insignificant when rate saturation of the control surfaces did not occur. When rate saturation did occur, those gust shapes that were at their peak magnitude for the longest period of time (rectangular and trapezoidal) were found to be most critical. (The differences were again diminished, however, when the rate limits were increased.) These results support the view that the conventional (1-cos) type gust shape is appropriate for use as a discrete design gust.

f. Control power requirements of unstable aircraft are highly sensitive to aerodynamic characteristics at high angles of attack.

g. The gust upset boundary was found to drop off sharply when the gust was applied at a significant angle from the vertical. Quantitative results would seem to be configuration dependent but again point out the need for a complete and accurate data base at high angles of attack.